THE DETERMINATION OF RATE-LIMITING STEPS DURING SOOT FORMATION

Final Report

for

February 1988 to January 1991

Prepared by

M. B. Colket III
R. J. Hall
J. J. Sangiovanni
D. J. Seery

United Technologies Research Center
East Hartford, CT 06108

UTRC Report No. UTRC91-21

For

Air Force Office of Scientific Research
Bolling Air Force Base
Washington, D.C. 20332

Contract No. F49620-88-C-0051

J. M. Tishkoff
Program Manager

August 14, 1991

(a)

SECURITY CLASSIFICATION OF THIS PAGE

REPORT DOCUMENTATION PAGE

Form Approved
OMB No. 0704-0188

1a. REPORT SECURITY CLASSIFICATION Unclassified	1b. RESTRICTIVE MARKINGS
2a. SECURITY CLASSIFICATION AUTHORITY	3. DISTRIBUTION/AVAILABILITY OF REPORT Approved for public release; distribution is unlimited.
2b. DECLASSIFICATION/DOWNGRADING SCHEDULE	
4. PERFORMING ORGANIZATION REPORT NUMBER(S) UTRC91-21	5. MONITORING ORGANIZATION REPORT NUMBER(S) AFOSR-TR- 91 0736
6a. NAME OF PERFORMING ORGANIZATION United Technologies Research Center 6b. OFFICE SYMBOL (If applicable)	7a. NAME OF MONITORING ORGANIZATION AFOSR/NA
6c. ADDRESS (City, State, and ZIP Code) East Hartford, CT 06108	7b. ADDRESS (City, State, and ZIP Code) Building 410, Bolling AFB DC 20332-6448
8a. NAME OF FUNDING/SPONSORING ORGANIZATION AFOSR/NA 8b. OFFICE SYMBOL (If applicable) NA	9 PROCUREMENT INSTRUMENT IDENTIFICATION NUMBER F49620-88-C-0051
8c. ADDRESS (City, State, and ZIP Code) Building 410, Bolling AFB DC 20332-6448	10. SOURCE OF FUNDING NUMBERS PROGRAM ELEMENT NO. 61102F; PROJECT NO. 2308; TASK NO. A2; WORK UNIT ACCESSION NO.

11. TITLE (Include Security Classification)

(U) The Determination of Rate-Limiting Steps During Soot Formation

12. PERSONAL AUTHOR(S)

Colket, M. B., Hall, R. J., Sangiovanni, J. J. and Seery, D. J.

13a. TYPE OF REPORT	13b. TIME COVERED	14. DATE OF REPORT (Year, Month, Day)	15. PAGE COUNT
Final	FROM 2/1/88 TO 1/31/91	1991 - August 14	96

16. SUPPLEMENTARY NOTATION

17. COSATI CODES			18. SUBJECT TERMS (Continue on reverse if necessary and identify by block number)
FIELD	GROUP	SUB-GROUP	modeling of soot formation growth of aromatic rings, pyrolysis of cyclopentadiene

19. ABSTRACT (Continue on reverse if necessary and identify by block number)

A detailed model for soot formation has been developed for describing soot production in laminar, premixed flames. The analysis is based on detailed chemical kinetic modeling, a simplified inception model, kinetic calculations of surface soot growth, and coalescing particle collisions. Several different models for surface growth are compared. Sensitivities to flame parameters and many of the assumptions were determined. Comparisons have been made to several flames with varying stoichiometry, temperature, fuel type, and pressure.

A mechanism for the pyrolysis of cyclopentadiene has been developed. In addition, mechanisms for the addition of acetylene to cyclopentadiene to form toluene are discussed.

20 DISTRIBUTION/AVAILABILITY OF ABSTRACT	21. ABSTRACT SECURITY CLASSIFICATION
☒ UNCLASSIFIED/UNLIMITED ☒ SAME AS RPT ☒ DTIC USERS	Unclassified
22a NAME OF RESPONSIBLE INDIVIDUAL Julian M. Tishkoff	22b TELEPHONE (Include Area Code) (202) 767-0465
	22c. OFFICE SYMBOL AFOSR/NA

DD Form 1473, JUN 86 Previous editions are obsolete. SECURITY CLASSIFICATION OF THIS PAGE

THE DETERMINATION OF RATE-LIMITING STEPS DURING SOOT FORMATION

Final Report

for

February 1988 to January 1991

Prepared by

M. B. Colket III
R. J. Hall
J. J. Sangiovanni
D. J. Seery

United Technologies Research Center

East Hartford, CT 06108

UTRC Report No. UTRC91-21

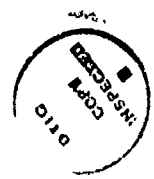

For

Air Force Office of Scientific Research
Bolling Air Force Base
Washington, D.C. 20332

Contract No. F49620-88-C-0051

J. M. Tishkoff

Program Manager

August 14, 1991

UTRC91-21

THE DETERMINATION OF RATE – LIMITING STEPS DURING SOOT FORMATION

Final Report

Table of Contents

List of Figures

UTRC91-21

DETERMINATION OF RATE-LIMITING STEPS DURING SOOT FORMATION

FINAL REPORT

I. Summary

A detailed model for soot formation has been developed for describing soot production in laminar, premixed flames. The analysis is based on detailed chemical kinetic modeling, a simplified inception model, kinetic calculations of surface growth, and coalescing particle collisions. Several different models for surface growth are compared. Sensitivities to flame parameters and many of the assumptions were determined. The importance of inception to the amount of soot formed has been verified for several premixed flames. Comparisons have been made to several flames with varying stoichiometry, temperature, fuel type, and pressure.

A mechanism for the pyrolysis of cyclopentadiene has been developed. In addition, mechanisms for the addition of acetylene to cyclopentadiene to form toluene are discussed. The formation of a bicyclic intermediate species is favored.

II. Introduction

There is substantial experimental evidence that important rate-limiting steps to soot formation are the production and growth of aromatic and polyaromatic hydrocarbons. Detailed modeling and comparison to experimental data has led to a good understanding of mechanisms and rates for the production of benzene (and phenyl radical). A major unknown is the importance of C_5-species on ring growth. Flame studies indicate that cyclopentadiene has sooting characteristics similar to that of aromatics, but mechanisms are lacking to explain the rapid conversion to C_6-rings which are believed to dominate in ring growth processes. Another large uncertainty in soot formation mechanisms is the effect of oxidation. Under many conditions, growth of polyaromatic hydrocarbons (PAHs) may be quite fast but is counterbalanced by oxidation. Therefore, the net production rate of PAHs, and therefore of soot, is only a small fraction of the "gross" production rate of PAHs. Oxidation processes (mechanisms and rates) of aromatic hydrocarbons at elevated temperatures ($T > 1200K$) are unfortunately very poorly known. Also, growth mechanisms of soot are poorly understood and models for growth mechanisms are few. Yet, this process, together with 'inception', plays an important role in the amount of soot produced in a given flame.

To investigate these important and competitive phenomena, an experimental and modeling program has been performed. The experimental phase of the program included the use of a single-pulse shock tube to thermally stress mixtures of gases, which are then quenched, and the reaction products are analyzed. In support of this work and under corporate sponsorship, the gas sampling system has been modified to collect and detect high molecular weight species. Results of these modifications were extremely successful and the modified facilities were described in the first year's annual report. To examine the importance of C_5 rings, cyclopentadiene has been pyrolyzed, oxidized and copyrolyzed with acetylene, biacetyl, and benzene. These results, as well as data on the rich oxidation of benzene, were reported in first two annual reports. Listings of mixtures examined

during the duration of this program are provided in Table I, II, and III, where the third table lists compounds examined in the past year under corporate sponsorship. Results of the corporate-funded experiments are not reported here but have provided insight to help guide the AFOSR-funded efforts. In order to help obtain additional information on species identification, a mass spectrometer has been added to the gas chromatograph. This added diagnostic insures greater confidence in the identification of high molecular weight intermediates.

In two annual reports (Colket, et al., 1989, 1990) for this program, much of the experimental results obtained in this study have been described. In addition, the preliminary modeling efforts of gas-phase kinetic processes and soot formation were presented. In the last year of this three year program, efforts have focused on soot modeling and some reinterpretation of the data on cyclopentadiene thermal decomposition.

The results of the soot modeling are described in Appendix A with enough detail that the procedures can be evaluated and duplicated at other laboratories as required. The document has been issued as a UTRC report (UTRC91-20) and its publication is being considered as either part of a collection of papers presented at the workshop on Mechanisms and Models of Soot Formation to be held in Heidelberg on September, 30 - October 1, 1991 (publication in "Springer Series of Chemical Physics"), or submitted to a journal, depending on constraints defined by the editors for length of paper, etc. Since the document is duplicated in its entirety in an appendix, only summary statements are included in the main body of this report.

Recent work has also been performed on the decomposition of cyclopentadiene. Experimental data and a preliminary interpretation was reported in last year's annual report and at the Eastern Section of the Combustion Institute, 1990. A copy of the ES/CI abstract is included in this report (Appendix B), although several refinements to the preliminary mechanism were recognized prior to the actual presentation, and since these new thoughts were presented at the Eastern Section meeting, they are briefly discussed here. Also, based on the analysis of the growth processes observed in the cyclopentadiene system, an alternative ring growth mechanism has been identified. These results will be presented at the 1991 Eastern Section of the Combustion Institute and a copy of the abstract is also included in Appendix C of this report.

III. Results

A. Summary of Soot Formation Modeling

An analytic model of soot formation in laminar, premixed flames has been developed which is based on coupling the output of flame chemical kinetics simulations with a sectional aerosol dynamics algorithm for spheroid growth. A flow chart describing the model is provided in Figure 1. A provisional particle inception model in which benzene acts as a surrogate for the inception species is employed. Justification for the use of this simplified model is based on experimental evidence relating ring formation to soot production, to the fact that soot predictions are strongly sensitive to the selection of the inception species so that any model will implicitly have empirical correction factors, and to the fact that the actual inception process is still unknown. Futhermore, there are at present uncertainties in modeling formation of PAHs, and long computational times are required for such efforts. The use of this inception model is motivated by a desire to develop a simple procedure which might be useful for predictions in more practical flames. This simplified inception model overstates the actual rate of inception and several compensatory factors are included in the model, including a slightly low specific surface growth rate and coagulation of low molecular weight aromatics. Surface growth has been based on experimental measurements and ab initio calculations using various possible mechanisms for the surface chemistry. In the latter, the surface growth rate becomes a function of the local values of certain gas phase species concentrations and

Table I

Series of Experiments Completed During the First Year of AFOSR Program

Reactants	Initial Concentrations
Toluene	1%
Benzene	1.1%
Benzene/oxygen	1.1/0.22%
Benzene/oxygen	0.11/0.022%
Benzene/oxygen	1.1/1.1%
Dicyclopentadiene	0.125%
*Acetylene/ethene	1.1/2.2%
*Acetylene/ethene	0.125/0.25%
*Toluene/methanol	1.0/0.15%
*Toluene/hydrogen	1.0/3.1%
*Methylcyclohexane	1%
*Methanol	4%
*Natural Gas/oxygen	4/1%
*Methane/oxygen	4/1%
*Cyclopentadiene	1.4%
*Cyclopentadiene	0.1%

* Performed under corporate sponsorship

Table II

Series of Experiments Completed During the Second Year of AFOSR Program

Reactants	Initial Concentrations
CPD^{+}/oxygen	1.4%/0.91%
CPD/oxygen	0.1%/0.065%
CPD/benzene	1.4%/0.4%
CPD/benzene	0.1%/0.03%
CPD/biacetyl	1.4%/0.35%
CPD/biacetyl	0.25%/0.062%
CPD/acetylene	1.4%/1.05%
CPD/acetylene	0.14%/0.105%
Benzene/hydrogen	1.1%/3.3%
Benzene/hydrogen	0.335%/1%
*Methane/oxygen	4%/0.5%
*Methane/oxygen	0.6%/0.075%
*Toluene/oxygen	1%/1%
*Toluene/oxygen	0.255%/1%
*Heptane	1%
*Heptane	0.1%
*Heptane/oxygen	1.0%/0.5%
*Heptane/oxygen	0.1%/0.05%

+cyclopentadiene

* performed under corporate sponsorship

Table III

Series of Experiments Completed During the Third Year of AFOSR Program

Reactants	Initial Concentrations
*Heptane/toluene	0.9/0.1%
*Heptane/toluene	0.09/0.01%
*Ethylene	3.5%
*1,3-Butadiene	1.75%
*1,3-Butadiene	0.175%
*Benzene	1.1%
*Benzene	0.11%
*Penten-3-yne	1.4%
*Biacetyl/nitric oxide	0.1/0.5%
*Biacetyl/nitric oxide	0.01/0.05%
*Biacetyl/nitrogen	0.1/0.5%
*Toluene	1.%
*Norbornadiene	1.%

* Performed under corporate sponsorship

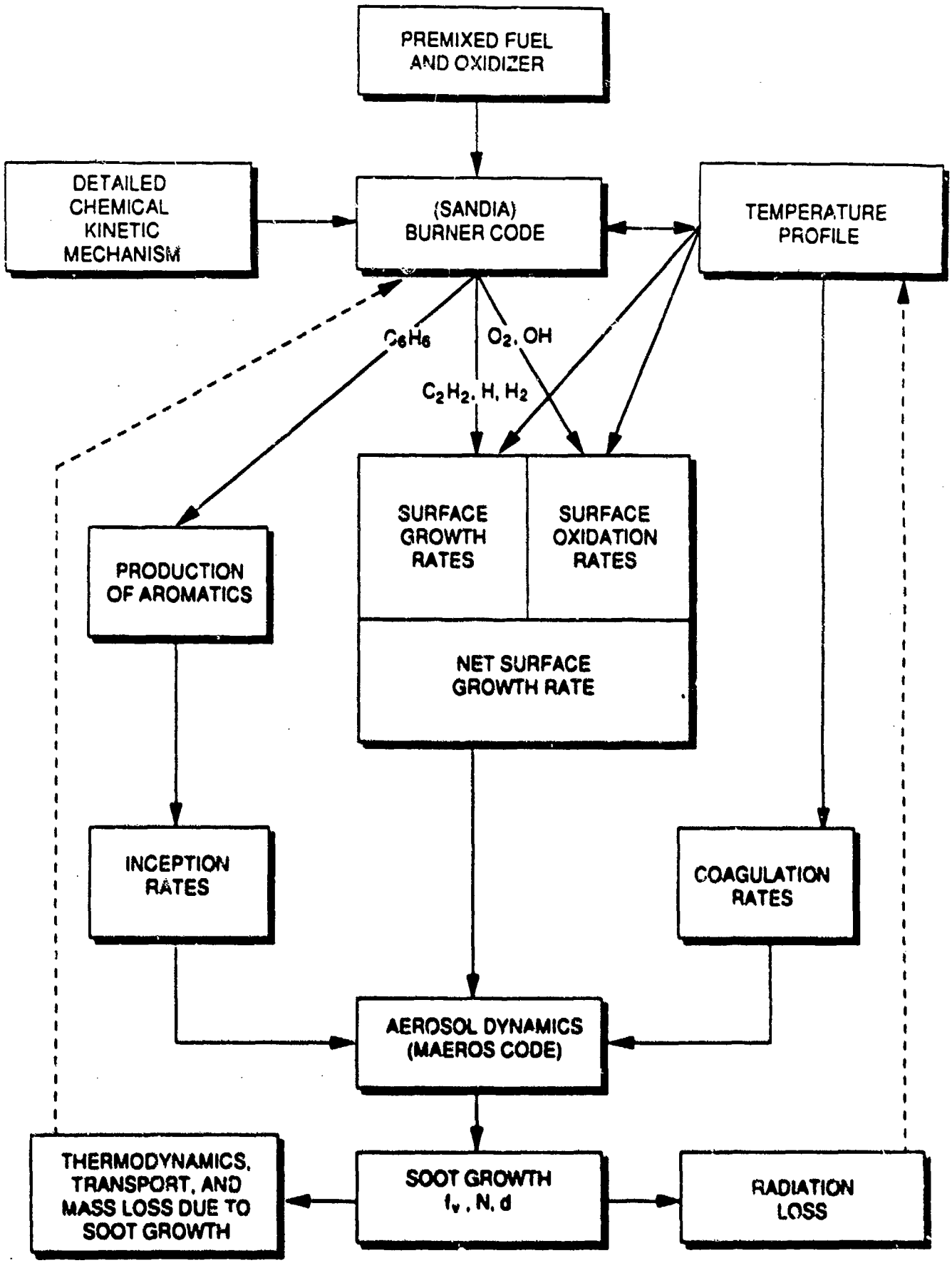

Figure 1: A Soot Growth Model for a Premixed, Laminar Flame.

the gas temperature. Adjustments have been made to rate constants for some reactions in order to improve agreement with experiment. Such adjustments, however, were made within the bounds of uncertainty associated with the rates, and the overall mechanisms are presented only as possible explanations for observed growth rates. Detailed comparisons have been made with various flame data by using experimental temperature profiles and calculating profiles of species concentrations needed for the inception rate and surface growth/oxidation calculations. Five separate models for surface growth were examined, including the Frenklach and Wang proposal (1990) and that by Harris and Weiner (1983). Most of the models appear to overestimate soot production high in the flames. This overestimation is undoubtedly due to the fact that none of the mechanisms include effects due to particle ageing. Recent suggestions that decay of H-atoms is the cause of this 'ageing', although plausible, are inadequate because of differences between the spatial (or temporal) dependence of the decay in the H-atom profiles and the fall-off in specific growth rates observed in laboratory flames. Among the various models for the soot surface growth, best overall agreement is obtained with a modified form of the approach taken by Frenklach and Wang. As shown in Fig. 2, model calculations are compared to experimental data for four separate flames: three ethylene flames at atmospheric pressure with varying carbon to oxygen ratios which were examined by Harris and Weiner (1983) and one low pressure acetylene flame studied by Bockhorn, Fetting and Wenz (1983). The figure shows that soot production is predicted reasonably accurately over a range of about two orders of magnitude in soot volume fraction.

The procedure described in Appendix A is highly efficient; accurate soot volume fraction calculations can be obtained with only a few growth equations. While various aspects of this simple model can be challenged, it yields agreement with experiment that is comparable to that obtained using more elaborate models.

The alternative mechanism referred to above (and as MODFW within Appendix A) avoids the assumption of a high temperature steric factor, yet reproduces growth profiles while also providing a 'linear' df_v/dt vs. f_v relationship. Limitations were found with the Frenklach and Wang mechanism in that it does not properly describe the stoichiometric dependence observed in the Harris and Weiner flames, and the temperature dependence of this mechanism seems to be above 50 kcal/mole while experimental evidence supports 20 to 35 kcal/mole. The very simple Harris and Weiner expression describes the stoichiometric variations well and also predicts soot production in the acetylene flames when the high temperature steric factor (as used in the Frenklach and Wang mechanism) is also used. Sensitivity analyses have been performed for parameters such as temperature, oxidation, number of size classes, sticking coefficients, inception rates, and coalescence of low molecular weight polyaromatic hydrocarbons. Each of these can have a significant effect on predictions of soot concentration depending on specific flame conditions. Details of the sensitivity results are provided in the appendix.

A radiative power loss term has also been incorporated into the soot growth model. At the wavelengths of importance in thermal radiative emission the soot particles will be in the Rayleigh range, and thus the emission coefficient (equal to the absorption coefficient by Kirchoff's Law) will be proportional to the volume fraction. If the soot index of refraction dispersion is ignored, and if the flame is optically thin, the net rate of radiative power loss per unit volume will be proportional to the product of volume fraction and the fifth power of temperature. With a specified temperature distribution, and the calculated soot volume fraction, this analysis makes it possible to calculate the integrated power loss due to radiation. In future work, the power loss term will be included in the energy equation for counterflow diffusion flames, making it possible to calculate the depression of temperature due to radiation, and any coupling effects between radiation and temperature-dependent processes governing chemical kinetics and soot growth. Using this analysis technique, we estimate that for the C/O=0.96 flame of Harris and Weiner, about 20% of the chemical energy

Figure 2

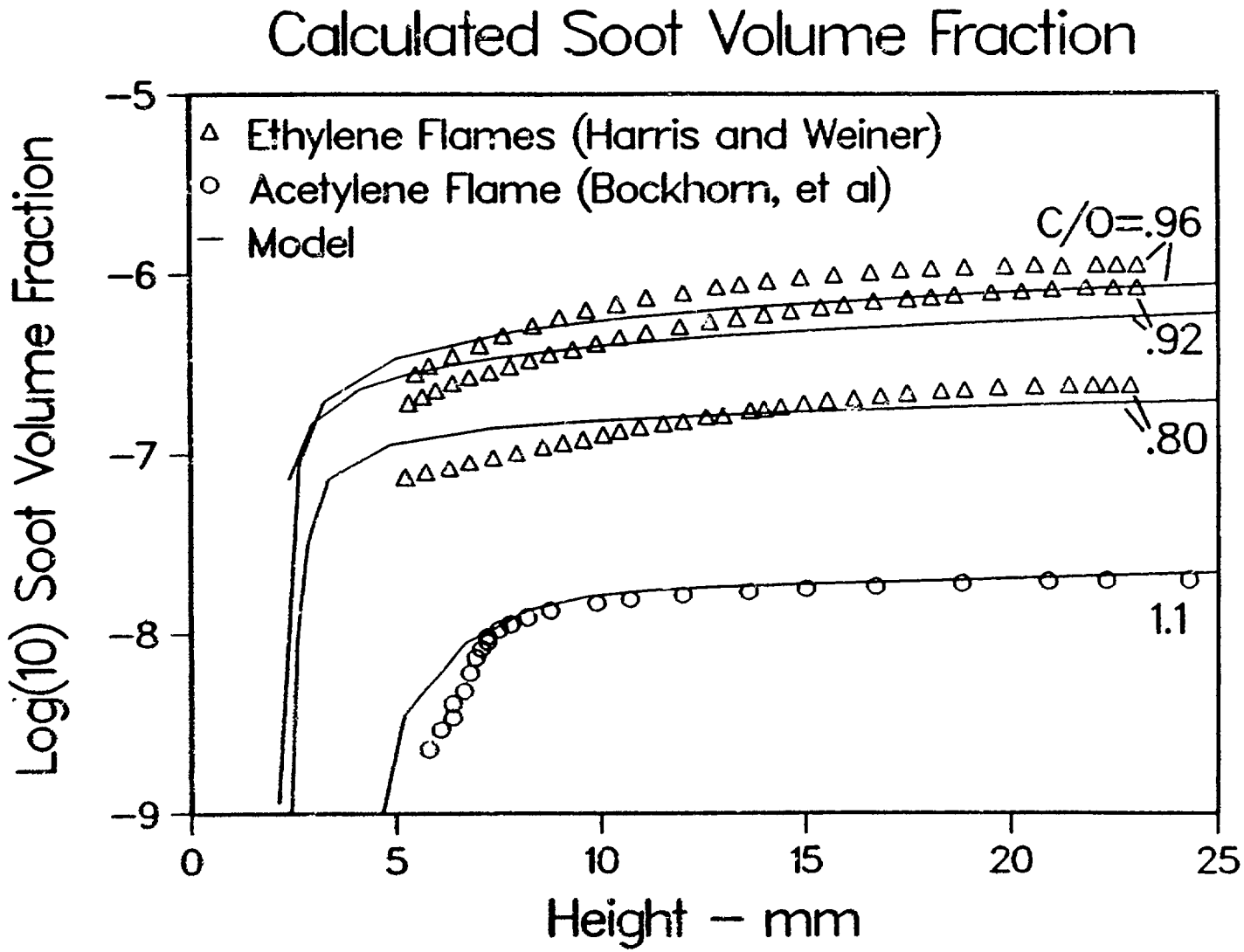
Calculated Soot Volume Fraction
Ethylene Flames (Harris and Weiner)
Acetylene Flame (Bockhorn, et al)
Model
C/O=.96
.92
.80
1.1
Log(10) Soot Volume Fraction
−5
−6
−7
−8
−9
0
5
10
15
20
25
Height − mm

produced in the fuel-rich flame (based on observed products) is lost to radiation from soot particles. If the remaining species are fully oxidized to carbon dioxide and water, then the radiative energy (from soot) amounts to nearly five percent of the total heat released. These percentages support arguments and efforts to include the effects of radiation in flame modeling.

B. Cyclopentadiene Decomposition

A difficulty in describing the decomposition of cyclopentadiene is that the primary radical, formed after loss of a weakly-bound H-atom, is the cyclopentadienyl radical whose stability is enhanced by resonance. As shown in Fig. 3, high concentrations of this radical can be produced without substantial decomposition of the ring, as indicated by the production of low molecular weight species shown in Fig. 4. A mechanism for cyclopentadiene pyrolysis (used in this prediction) was presented in the abstract to the Eastern Section meeting and was based in part on an analysis of the reverse of a process suggested by Dean (1990) for the addition of allyl radicals to acetylene (see Fig. 5). This mechanism was important since it helped to describe at least some of the methane produced during the pyrolysis (see Fig. 4). An enhancement to this mechanism was also identified and presented at the Eastern Section Meeting (although not included in the abstract). If H-atoms add to cyclopentadiene at the two (rather than the three) position, then the resulting adduct can readily decompose into a 1,3-pentadien-5-yl radical whose stability is enhanced through resonance. This radical should have a long lifetime and reach high intermediate concentrations. H-atom addition to this radical as shown in Fig. 6 can lead to production of methyl radicals and butadienyl radicals. Butadienyl can either abstract a weakly held H-atom from cyclopentadiene or decompose into acetylene and vinyl radicals, and the latter could easily produce ethylene under conditions of these experiments. Consequently, this additional sequence could explain the additional formation of methane which was underpredicted by the old model and describe the production of butadiene and ethylene as well. We plan to complete modeling of this system shortly and submit the results to the Twenty-Fourth International Symposium on Combustion.

Figure 3

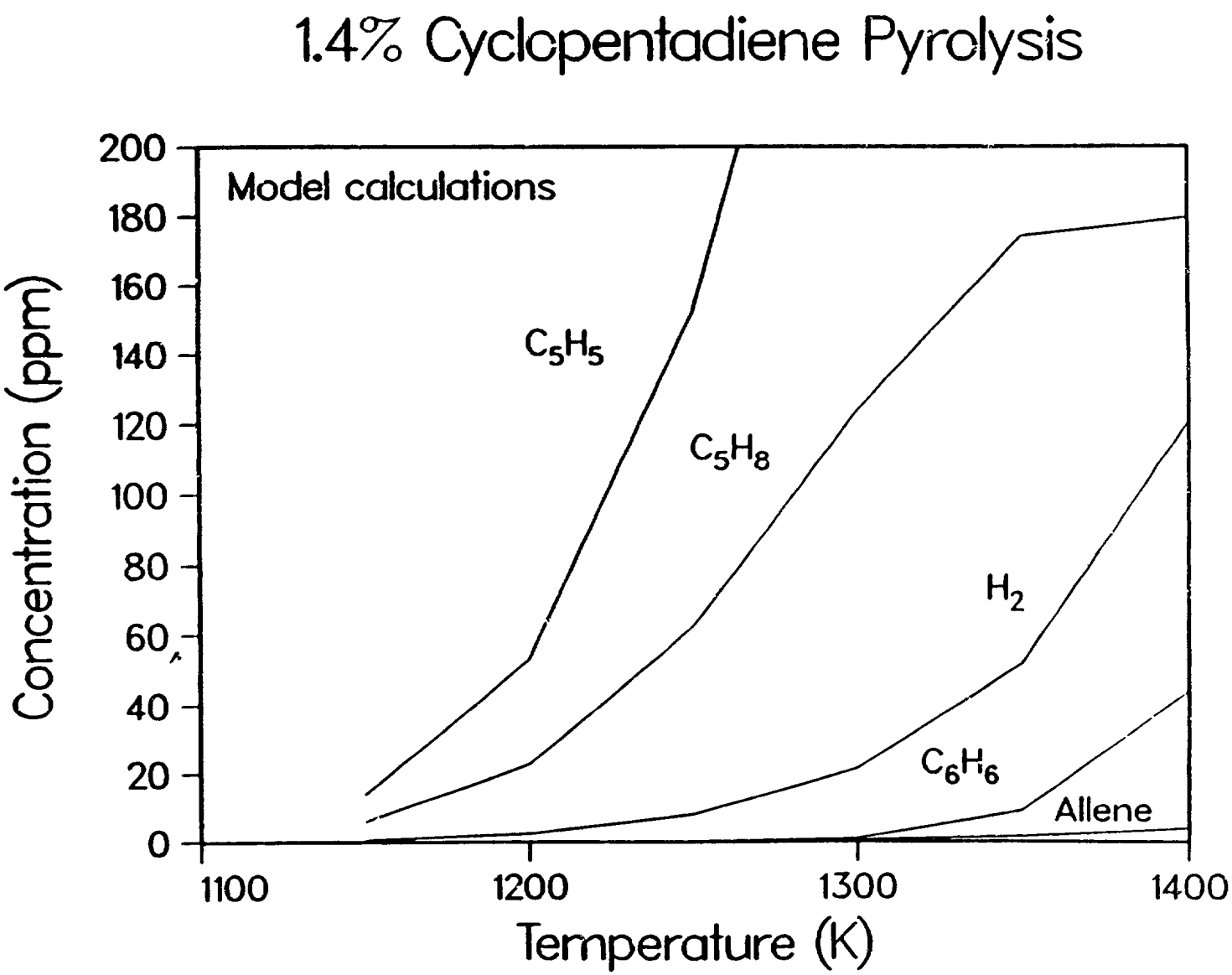
1.4% Cyclopentadiene Pyrolysis
Model calculations
C_5H_5
C_5H_8
H_2
C_6H_6
Allene
Concentration (ppm)
200
180
160
140
120
100
80
60
40
20
0
1100
1200
1300
1400
Temperature (K)

Figure 4

1.4% Cyclopentadiene Pyrolysis

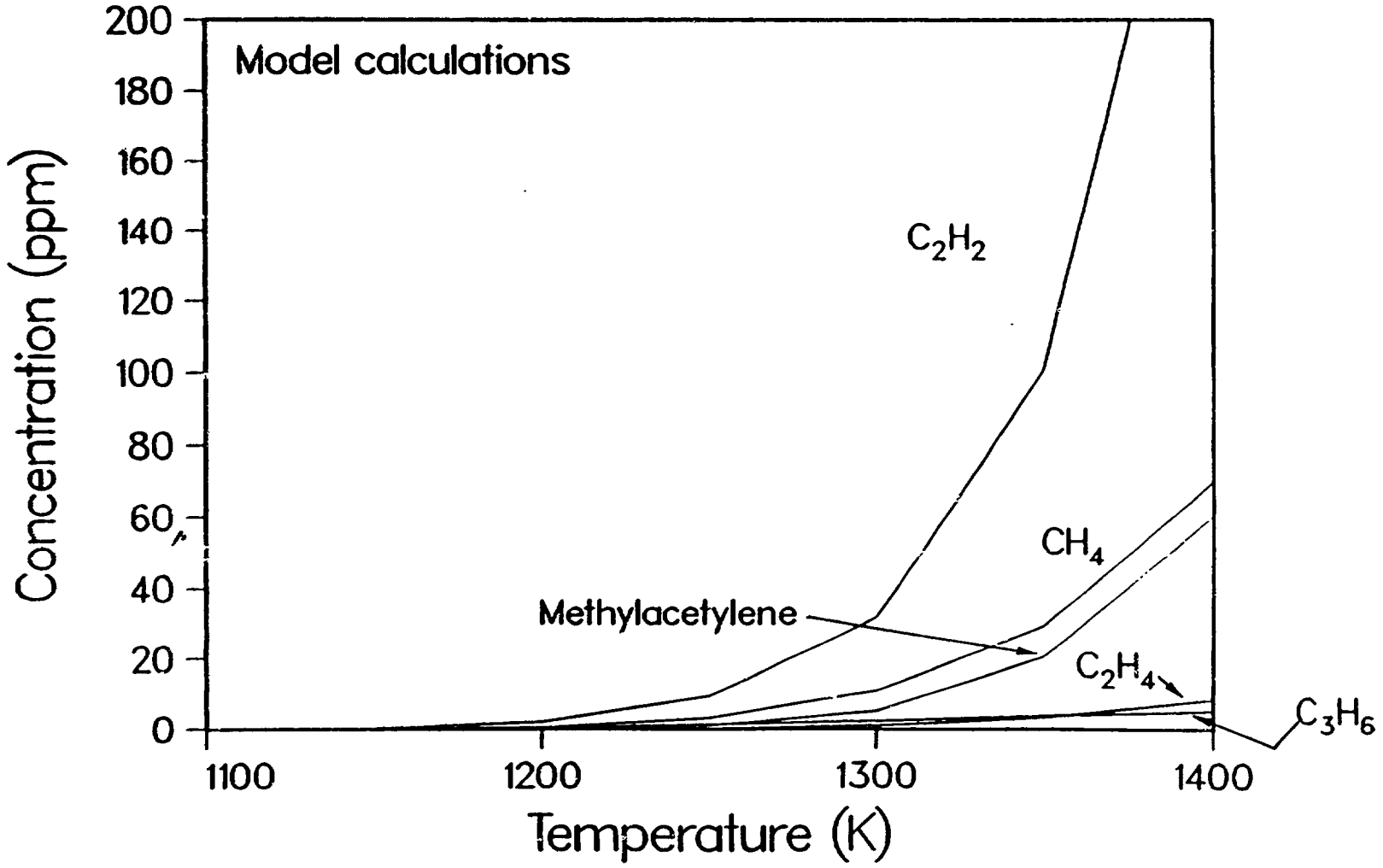

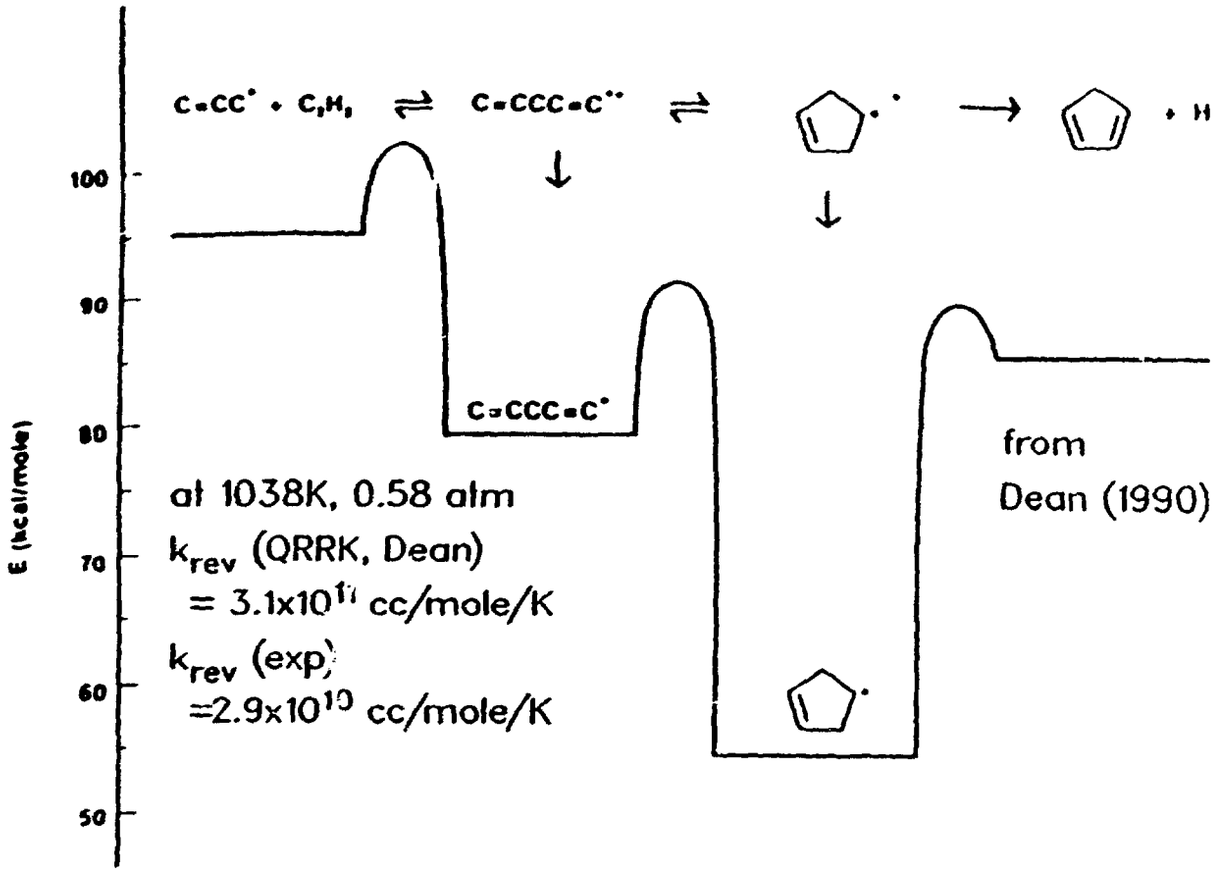

Figure 5 Potential energy diagram for the addition of allyl radical to acetylene, illustrating the possible pathways for reactions of the intermediates.

Figure 6

POTENTIAL ENERGY DIAGRAMS of 1,3-PENTADIEN-5-yl

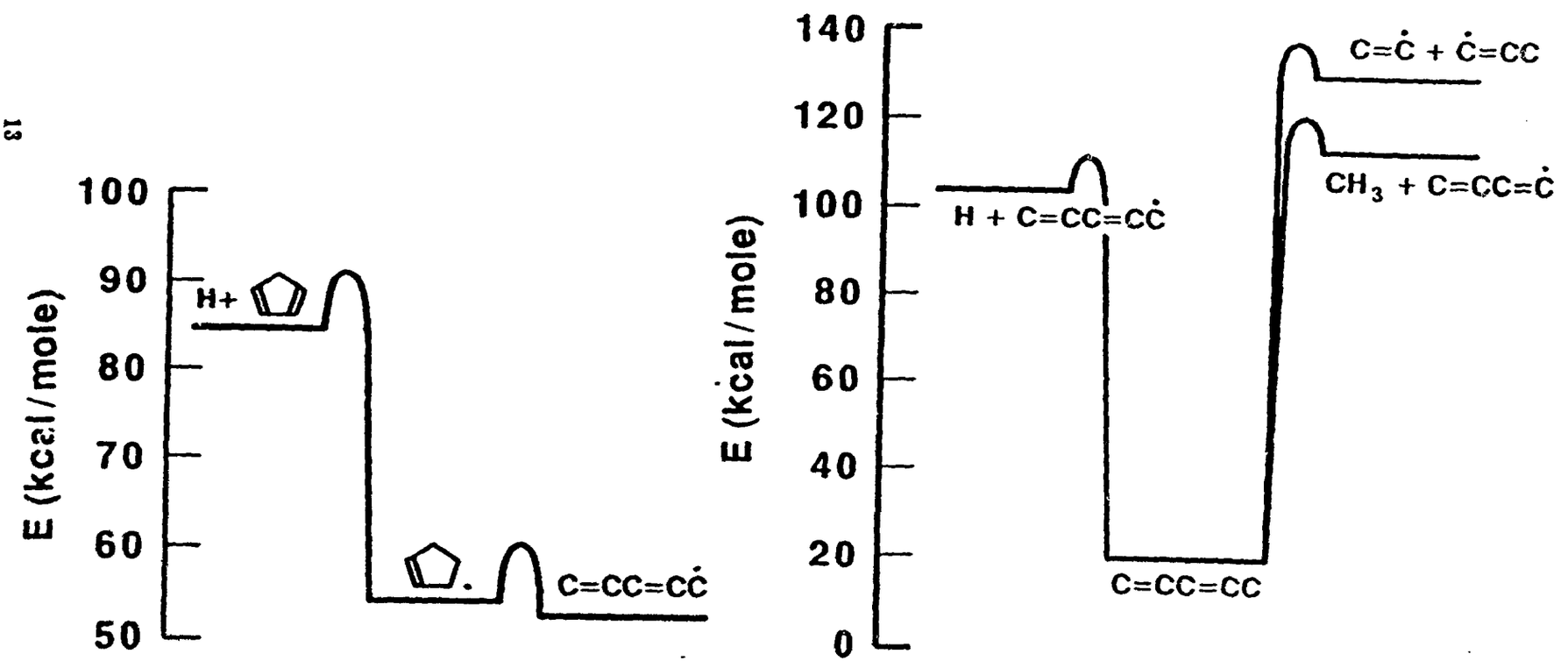

RC3145TX.001

IV. List of Publications

three year summary

A paper entitled "The Pyrolysis of Acetylene Initiated by Acetone" by M. B. Colket, H. B. Palmer and D. J. Seery has been published in Combustion and Flame, Vol. 75, pp. 343-366, 1989. This work was initiated under contract F49620-85-C-0012, and revisions to the manuscript were performed under this contract. A reprint of the manuscript was provided in the first annual report for this contract.

A four page abstract entitled "Simplified Models for the Production of Soot in a Premixed Flame" by R. J. Hall and M. B. Colket was published in Chemical and Physical Processes in Combustion, Paper no. 58, October, 1989.

An article entitled "Shock Tube Pyrolysis of Pyridine" by J. C. Mackie, M. B. Colket, and P.F. Nelson has been published by the Journal of Physical Chemistry, Vol. 94, No. 10, pp. 4099-4106, 1990. A copy of the manuscript was included in the first annual report for this contract. The research was performed under corporate sponsorship.

A four page abstract entitled "The Pyrolysis of Cyclopentadiene" by M. B. Colket was published in Chemical and Physical Processes in Combustion, Paper no. 1, December, 1990. A full paper based on this work will be submitted to the Twenty-Fourth Symposium on Combustion. A copy of the abstract is provided in Appendix B.

A manuscript entitled "Shock Tube Pyrolysis of Pyrrole and Kinetic Modeling" by J. C. Mackie, M. B. Colket, P. F. Nelson and M. Esler has been accepted by the International Journal of Chemical Kinetics for publication. A copy of the manuscript was included in the second annual report of this contract. The research was performed under joint sponsorship from UTRC and the University of Sydney.

A reply (to a comment) entitled "On Impurity Effects in Acetylene Pyrolysis" by M. B. Colket, H. B. Palmer and D. J. Seery has been published in Combustion and Flame, Vol. 84, pp. 434-437, 1991. A reprint of this article is provided in Appendix D.

A four page abstract entitled "A Soot Growth Mechanism Involving Five-Membered Rings" by M. B. Colket and R. J. Hall has been submitted to the Eastern Section of the Combustion Institute for publication in Chemical and Physical Processes in Combustion, October, 1991. A copy of this abstract is provided in Appendix C.

A manuscript entitled "Description and Discussion of a Detailed Model for Soot Formation in a Laminar, Premixed Flame" has been written. The manuscript has been assigned a UTRC report number (UTRC91-20) and decisions regarding the publication medium will be made shortly. A copy of the entire manuscript is included in Appendix A.

V. Meeting Interactions and Presentations

three year summary

1. Eastern Section of the Combustion Institute, Clearwater Beach, Dec. 5-7, 1988. M. Colket presented an invited talk entitled "The Role of Oxidative Pyrolysis in Preparticle Chemistry".

2. A round table discussion on "Current Problems in Soot Formation During Combustion, Especially the Mechanism of Soot Formation" was held in Göttingen, West Germany on March 29-30, 1989. The meeting was organized by Professor H. Gg. Wagner and was attended by about twenty engineers/scientists currently involved with understanding soot formation phenomena. Financial support was provided by the Commission for Condensation Phenomena of the Academy of Sciences in Göttingen, West Germany.

3. A paper entitled "Simplified Models for the Production of Soot in a Premixed Flame" by R. J. Hall and M. B. Colket was presented at the Eastern Section of the Combustion Institute on October 30th - November 1st, 1989. The meeting was held in Albany, New York.

4. Department of Energy - Office of Basic Energy Sciences Combustion Research Meeting held at Lake Geneva, Michigan, June 1-3, 1988. M. Colket was invited by W. H. Kirchhoff to be an observer and participant at this D.O.E. contractor's meeting. The meeting was attended under corporate sponsorship.

5. Brookhaven National Laboratory, Upton, New York, November 9, 1989. M. Colket presented an invited seminar entitled "Kinetic Mechanisms for the Pyrolysis of Unsaturated Hydrocarbons". Financial support provided by BNL.

6. Department of Energy - Office of Basic Energy Sciences Combustion Research Meeting held at Hofstra University on Long Island, June 7-9, 1989. M. Colket was invited to be an observer and participant at this contractor's meeting. The meeting was attended under corporate sponsorship.

7. M. B. Colket presented an invited lecture entitled "Progress Towards Understanding Soot Formation and Development of Global Models" to the Diesel Cooperative Meeting held at United Technologies Research Center on May 17-18, 1990.

8. Under joint corporate and AFOSR sponsorship, M. Colket attended the Twenty-Third International Symposium on Combustion in Orleans, France, July 22-27, 1990 and presented a poster paper entitled "The Rich Oxidation of Ethylene in a Single-Pulse Shock Tube".

9. In January, 1991, M. Colket traveled to Yale University and held technical discussions with Professors L. Pfefferle and M. Smooke on subjects related to pyrolysis of hydrocarbons and modeling of soot formation in diffusion flames.

10. Department of Energy - Office of Basic Energy Sciences Combustion Research Meeting held at Lake Geneva, Michigan, May 29-31, 1991. M. Colket was invited to be an observer and participant at this contractor's meeting. The meeting was attended under corporate sponsorship.

11. M. Colket attended an ARO Particulates Conference entitled "Particulates in Heterogeneous Combustors" on June 12-13, 1991 in Boulder, Colorado.

12. R. Hall will present a poster paper entitled "Aerosol Dynamics of Soot Particle Growth in Flames" at the 10th Annual Meeting of the American Association for Aerosol Research on October 7-11, 1991. (See abstract in Appendix E.)

VI. References

H. Bockhorn, F. Fetting and H. W. Wenz, *Ber. Bunsenges. Phys. Chem.*, 87:1067, (1983).

M. B. Colket, R. J. Hall, J. J. Sangiovanni, and D. J. Seery, "The Determination of Rate-Limiting Steps During Soot Formation", Annual Reports to AFOSR, under Contract No. F49620-88-C-0051, UTRC Report nos. 89-13 and 90-23, April, (1989) and June 8, (1990).

M. Frenklach and H. Wang, *Twenty-third Symposium (International) on Combustion*, The Combustion Institute, p. 1559, July, (1990).

S. J. Harris and A. M. Weiner, *Combust. Sci. Tech.*, 31:155-167, (1983).

APPENDIX A

Description and Discussion of a Detailed Model for Soot Formation in a Laminar, Premixed Flame

DESCRIPTION AND DISCUSSION OF A DETAILED MODEL FOR SOOT FORMATION IN LAMINAR, PREMIXED FLAMES

by

Meredith B. Colket, III and Robert J. Hall
United Technologies Research Center
East Hartford, CT 06108

UTRC Report No. UTRC91-20

August 9, 1991

Abstract

A model for soot formation in laminar, premixed flames is presented. The analysis is based on a simplified inception model, detailed kinetic calculations of soot surface growth, and coalescing particle collisions. A sectional aerosol dynamics algorithm which involves solving a master equation set for the densities of different particle size classes provides an efficient solution scheme. The calculation of surface growth and coalescence sectional coefficients has been simplified and extended to the entire temperature range of interest in flame simulations. In order to test convergence properties, the former geometric limitation on the number of size classes has been relaxed. Convergence of the soot volume fraction typically requires only a few size classes and balance equations. Several possible soot surface growth models have been compared. The inception and surface growth models require profiles of temperature and important species like benzene, acetylene, and hydrogen atoms, and oxidizing species. Extensive comparisons have been made with well-characterized flame data by using experimental temperature profiles and calculating the concentrations of the important species with a burner code. Excellent agreement has been obtained with experimental species profiles where data are available. The calculated species concentrations and surface growth/oxidation rates are input to the aerosol dynamics program, which calculates the evolution of various soot size and density parameters. While aspects of the model are highly simplified, on balance it appears to give agreement with experiment that is comparable to that obtained from more elaborate models. The calculated sensitivity of soot growth to temperature and the important inception and coalescence parameters is discussed.

Introduction

Many of the effects of soot formation in flames have been listed and discussed in detail in a great number of technical and review papers (Wagner, 1979; Haynes and Wagner, 1981; Glassman, 1988; Smith, 1981; and Barfknecht, 1983). These articles have discussed effects on pollutants (including carcinogenic processes), plume visibility, component lifetimes, and radiation. More recently as computer and flame modeling capabilities have advanced, the importance of soot formation to flame modeling has also been recognized.

The most obvious and acknowledged flame process affected by soot is radiation which can lead to substantial fractions of energy lost from the immediate flame environment (Bhattacharjee and Grosshandler, 1988; Kennedy, et al., 1990). Twenty percent energy loss due to radiation is not atypical for a coflowing sooting diffusion flame (Hall and Bonczyk, 1991). This energy loss leads directly to a temperature reduction (and therefore affects kinetics of pollution formation), a change in density (and local gas velocity), as well as reductions in flame length.

A secondary and often unrecognized phenomenon is the effect on flame thermochemistry and kinetics. The thermochemistry of soot formation and oxidation can dramatically affect the heat release profile in a flame. The conversion of alkanes, for example, to acetylene (a principal soot intermediate) is nearly one-fifth as endothermic as the oxidation process is exothermic. Thus, a strongly endothermic process can occur just inside the flame front to form soot. The soot may be transported to another region and oxidized. The oxidation rates of soot particles are dramatically different than those of gas-phase species. Local flame temperatures may be lowered in order to provide energy to drive the endothermic soot forming reactions. This process is also strongly dependent on fuel-type and often has not been considered by researchers addressing fuel-type effects on soot formation. The importance of the thermochemistry of fuel components is dramatically demonstrated in the recent analysis of Smooke, et al. (1990). Their model indicates the existence of a region of negative heat release just below the apex of a coflowing diffusion flame! This effect is attributed principally to the strongly endothermic reaction, $2CH_4 \rightleftharpoons C_2H_2 + 3H_2$.

We believe that the modeling of practical (soot-containing) flames will be highly inaccurate without predictions of soot formation as part of the flame modeling process. Further support for modeling efforts comes from the more commonly recognized deleterious effects of soot formation, such as pollution, hardware lifetimes, and plume visibility.

Consequently, over the past several years, we (Colket, et al., 1989, 1990; Hall and Colket, 1989) have been developing a procedure for calculating soot production in one-dimensional laminar, premixed flames. These procedures have similarities with techniques examined at other laboratories (Frenklach and Wang, 1990; McKinnon, 1989; Mckinnon and Howard, 1990). It is a hope that these or similar procedures could be used for predicting soot in more complex flame systems. Although there are limitations and uncertainties with the developed code, it also is quite versatile and is quite successful in predicting soot production from several different laboratory flames. A detailed description of the calculation procedure is provided in this manuscript as well as a discussion of the principal assumptions, successes, and uncertainties. Despite the uncertainties, we feel that the code in its present form is a useful tool for evaluating the controlling soot formation processes in different flames and for providing valuable understanding to the many interrelated and competitive processes of soot formation.

One of the important issues discussed in this manuscript is that of particulate inception. Kennedy, Kollman, and Chen (1990) recently found that soot production in a coflowing laminar, diffusion

flame was nearly independent of the rate assumed for particle inception; however, several studies in the early 1980's indicated that the amount of soot production varies nearly linearly with particle inception. Indeed, much of the work on hydrocarbon pyrolyses and aromatic growth processes was motivated by this assumption. Consequently, the recent results of Kennedy, et al., if true, could dramatically simplify soot modeling efforts. As part of this study, we have varied the inception rate for several flames in order to determine its importance in premixed, laminar flames.

The soot formation model is sufficiently versatile that the sensitivity of soot production to a variety of flame parameters can easily be examined. These studies are described in the manuscript in order to provide the reader with some understanding of the successes and limitations of soot formation modeling.

Brief Description of Model

A flow chart of the model used to describe soot formation processes is provided in Fig. 1. Dashed lines are used for portions of the code which have not yet been implemented. The model couples detailed chemical kinetics calculations of gas-phase processes with mechanisms for particle surface growth, oxidation, and agglomeration. MAEROS, a widely-used aerosol dynamics code (Gelbard, 1982), has been modified for the latter part of the analysis.

The soot growth/aerosol dynamics program is based on a sectional representation of the growth equations with provision for inception source terms, surface growth through condensible vapor deposition, and coagulation. The program has been modified in a number of ways for the soot growth problem. Its temperature range capabilities have been extended to the full range of interest in combustion problems by a reformulation of the surface growth and coalescence sectional coefficient calculations. Provision for oxidizing vapors (oxygen and hydroxyl radicals) has also been made. The simulations require as input profiles of temperature, aromatics (C_6H_6), condensible (C_2H_2) and oxidizing vapor concentrations (OH and O_2), and the concentrations of other flame species (such as H-atoms and H_2). The input of the aerosol dynamics program has been made compatible with the output of the Sandia premixed, laminar flame program (Kee, et al., 1985, 1989). The facility to exclude small mass spheroids from coagulative processes has also been added. The code also calculates the radiative energy loss from soot assuming optical thinness and neglecting soot refractive index dispersion.

In the present version of the model, the (mass) rate of particle inception is equated to the rate of formation of benzene (as mass of carbon atoms). The model is not limited to this assumption but, as will be seen, the results obtained using this simple, provisional assumption may on balance be just as good as those presently obtainable from more elaborate calculations of the inception species, given the uncertainties presently associated with the latter. As additional information becomes available, this assumption may be modified as required.

Acetylene is assumed to be the surface growth species. The growth rate has been calculated using the Harris-Weiner value (1983a), the Frenklach-Wang expression (1990), as well as several other steady-state expressions. Local values of acetylene and hydrogen atom/molecule concentrations as well as estimates of rate coefficients for certain kinetic processes are required for these calculations. Oxidation is assumed to be given by the Nagle and Strickland-Constable expression (1963), and oxidation by OH by a gas kinetic rate multiplied by a collision efficiency of 0.13 (Neoh, et al., 1981). Recent studies have shown that soot mass also grows by the addition of polyaromatic hydrocarbons. These processes are included in the present model since low molecular weight polyaromatic hydrocarbons are included in the total soot mass (according to the model used in this study) and

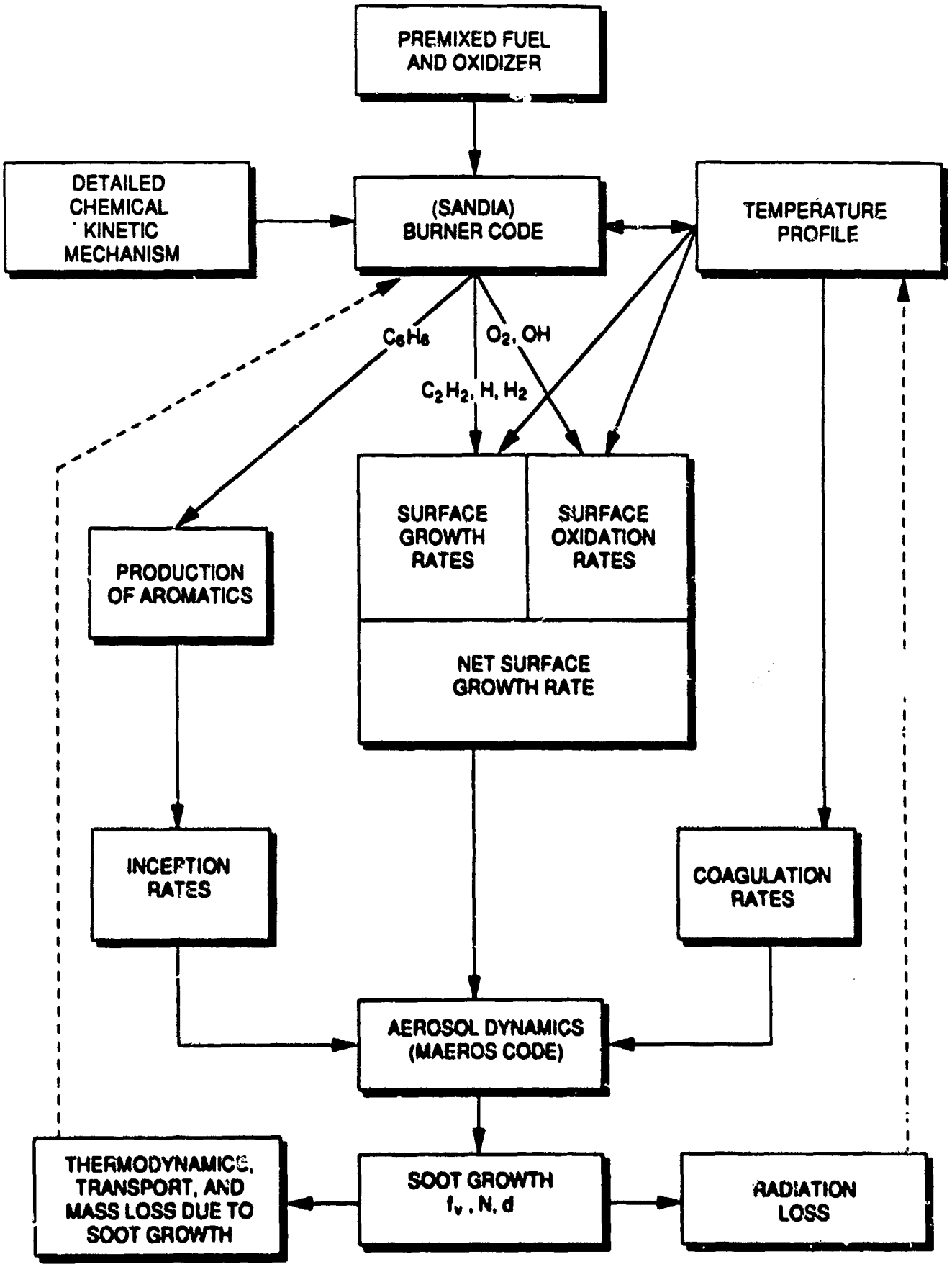

Figure 1: A Soot Growth Model for a Premixed, Laminar Flame.

91-7-33-1

these species are allowed to grow by acetylene addition as well as by coagulation with other 'soot' particles.

Modeling of Gas Phase Chemistry

In this investigation, extensive comparisons were made with the well-characterized, premixed, burner-stabilized flames examined by Harris and Weiner (1983a) and by Bockhorn, Fetting, and Wenz (1983). Concentrations of gas-phase species were calculated using detailed chemical kinetic models with CHEMKIN II (Kee, et al., 1989) and the SANDIA premixed flame code (Kee, et al., 1985). The purpose of these calculations is to determine concentrations of gas-phase species as a function of height above the burner. These data in turn are used to calculate inception rates and specific growth rates. Thus far, experimentally determined temperature profiles have been used; in general, a code could calculate the temperature profile once radiation, thermodynamics of soot formation, and burner effects are included in the model. Results from the kinetic modeling efforts are described in the following paragraphs. Since benzene has been assumed to be the incepting particle in the present calculations, the discussion is focused on the predictions of benzene profiles.

For the atmospheric pressure, $C_2H_4/O_2/Ar$ flames examined by Harris and Weiner (1983a), the kinetic code of Harris, Weiner and Blint (1988) was used with the addition of the reaction

$$C_3H_3 + C_3H_3 \leftrightarrow C_6H_5 + H \qquad (1)$$

Recently, this and related reactions have been found to contribute significantly to benzene formation in rich flames. The rate constant for Reaction 1 was 10^{13} cm^3/mole/sec (Miller and Melius, 1991) For the C/O = 0.92 flame, it contributes approximately 50% of the total formation of benzene (see Fig. 2). Without this reaction, we calculate a benzene profile lower than the data of Harris, Weiner and Blint (1988) as well as lower than their calculations (presumably due to a different set of thermodynamics for the higher hydrocarbons). Yet, we slightly overpredicted the experimental profile when Reaction 1 was added. Although we observed a factor of two difference in benzene profiles with and without Reaction 1, recent modeling efforts of Frenklach and Wang (1991) indicate that Reaction 1 has a negligible contribution. Presumably the difference is due to a difference in kinetics and thermodynamics related to the formation of C_3-species. In the present study, this reaction was included in all calculations. Calculated benzene, acetylene, and H-atom profiles are shown in Fig. 3 for the C/O = 0.96, 0.92, and 0.80 flames.

For the low pressure acetylene (0.12 atm) and propane (0.15 atm) flames studied by Bockhorn, Fetting and Wenz (1983), species profiles were calculated using a modified version of the kinetic code of Miller and Bowman (1989) with propane kinetics from Westbrook and Dryer (1984). (Numerical problems were encountered with the Harris kinetics.) The same ring-forming reactions used to model the Harris and Weiner flames were also included in this kinetic sequence. A sensitivity analysis on benzene formation in the acetylene flame indicates that its formation is principally dependent on chain branching and termination steps as well as on reactions linked to the formation and destruction of C_3H_3. These results support the recent findings in several studies (Miller and Melius, 1991; Communal, et al., 1990; and Stein, et al., 1990) regarding the significance of C_3-species to benzene formation in flames.

Calculated benzene profiles for the acetylene and propane flames are compared to the experimental values in Figs. 4 and 5. Peak benzene concentrations in the flame front are predicted fairly well by the kinetics model, as well as the qualitative decay and slow recovery downstream of the flames. Two obvious discrepancies are the location of the peak benzene concentrations and value of the minimum benzene concentration in the acetylene flame. These same discrepancies are also apparent in the

Figure 2

Benzene Formation in Premixed, Laminar Ethylene Flame (Harris and Weiner, 1983)

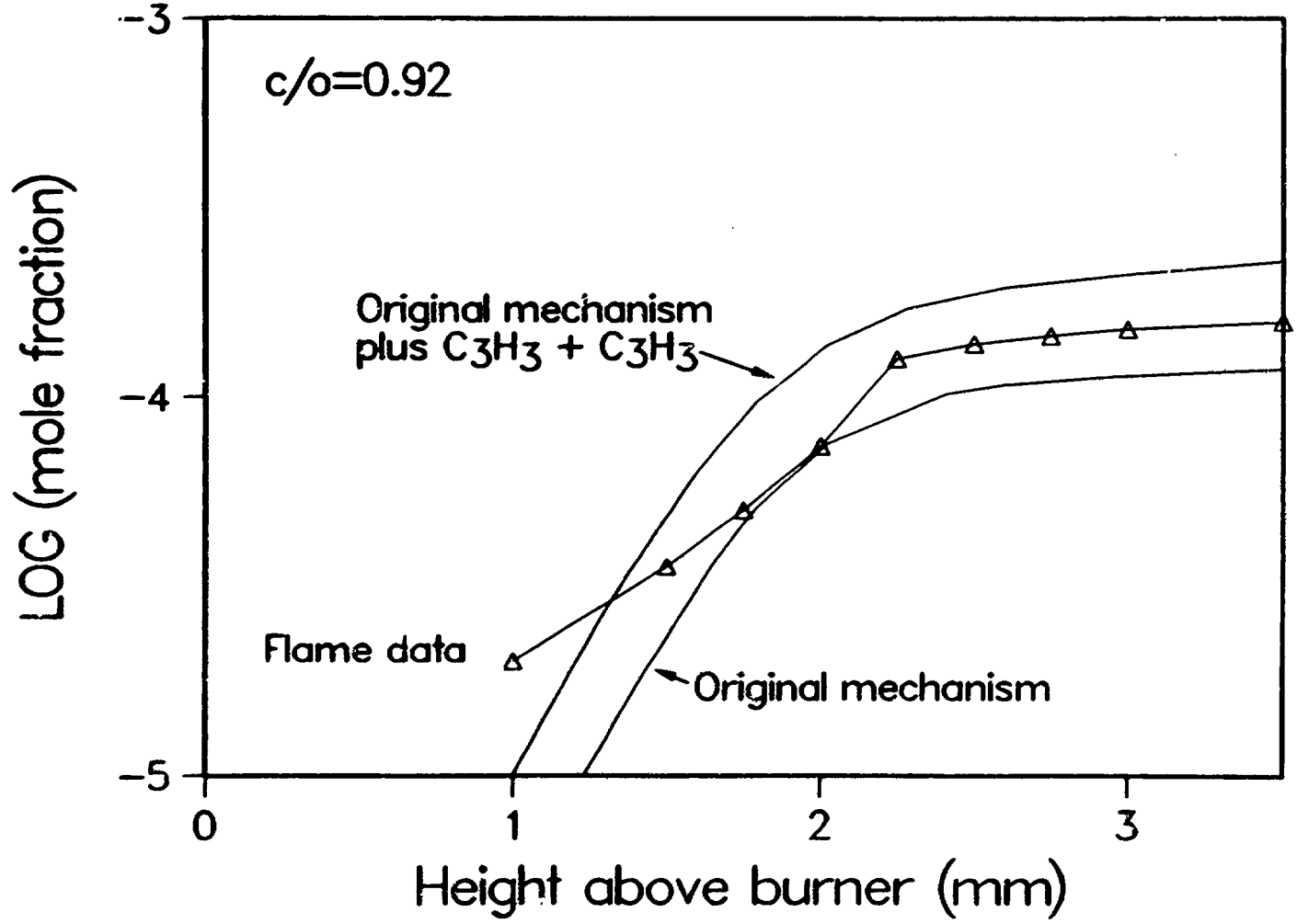

Figure 3

Calculated Species Profiles for Harris and Weiner Flames

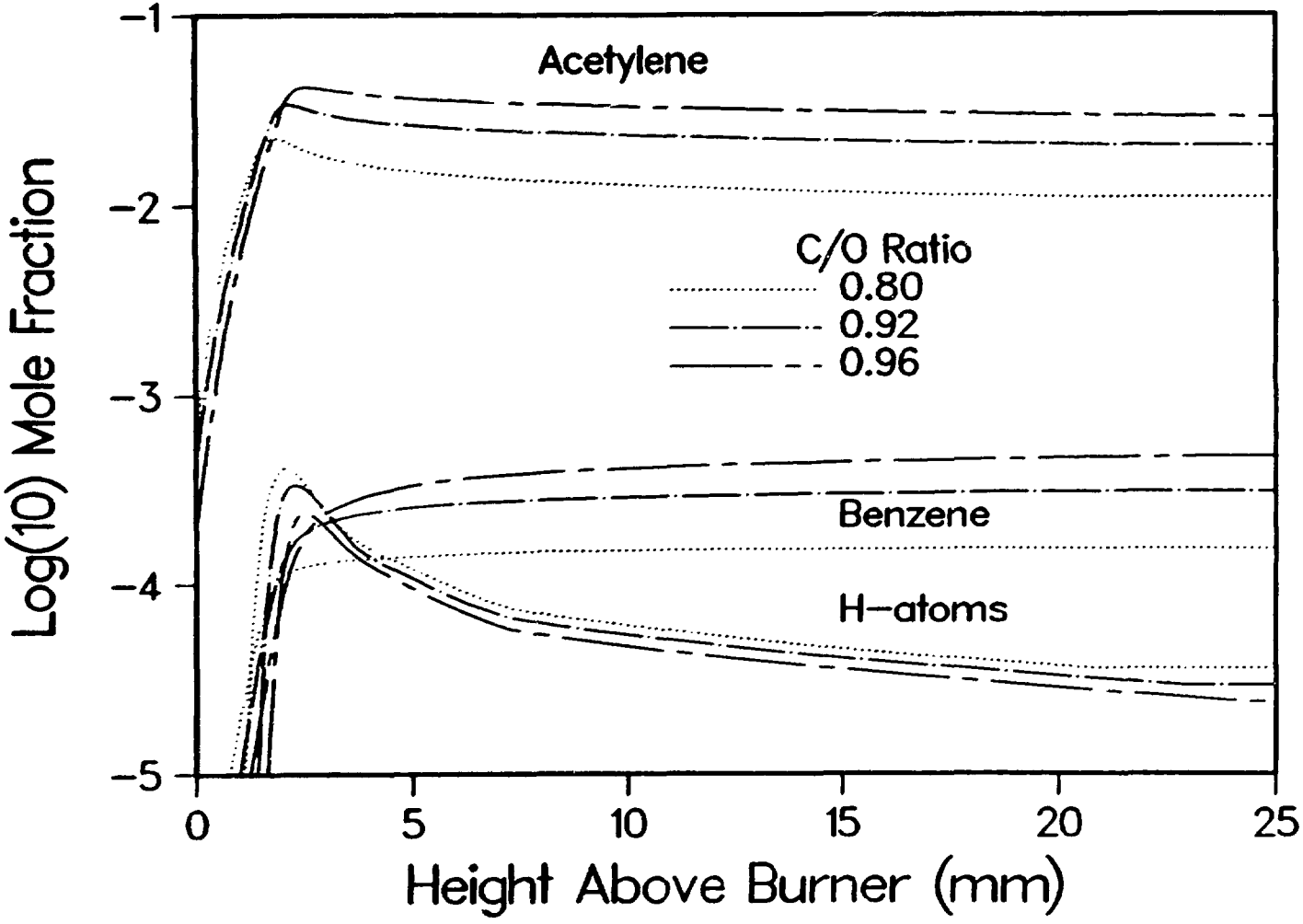

Figure 4

Comparison of Experiment and Kinetics Model for Acetylene Flame

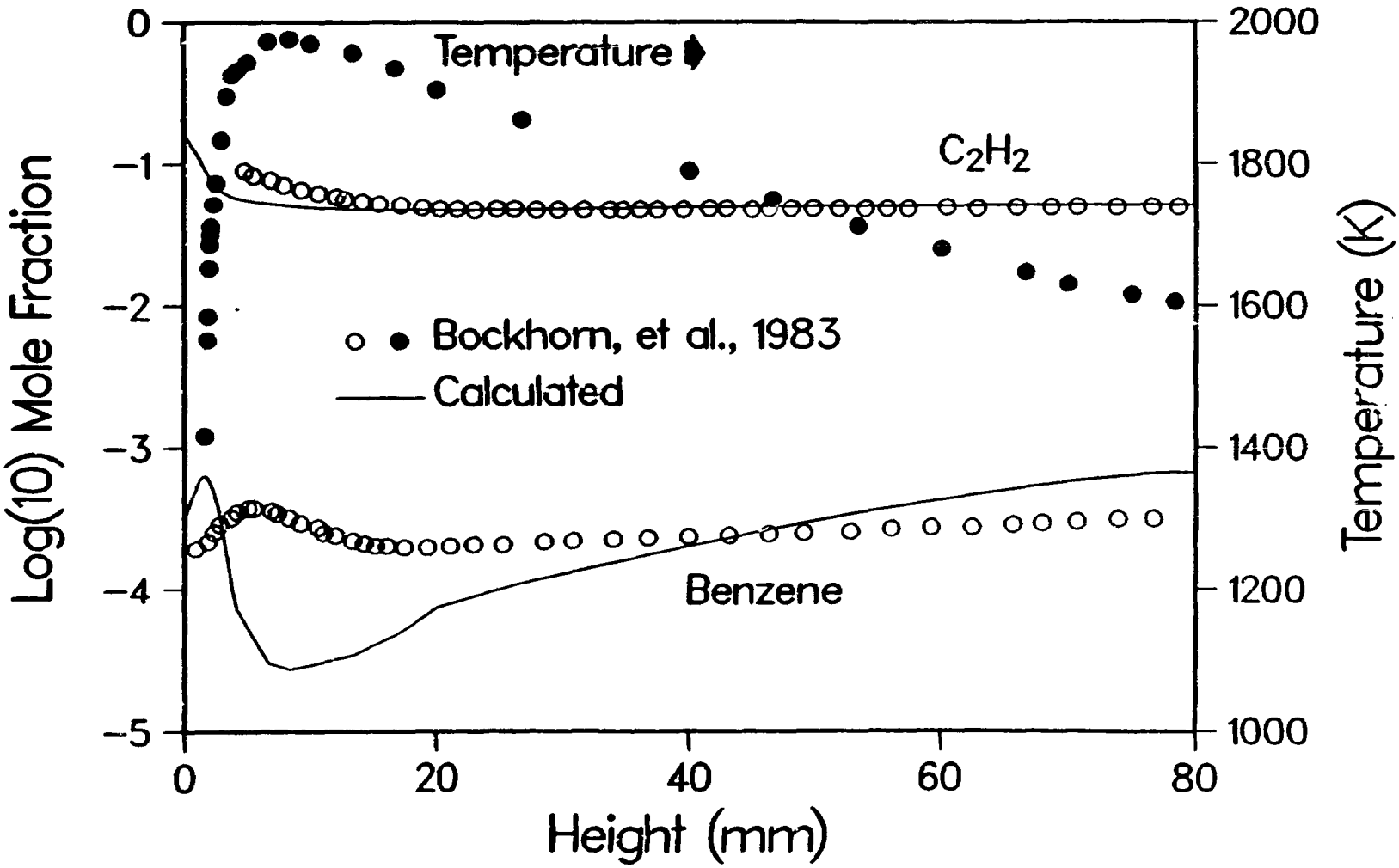

Figure 5

Comparison of Experiment and Kinetics Model for Propane Flame

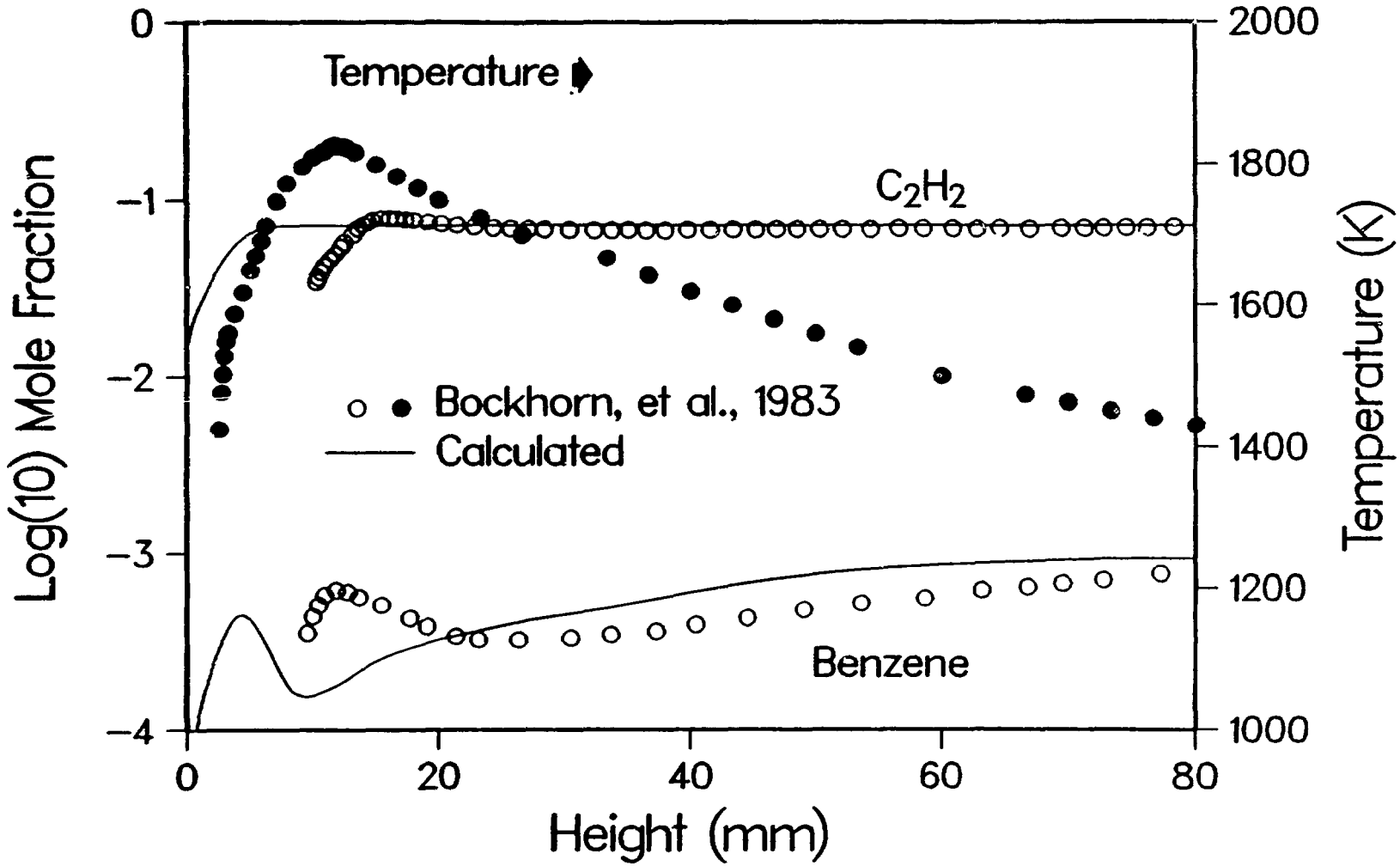

modeling work of Wang and Frenklach (1989), who modeled a slightly richer acetylene flame. Of interest to note is the location of the temperature peaks (See Figs. 4 and 5) for these two flames which nearly coincides with the benzene minimums in the calculated profiles. Since the kinetic model does not include the formation of high molecular weight species, the dramatic decay in the benzene concentration (and those for other low molecular weight aromatic species) is due to the fracturing of aromatic rings at elevated temperatures. This statement was confirmed by shifting the location of the peak temperature (in the model) and the calculated location of the minimum benzene concentration shifted correspondingly. This observation raises some questions about the internal inconsistency of the data reported by Bockhorn, et. al (1983), since the 'experimental' temperature peak occurs approximately 8 and 10 mm before the minimum in the experimental benzene profiles for the acetylene and propane flames, respectively. Bockhorn, et. al, state that disturbances from the sampling probe could shift profiles by as much as a few millimeters, but the shift observed seems larger. Another potential problem is that identified by Zabielski, et al. (1990) for porous plug burners in low pressure flames. They found that small, effective 'open' areas led to local velocities at the burner exit much higher than averaged velocities based on total burner areas. Thus, the early portion of the flame front can be altered from one in which lower velocities exist throughout. Significant differences in flame structure can result for different burners with the same mixture ratio, pressure, and flow rates. This effect is perhaps less important in the Bockhorn, et. al flames since hypo tubing was used in construction of the burner. Even so, we estimate the actual exit velocities are four to five times higher than an area-weighted average.

The inability of the kinetics model to predict accurately the benzene profile at elevated temperatures was examined. Overprediction of the amount of decomposition is particularly alarming since the kinetics model does not include decomposition routes associated with oxidative attack on the phenyl radical. Reductions in the rate constants for phenyl decomposition lead to virtually no change in the benzene profile, suggesting quasi-equilibrium might be controlling the benzene profile. Reduction in the peak temperature by 30K (for the acetylene flame) led to about a 20% increase in the benzene minimum for the acetylene flame. Since it is unlikely that the error in temperature is large enough to account for a difference of about an order of magnitude, we conclude that there may be some errors in thermodynamics (such as for l-C_6H_5 or C_4H_3) or uncertainties in the experimental data or some combination, thereof.

The inaccuracies in the predictions of the benzene minimum as well as its location are raised principally to point out that, in addition to uncertainties in the modeling efforts, there are difficulties and uncertainties in collecting the experimental data as well. Nevertheless, all species profiles as calculated were used in the subsequent soot modeling, except for the benzene profile in the acetylene flame, which was significantly underpredicted just after the flame front and slightly overpredicted higher in the flame. In this case, the experimental profile for benzene was used.

Simplified Inception Model: Justification, Motivation and Implications

In the aerosol dynamics simulations, the smallest size class is given a finite source rate, and is regarded as the inception species. This would ordinarily be a high molecular weight polyaromatic hydrocarbon. The present version of the model is based on the zero order assumption that the inception source rate can be approximated by that of benzene; that is,

$$S_i(t) = 6\, m_c\, N_a\, \frac{d[C_6H_6]}{dt} \qquad (2)$$

where m_c is the mass of a carbon atom and N_a is Avogadro's number. Frenklach and Wang (1990) have selected a model for inception which is physically much more realistic and have pointed out that the assumption used in the present study is unrealistic. While we appreciate its limitations,

we, for a variety of reasons, elect to retain the use of this assumption in this study. Justification for, motivations for, and implications of the use of this simplifying assumption are provided in the following paragraphs.

The use of benzene as the incepting species is justified based on several facts. First of all, benzene has been found in this laboratory as well as by Kern, et al. (1987) to correlate directly with sooting tendencies for a variety of aliphatic hydrocarbons; secondly, while relatively small uncertainties exist in our ability to predict benzene concentrations (factor of two), large uncertainties exist in the prediction of multi-ringed aromatics (probably a factor of ten or more), so calculations of inception based on concentrations of these high molecular weight species are at the present time subject to large error; thirdly, results can be very sensitive to the selection of the incepting species and its selection appears to be somewhat arbitrary; and fourthly, the actual mechanism for inception is not yet known (although some good speculation is available). Consequently, we conclude that there are significant uncertainties in calculating the true inception rate and, therefore, at the present time, the use of benzene as the incepting species is as good as other uncertain alternatives. As will be seen, use of this assumption yields reasonable agreement with experimental data in many regards.

In addition to these justifications, there is a strong motivation for using a simplified inception process. Calculation times for solutions of flame systems increase dramatically as the number of flame species increase. This concern becomes even greater as multi-dimensional flames are considered. Already, the calculation time for solution of the gas-phase kinetics (many hours) by far dominates over the solution times of the aerosol dynamics (seconds to a couple of minutes on an IBM 486 pc).

One of the obvious errors in using benzene as the inceptor is that it must significantly overestimate the true rate of inception. A second effect is that the dependency on the concentration of aromatic hydrocarbons (or other parameters such as temperature, pressure, or other species) may not be properly reproduced. For example, Frenklach and Wang (1990) assumed that bimolecular collisions between species with four or more rings were responsible for inception. Obviously the rate of this process must be much lower than that calculated from Eqn. 2. Furthermore, the Frenklach and Wang inception rate is dependent on the square of the concentration of the higher order aromatics rather than the rate of formation of aromatic species. In addition, there may be a temperature dependence to this 'sticking' process. These differences in magnitude and dependency may have a significant impact on predictions of soot, but as has been pointed out (Kennedy et al., 1990) the total soot production may be a relatively weak function of the inception rate at least for heavily sooting flames. For the flames studied herein, soot production is dependent on inception rate although less than first order dependence is generally observed (see later discussion).

As will be seen in the subsequent discussions, the model compensates for the overprediction of the inception rate in several ways. First of all, coagulation is allowed to occur for unreasonably low molecular weight aromatics. By allowing such coagulation, total surface area is reduced more rapidly at early stages of soot growth, and hence total mass growth of soot is limited. A second compensator is that we use predictions of specific soot growth rates which are sometimes slightly lower than experimental measurements. (In fact, if growth rates were raised, all models examined in this study would dramatically overpredict growth rates at extended times and hence overpredict soot growth high in the flames.) Because of these compensatory factors, we expect that as additional information becomes available on the inception process as well as the ageing process, such corrections can be implemented into the soot growth model.

Soot Growth Mechanisms

Soot growth rates were calculated using a variety of procedures, each of which exhibit different features. Two literature 'mechanisms' were used, i.e., the Harris and Weiner (HW) expression

(1983a) and the Frenklach and Wang (FW) mechanism (1990). In addition, three other mechanisms (MODFW, 8STEP, 5RING) are evaluated. For the latter four mechanisms, steady-state assumptions are made for all intermediate 'species' and expressions for overall soot growth rates were determined. In the latter three cases, rate constants were initially selected based on literature expressions but then adjusted (typically less than a factor of four) in order to provide better agreement with experimental data (that is, specific surface growth rates from Harris and Weiner and the soot profiles from Bockhorn, et al). Frenklach and Wang's approach of not altering rates from those which describe reactions for low molecular weight species is admirable. However, we justify our adjustments due to the fact that rate constants between low and high molecular weight species are not necessarily identical for similar processes (due to changes in molecular structures as well as reduced masses) and since a simplified sequence is used to describe what is probably a very complex process.

Net growth rates are determined by subtraction of oxidative terms (due to oxidation by oxygen and hydroxyl radicals) as described in the section on aerosol modeling. Only growth mechanisms are described in this section.

HW Mechanism -

Harris and Weiner (1983a,b) found that soot growth rates were proportional to acetylene to the power of 1.2 ± 0.6 (2 σ) for a series of premixed, laminar ethylene flames (0.70≤C/O≤0.79) and 0.9 ± 0.7 (2 σ) for a series (0.76≤C/O≤0.94) of richer flames. Several previous investigators (Narasimham and Foster, 1965; Arefeva, et. al, 1977; and Tesner, 1979) had found soot growth rates to be proportional to acetylene concentrations. Based on these experimental results, Harris and Weiner suggested that the per particle growth rate of soot (grams/sec) follows the expression:

$$\frac{d[m]}{dt} = k_{HW}\, A\, P_{C_2H_2} \qquad (3)$$

where A is the surface area of the soot particle, and $P_{C_2H_2}$ is the partial pressure of acetylene in atmospheres. Using an overall activation energy for the soot growth process of 31.8 kcal/mole (Hura and Glassman, 1988) and Harris and Weiner's rate at 1650K of 3×10^{-3} grams/sec/cm^2/atm, we calculate k_{HW} = 47 exp(-31800/R/T) grams/sec/cm^2/atm.

Alterations to this simple equation have been considered. In some flames (see Frenklach and Wang, 1990; Howard, 1988; and Harris and Weiner, 1988), significant growth rates of soot (especially early in the flame) can be dramatically enhanced by addition of polyaromatic hydrocarbons to soot particles. This enhancement to the soot growth rate is implicitly included by the approach described in the present study since coagulation processes are included and since the model does not distinguish between gas phase PAH species and condensed 'soot' particles.

The experiments of Wieschnowsky, et. al (1988) on seeded flames have indicated that some alterations to this very straightforward equation may be required. Harris (1990), Frenklach and Wang (1990) and Woods and Haynes (1991) have all offered explanations and revised mechanisms. Until additional information is available, however, we elect to retain the original HW mechanism for the purposes of this study.

A possible mechanistic explanation of this linear dependence on acetylene could be that acetylene isomerizes to vinylidene which subsequently inserts itself into a surface bond. However, the isomerization process is about 40 kcal endothermic, which is noticeably higher than the 20 to 35 kcal activation barrier normally observed for the soot formation process. Alternatively, acetylene could add to a soot particle via a Diels-Alder reaction, such as

$$C_4H_6 + C_2H_2 \leftrightarrow c - C_6H_8 \leftrightarrow \text{benzene} + H_2$$

or

$$\text{phenanthrene} + C_2H_2 \leftrightarrow \text{dihydropyrene} \leftrightarrow \text{pyrene} + H_2$$

Rate constants for the initial rate limiting steps can be estimated by the rate for the addition of ethylene to butadiene (Benson and O'Neal, 1970) or about 1.5×10^{10}exp(-27500/R/T) cm^3/moles/sec which converts to 10^{-3}exp(-27500/R/T) grams/sec/cm^2/atm at 1650K and for a small soot particle of 2×10^{-15} cm^2 surface area. The activation energy for this process is very close to experimental values, but the pre-exponential is orders of magnitude too low. Calculations such as these support efforts (Frenklach and Wang, 1990) to explain the soot growth process as a radical process.

FW Mechanism -

Based on an extensive set of prior work (Frenklach and coworkers, 1984, 1987, and 1988), Frenklach and Wang (1990) derived a soot growth rate expression from a steady state analysis of a reaction mechanism for soot growth. The proposed mechanism

Table I: Frenklach and Wang Soot Growth Mechanism (FW)

	Reactions Considered	$\log_{10}(A_f)$	n_f	E_f	$\log_{10}(A_r)$	E_r
1.	$H+C(s)\leftrightarrow \dot{C}(s)+H_2$	14.40	-	16	12.55	9.8
2.	$H+\dot{C}(s) \rightarrow C(s)$	12.26	0.68	8.6	-	-
3.	$C_2H_2+\dot{C}(s)\leftrightarrow C'(s) + H$	13.6	-	10.1	-	-

is modeled after an acetylene addition process to aromatic rings. Using a steady-state analysis, the rate of mass growth of soot due to acetylene addition (ignoring oxidation) is

$$\frac{dm}{dt} = 2m_c\frac{d[C'(s)]}{dt} = 2m_c\alpha\frac{k_1k_2[H][C_2H_2]\chi A}{(k_{-1}[H_2] + k_2[C_2H_2] + k_3[H])} \quad (4)$$

where m_c is the mass of a carbon atom, χ is a surface density of C_{soot}-H sites ($\approx 2.3\times10^{15}$ cm^{-2}, according to Frenklach and Wang), and α is a steric factor equal to one for the lower temperature flames of Harris and Weiner and equal to 0.1 for the higher temperature acetylene flame examined by Wieschnowsky and coworkers (1988). Expressions for the rate constants were obtained from Frenklach (1991) and are reported in Table I. These rate constants are literature expressions for the counterpart reactions with the benzene molecule. The steady-state expression is attractive since it contains a dependence on the hydrogen atom concentration. Frenklach and Wang argued that this feature helps to explain the fall-off of soot growth rates with increasing height above the burner. Conceptually, we favor this feature. Surface activation by H-atoms seems very reasonable and is consistent with proposed concepts for other surface deposition processes (such as for CVD diamond growth). Furthermore, calculated H/H_2 ratios fall off more rapidly than the $(H/H_2)_{eq}$ ratio with decreasing temperature in the post-flame zone for all the flames examined in this study. Unfortunately, as will be shown later in this paper, the fall-off of the soot growth rates as modeled by this mechanism (as well as others) occurs prematurely for the Harris and Weiner flames. Thus, previous proposals which attribute reductions in soot growth rates to particle ageing cannot be entirely discarded.

Despite the pioneering effort which the Frenklach and Wang work represents, constructive criticism of their mechanism is fruitful since it can lead to further understanding of the soot growth process. One of our principal concerns of this mechanism is that under the conditions of the Harris flames, the middle term in the denominator of Eqn. 4 dominates and the above steady-state expression reduces to

$$\frac{dm}{dt} \approx 2m_c \alpha k_1 [H] \chi A \tag{5}$$

which is directly proportional to H-atoms and independent of the acetylene concentration. The lack of a dependency on acetylene conflicts with the experimental conclusions of the Harris and Weiner works (1983a,b) as well as those of several other workers. More importantly, and as will be shown in a later section, this inadequacy leads to an inability to predict the stoichiometric dependence of soot formation for the Harris and Weiner flames. A second, important issue is that the overall activation energy of the above expression can be estimated as

$$E_{ov} = E_1 + E_H \approx 68 \text{kcal/mole}$$

where E_H, the effective activation energy of the H-atom concentration, is estimated to be 52 kcal/mole. This overall activation energy is substantially higher than literature values for soot growth rates, typically 20 to 35 kcal/mole. A third uncertainty about the FW mechanism is that an efficiency factor of 0.1 was used in order to describe a flame examined by Wieschnowsky and coworkers (1988). Frenklach and Wang justified its use by arguing that there are temperature dependencies to the probability for a gaseous species to collide with the edge plane instead of the unreactive basal plane of a particle and to the probability of the number of edge carbon atoms available for a given reaction. Such rationalization appears plausible, but self-consistency raises the question of whether it is fair to assume a constant value for a temperature-dependent steric factor in a flame for which temperatures vary strongly as a function of height. Despite such concerns, Frenklach and Wang had no other alternative which simultaneously described soot growth rates while providing a linear df_v/dt vs. f_v relationship which was found to be true for many of the flames studied by Bockhorn and co-workers (1984).

Modified FW Mechanism -

As an alternative to the multiplying factor used to explain the high temperature flame data, we attempted (Frenklach and Wang also tried a similar approach) to include some reversibility in the acetylene addition process. The resulting mechanism (MODFW):

Table II: Modified Version of the FW Soot Growth Mechanism (MODFW)

	Reactions Considered	$\log_{10}(A_f)$	E_f	$\log_{10}(A_r)$	E_r
1.	$H+\dot{C}(s) \leftrightarrow \dot{C}(s)+H_2$	14.40	12	11.6	7.0
2.	$H+\dot{C}(s) \leftrightarrow C(s)$	14.34	-	17.3	109.
3.	$\dot{C}(s) \rightarrow$ products $+ C_2H_2$	14.48	62	-	-
4.	$C_2H_2+\dot{C}(s) \leftrightarrow C(s)CH\dot{C}H$	12.30	4	13.7	38
5.	$C(s)CH\dot{C}H \rightarrow C'(s)+H$	10.70	-	-	-

includes possible acetylene elimination from the soot radical (analogous to phenyl radical decomposition) and separates the acetylene addition process into a reversible formation of the radical adduct

and a cyclization reaction. Assuming steady-state conditions for all intermediate species, the rate expression for soot mass growth is calculated to be

$$\frac{dm}{dt} = 2m_c \frac{(k_1[H] + k_{-2}[C_2H_2])k_4k_5\chi A}{(k_{-1}[H_2] + k_2[H] + k_3)k_{-4}k_5 + k_4k_5[C_2H_2]} \tag{6}$$

where rate constants are listed in Table II.

8STEP Mechanism -

Another plausible reaction sequence is modeled after the sequence depicted in Fig. 6. At least one attractive feature of this more complex mechanism is that it includes reversible as well as irreversible reactions. The irreversible reaction (R8) 'pulls' the soot growth process along as described by Frenklach, et. al (1984). Alternatively, this sequence can be described by

Table III: Eight Step Soot Growth Mechanism (8STEP)

	Reactions Considered	$\log_{10}(A_f)$	E_f	$\log_{10}(A_r)$	E_r
1.	$H+\dot{C}(s) \leftrightarrow \dot{C}(s)+H_2$	14.15	16	11.3	10.0
2.	$H+\dot{C}(s) \leftrightarrow C(s)$	14.30	-	16.38	109
3.	$C_2H_2+\dot{C}(s) \leftrightarrow C(s)C_2H + H$	11.95	4	11.6	6
4.	$H+C(s)C_2H \leftrightarrow \dot{C}(s)C_2H + H_2$	14.18	16	12.0	4
5.	$C_2H_2 + \dot{C}(s)C_2H \leftrightarrow C(s)CH\dot{C}HC_2H$	12.48	4	14.0	30
6.	$C(s)CH\dot{C}HC_2H \leftrightarrow \dot{C}'(s)$	10.90	-	14.0	72.5
7.	$\dot{C}'(s) + C_2H_2 \leftrightarrow C'(s)CH\dot{C}H$	11.48	6	13.3	25
8.	$C'(s)CH\dot{C}H \rightarrow C''(s)+H$	10.90	-	-	-

Assuming steady-state concentrations of intermediates, the rate of soot growth is

$$\frac{dm}{dt} = 6m_c \frac{(k_1[H] + k_{-2})E[C_2H_2]^3\chi A}{(k_{-1}[H_2] + k_2[H])(B[H_2] + C[H_2][C_2H_2] + D[C_2H_2]^2) + E[C_2H_2]^3} \tag{7}$$

where

$$B = k_{-3}k_{-4}k_{-5}k_{-6}(k_{-7} + k_8)$$
$$C = k_{-3}k_{-4}(k_{-5} + k_6)k_7k_8)$$
$$D = (k_{-3} + k_4)k_5k_6k_7k_8$$
$$E = k_3k_4k_5k_6k_7k_8$$

Rate constants used for this mechanism are listed in Table III.

5RING Mechanism -

A soot growth mechanism was also constructed based on involvement of five-membered rings. Justification for these arguments are based on Colket's (1990) recent observation of rapid conversion of five-membered rings to six-membered rings as well as known processes causing ring enlargement and contraction(Gajewski, 1981; Benson and O'Neal, 1970; and Ritter, et. al, 1991).

Figure 6

Eight Step Ring Growth Process

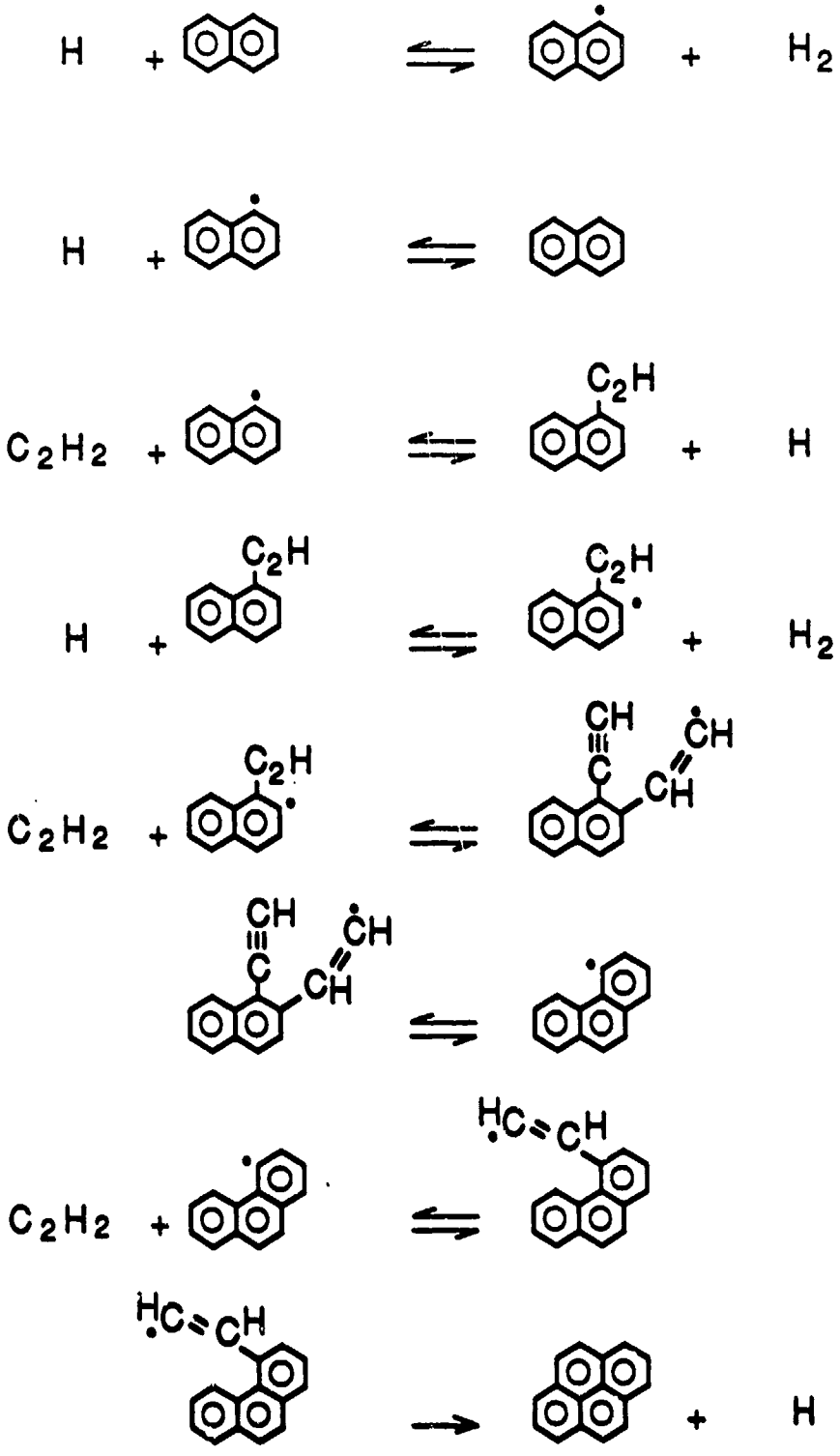

Ritter, et al. have recently examined the thermodynamics and kinetics of ring contraction, in particular, conversion from a C_6-ring to a C_5-ring. Colket (1990) recently added acetylene to the pyrolysis of cyclopentadiene (CPD) and observed substantial formation of toluene. A specific mechanism for this process was not identified. Kiefer (1991) suggested that the acetylene addition processes may be related to the Diels-Alder reaction of acetylene addition to CPD to form norbornadiene. Benson and O'Neal (1970) report rates for unimolecular decomposition of norbornadiene to CPD plus acetylene and for the isomerization of norbornadiene to toluene. Thus, one could speculate an overall process for ring enlargement:

$$C_5H_6 + C_2H_2 \leftrightarrow \text{norbornadiene} \leftrightarrow \text{toluene}$$

However, based on calculations of rate data and literature values, we concluded (Colket and Hall, 1991) that the dominant process observed in the SPST experiments is a radical process.

Assuming radical addition processes, we propose the reaction scheme in Fig. 7 as a possible alternative to a growth mechanism involving six-membered rings. The acetylene addition to cyclopentadienyl, formation of norbornadienyl, and isomerization to benzyl radical may be the reverse of a route for benzyl decomposition which has eluded researchers for years. Indene, formed in Reaction 7, has a five-membered ring and, after loss of an H-atom (analogous to Reactions 1 or 2), it may undergo subsequent acetylene addition for further growth of polyaromatic hydrocarbons. Rewriting this sequence as

Table IV: Soot Growth Mechanism Based on Five-Membered Rings (5RING)

	Reactions Considered	$\log_{10}(A_f)$	E_f	$\log_{10}(A_r)$	E_r
1.	$H+C(s)\leftrightarrow \dot{C}(s)+H_2$	14.40	6	13.70	36
2.	$\dot{C}(s)\rightarrow$ products + C_2H_2	13.70	60	-	-
3.	$C(s)\leftrightarrow \dot{C}(s)+H$	14.78	86	14.48	-
4.	$C_2H_2+\dot{C}(s)\leftrightarrow \dot{C}'(s)$	12.04	12	12.00	70
5.	$C_2H_2+\dot{C}'(s)\leftrightarrow C'(s)\dot{C}HCH$	13.00	5	12.30	21
6.	$C'(s)\dot{C}HCH \rightarrow C''(s)+H$	11.40	5	-	-

and assuming steady-state concentrations for all intermediate species, the expression for acetylene addition to 'soot' can be obtained:

$$\frac{dm}{dt} = 4m_c \frac{(k_1[H] + k_3)k_4k_5k_6[C_2H_2]^2\chi A}{(k_{-1}[H_2] + k_{-3}[H] + k_2)\{k_{-4}(k_{-5} + k_6) + k_5k_6[C_2H_2]\} + k_4k_5k_6[C_2H_2]^2} \qquad (8)$$

Reactions 4 and -4 represent the overall reversible process of acetylene addition to cyclopentadienyl to form benzyl radical. Rate constants were initially determined based on literature values for these processes (with CPD) or estimates as necessary. An important difference of this new mechanism from those based on six-ringed species is the lower C-H bond strength in the C_5 ring species. The rate constant for acetylene addition to cyclopentadienyl was initially taken to be the reverse of that for the decomposition of benzyl radical. Using the rate determined by Brouwer, et al., 1988 (for the reaction for which they assumed the products to be C_4H_3 + C_2H_2) and assuming reversibility, k_4 was initially estimated to be $10^{12}\exp(-15000/R/T)$ cm^3/mole/sec. The adjusted rate constant for k_4 which provides reasonable agreement to the soot growth data of Harris and Weiner (1983) and the soot production in the acetylene flame of Bockhorn, et al.(1983) has only a

Figure 7

Alternate Ring Growth Mechanism

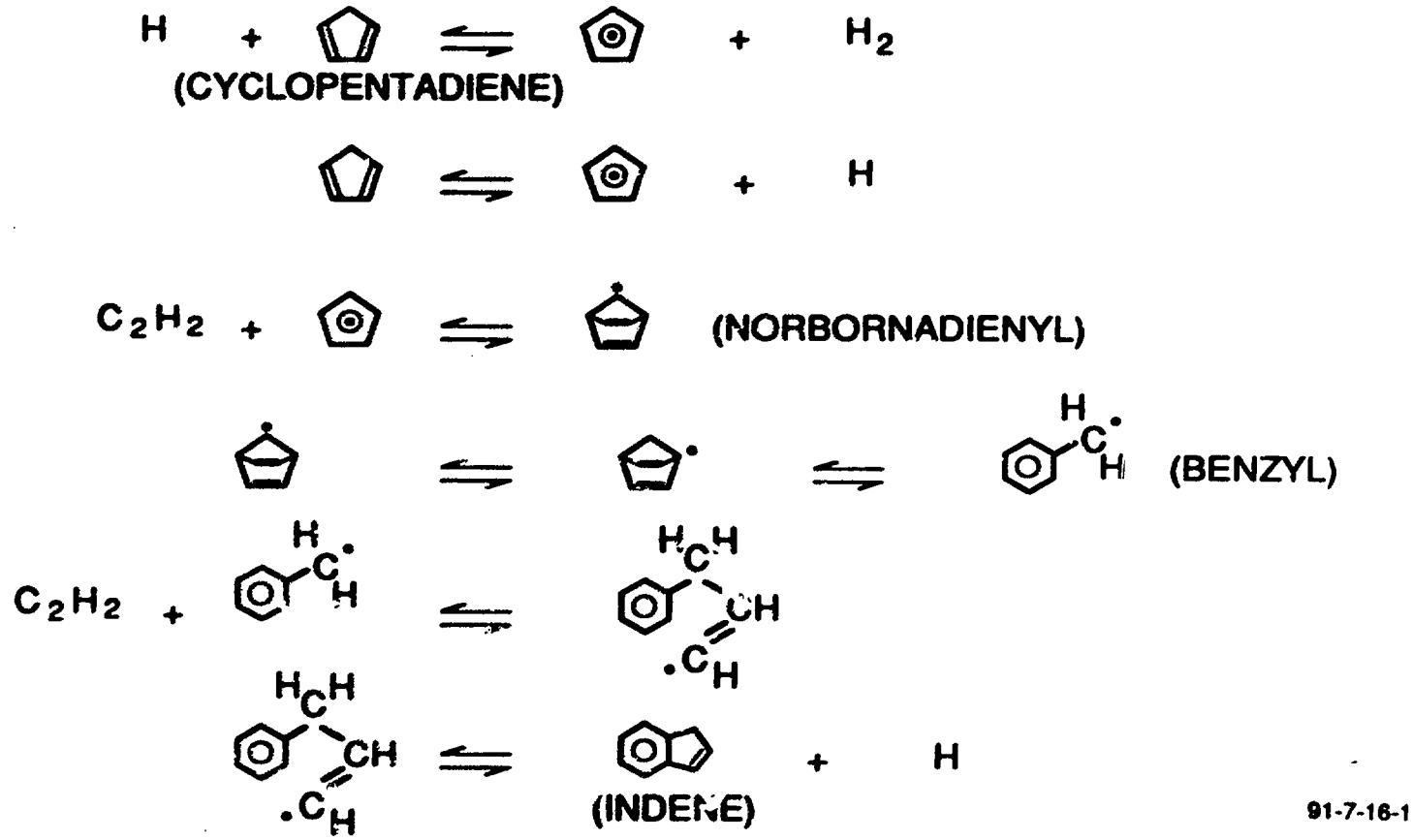

91-7-16-1

slightly increased activation energy. The equilibrium constant for Reaction 4 is within a factor of three of the equilibrium constant of the conversion from cyclopentadienyl and acetylene to benzyl radicals.

Predictions of Specific Surface Growth Rates

Specific surface growth rates, R_g, were calculated according to

$$R_g = \frac{dm/dt}{A} \tag{9}$$

for each of the above expressions and by using the same value (2.3×10^{15} sites/cm^2) as derived by Frenklach and Wang(1991) for χ, the surface density of C_{soot}-H sites. Comparisons of surface growth rates for four separate flames are shown in Figs. 8-11. The four flames include two of the (ethylene) Harris and Weiner flames (1983a) at differing stoichiometries and the acetylene and propane flames examined by Bockhorn and coworkers (1983). Net surface growth rates are reduced from the rates in these figures by the subtraction of oxidative terms. Oxidation has a negligible effect on the Harris and Weiner flames but affects the Bockhorn flames dramatically. The effect of oxidation will be discussed in more detail in the section on soot model predictions.

Harris and Weiner measured soot growth rates for a variety of flames ($0.76\leq C/O\leq0.94$), and these data are included for comparison in Figs. 8 and 9. No data were presented for the C/O=0.96 flame, but we assume such data would lie slightly above the highest set of experimental data. Although the experimental data nearly collapses to a single curve, there is a noticeable stoichiometric dependence with the soot growth rates in the richer flames about a factor of two above those for the C/O=0.80 flame (except high in the post-flame zone where the data converge fairly well). The predicted curves tend to peak early and are all concave upwards, whereas the experimental data is concave downwards. The shape of these 'theoretical' curves is at least partially due to their dependence on H-atom concentrations and partially due to the decay in temperature. For the richer flames, all of the calculated soot growth rates predict the initial magnitude of the soot growth rate fairly well, although they all fall off too rapidly with increasing height above the burner. Furthermore, none of the models adequately describes the fall-off observed for 'older' soot particles. Consequently, we favor proposals which attribute decreasing soot growth rates with the particle ageing process. For the C/O=0.8 flame, the FW expression does not decrease by a factor of two from that for the C/O=.96 flame (in fact the FW predictions for the two flames are nearly identical) as the experimental data indicates and leads to substantial overprediction of soot formation in this leaner flame. As described previously, the failure in the mechanism is due to the lack of dependency on the acetylene concentration. The alternative mechanisms described in this paper provide a slightly better description of the stoichiometric differences between flames. In fairness to the FW mechanism, the reader should be reminded that the rate constants used in the alternative mechanism were 'fitted' in order to obtain the agreement.

Although stoichiometric dependences can be described, it is also obvious that none of the models predicts the absolute magnitude of the soot growth rate data. Yet, despite the low predicted values of soot growth rates, reasonable agreement between the experimental soot profiles and the modeling of soot production is obtained. As has been discussed, the use of benzene production as a surrogate for the inception rate undoubtedly overstates the inception process. As a result, our present model favors the use of lower surface growth rates. In general, however, we do not feel that our model is far wrong because of its reasonable agreement with the results of Frenklach and Wang, who used a more elaborate scheme for simulating the inception process. In addition, uncertainties in χ as well as the rate constants, indicates that the predicted curves in Figs. 8-11 could easily shift up or down

Figure 8

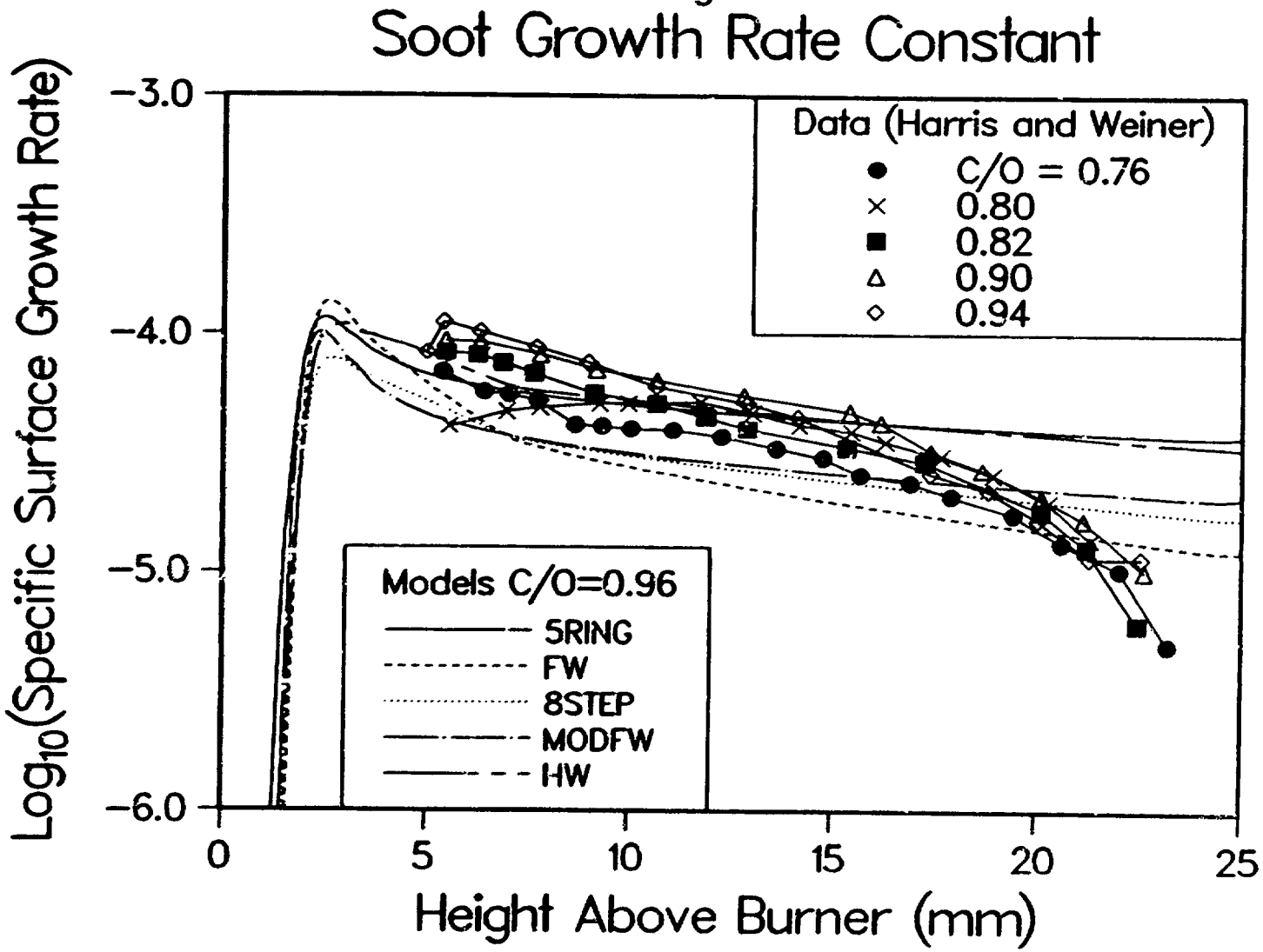
Soot Growth Rate Constant
Log10(Specific Surface Growth Rate)
-3.0
-4.0
-5.0
-6.0
0
5
10
15
20
25
Height Above Burner (mm)
Data (Harris and Weiner)
C/O = 0.76
0.80
0.82
0.90
0.94
Models C/O=0.96
5RING
FW
8STEP
MODFW
HW

Figure 9

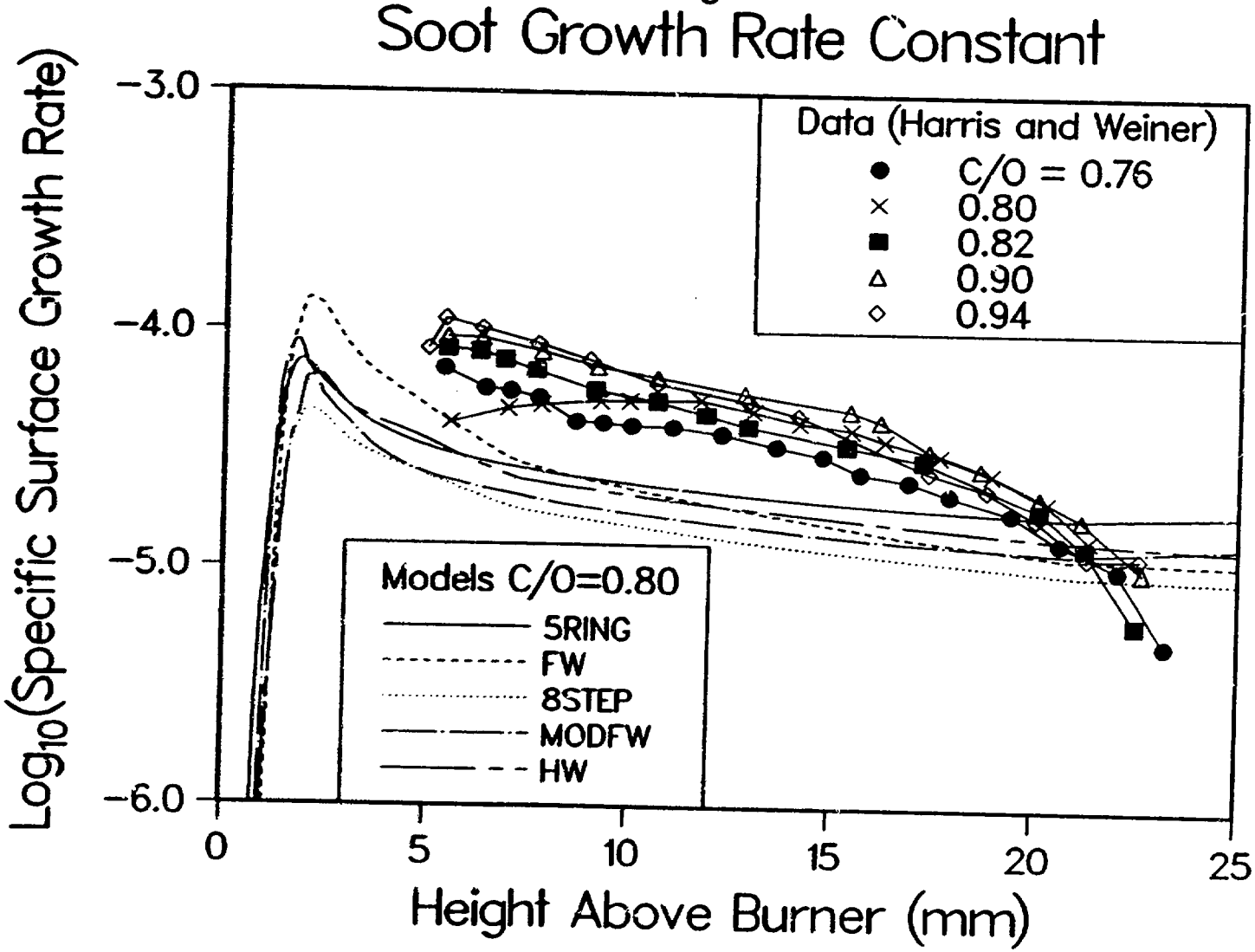
Soot Growth Rate Constant
Log10(Specific Surface Growth Rate)
-3.0
-4.0
-5.0
-6.0
0
5
10
15
20
25
Height Above Burner (mm)
Data (Harris and Weiner)
C/O = 0.76
0.80
0.82
0.90
0.94
Models C/O=0.80
5RING
FW
8STEP
MODFW
HW

Figure 10

Soot Growth Rate Constant
Acetylene Flame

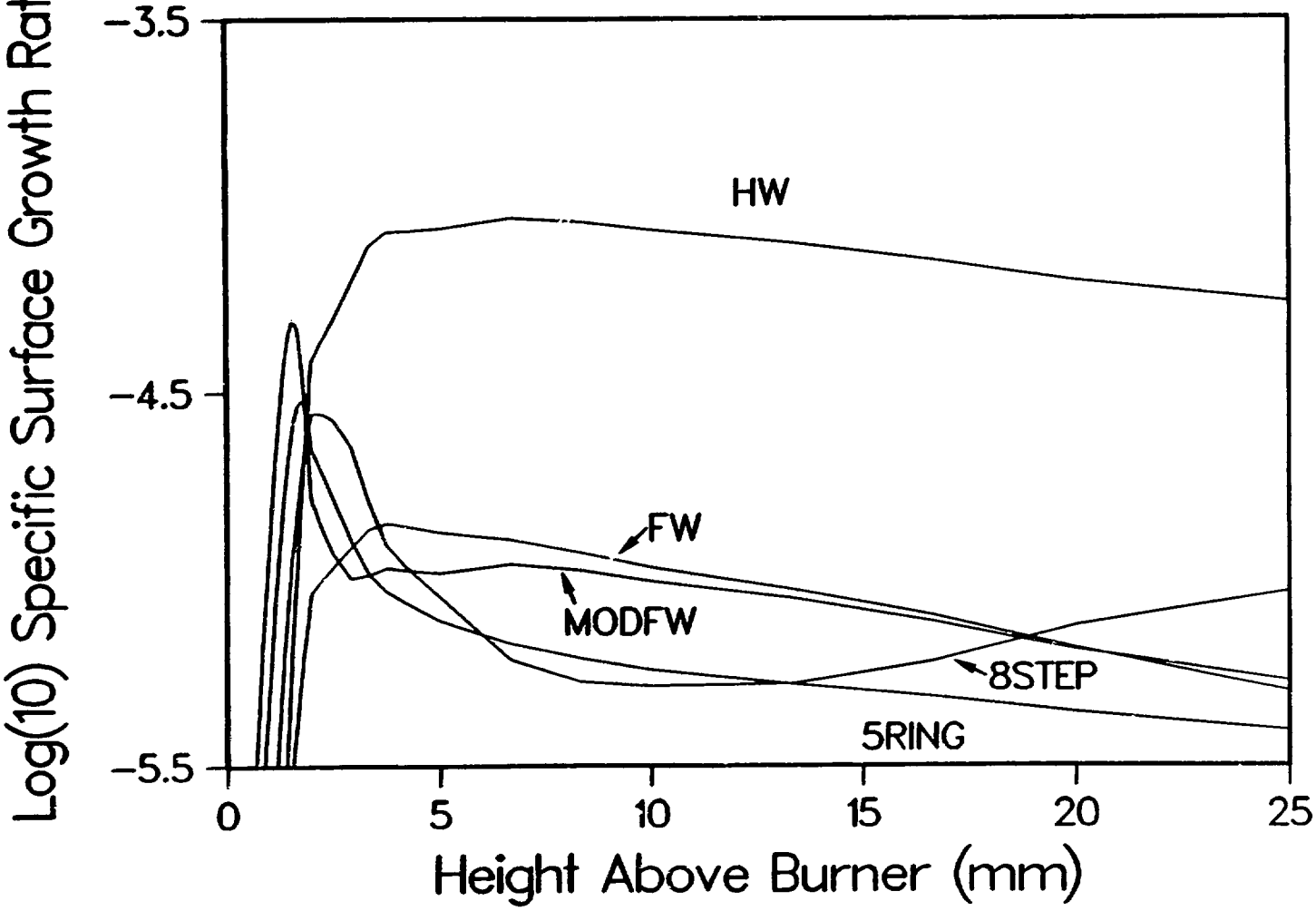

Figure 11

Soot Growth Rate Constant
Propane Flame

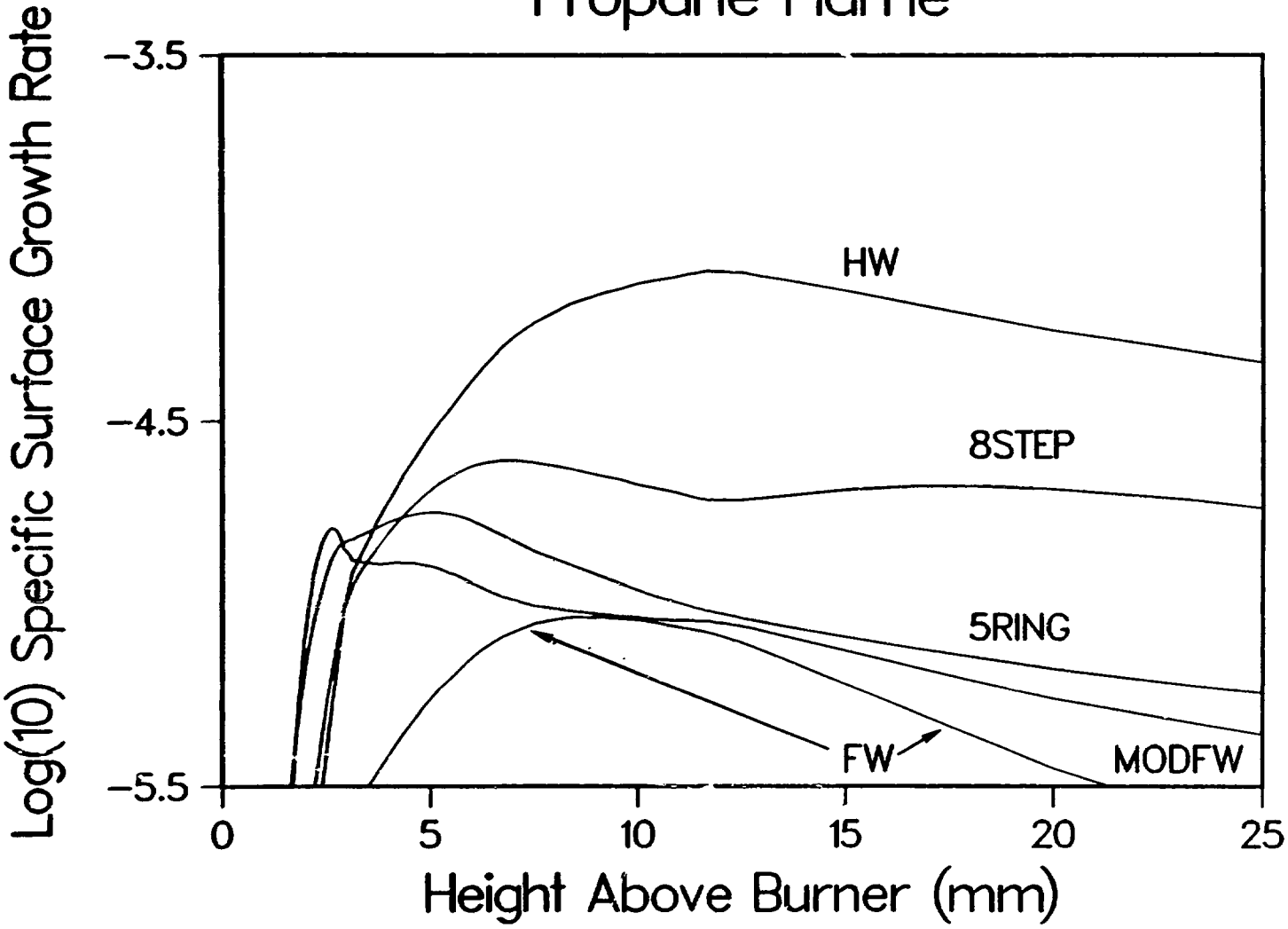

as much as a factor of two. We have not made such shifts in the present study since uncertainties still exist in the understanding of the inception process and since the fall-off in soot growth rates in the post-flame zone is not modeled by any of the mechanisms examined in this study. Without this fall-off, significant growth late in the post-flame zone would be predicted by our code (using any of the mechanisms described herein) if all curves were shifted upwards.

As a result of these issues, we believe that it is not the absolute magnitude that is of concern when comparing these different mechanisms, but rather the shape of the soot growth profiles within a given flame as well as the comparison of the mechanisms for several different flames.

Soot growth rates for the Bockhorn flames are presented in Figs. 10 and 11 for information. Experimental values for the surface growth rates for these flames have not been published. The FW expression has been calculated using α= 0.1 for the acetylene flame. Frenklach and Wang argued that this factor accounts for a steric reduction in the rate of growth processes and was required for the high temperatures in the acetylene flame. The same value for α was used for the propane flame even though the peak temperatures in the propane flame are about one hundred degrees lower than those in the acetylene flame and about 200 degrees higher than those in the Harris and Weiner flames. These same factors were used in subsequent soot calculations.

Soot Spheroid Growth Model

The growth of soot spheroids has been modeled as an aerosol dynamics problem, involving the division of the size range of interest into discrete intervals or classes, and then solving a master equation for the size class mass densities with terms representing inception, surface growth (or oxidation), and coagulation (coalescence). The spheroids are assumed to be comprised of the single component carbon only. The sectional analysis is discussed in by Gelbard and Seinfeld (1980) and Gelbard, Tambour, and Seinfeld (1980), and the computer program we have developed is an outgrowth of the well-known MAEROS program (Gelbard, 1982). Because our application is specialized, we were able to simplify the calculation of growth and coagulation coefficients, as will be discussed. The fundamental growth equations and numerical analysis algorithms are those of MAEROS, however. The important features of the aerosol dynamics analysis are provided below.

Soot spheroids vary in diameter from approximately one to 100 nanometers, representing a variation of six orders of magnitude in mass. In the sectional analysis, it is assumed that the boundaries of the sections vary linearly on a log scale. Thus, if we have M sections, with diameter minima and maxima D(0) and D(M), respectively, the sectional boundaries will be given by

$$D_\ell = D(0)\left(\frac{D(M)}{D(0)}\right)^{(\ell/M)} \tag{10}$$

where 0.75 and 300 nanometers are typical values for D(0) and D(M). Section ℓ ($1 \leq \ell \leq M$) will thus have the boundaries m(ℓ-1) and m(ℓ) in particle mass where

$$m = \rho_s \frac{\pi D^3}{6} \tag{11}$$

and the soot density ρ_s is taken to be that of solid carbon, 1.8 g/cc. If $n_\ell(m,t)$ represents the number density per unit mass of particles within a section, the total mass Q(ℓ) within the section is given by the integral

$$Q_\ell = \int_{m_{\ell-1}}^{m_\ell} m\, n_\ell(m,t)\, dm \tag{12}$$

Choosing, as in Gelbard, the form

$$n_\ell(m,t) = \frac{Q_\ell}{m^2}\, \Delta_\ell \tag{13}$$

where

$$\begin{aligned} \Delta_\ell &= \left(\ell n\, \frac{m_\ell}{m_{\ell-1}}\right)^{-1} = (X_\ell - X_{\ell-1})^{-1} \\ X &= \ell n(m) \end{aligned} \tag{14}$$

results in the following expression for the total number density of particles in class ℓ

$$N_\ell = \int_{m_{\ell-1}}^{m_\ell} n_\ell(m,t)\, dm = Q_\ell\, \Delta_\ell \left(\frac{1}{m_{\ell-1}} - \frac{1}{m_\ell}\right) = \frac{Q_\ell}{\overline{m}_\ell} \tag{15}$$

where the average particle mass $\overline{m}_\ell$ in section ℓ is given by

$$\begin{aligned} \overline{m}_\ell &= \int_{m_{\ell-1}}^{m_\ell} m\, n_\ell(m,t)dm \Big/ \int_{m_{\ell-1}}^{m_\ell} n_\ell(m,t)dm \\ &= \Delta_\ell^{-1} \left(\frac{1}{m_{\ell-1}} - \frac{1}{m_\ell}\right)^{-1} \end{aligned} \tag{16}$$

Equation 13 is equivalent to assuming that $dQ_\ell/d\,\ell n(m)$ is constant within a section, and represents the lowest order intra-class density distribution function.

The per particle net rate of growth due to surface mass addition and oxidation is assumed, as discussed, to be proportional to particle surface area (free molecule form)

$$\frac{dm}{dt} = G'(t)A = G(t)m^{2/3} \tag{17}$$

where A is the particle surface area, and the specific growth rate has the overall form

$$\begin{aligned} G'(t) = &(\text{Growth rate by acetylene or other growth species addition} \\ &- \text{oxidation rate by } O_2,\ OH)/\text{unit surface area.} \end{aligned} \tag{18}$$

$$\text{or} \quad G'(t) = R_G - R_{O_2} - R_{OH}$$

The mass addition term R_G (see Eqn. 9) has been derived for several kinetic models of the surface growth process, as discussed in the preceding section. Oxidation of soot by OH radicals is assumed to proceed at a gas kinetic collision frequency multiplied by a collision probability of 0.13 (Neoh, Howard, and Sarofim, 1981). Thus, with N_{OH}, N_A, and m_{OH} representing the OH number density, Avogadro's number, and the OH radical mass, respectively, the OH oxidation is

$$R_{OH} = (0.13) \times N_{OH} \sqrt{\frac{KT}{2\pi m_{OH}}} \times \frac{12}{N_A} = 16.7 \frac{P_{OH}}{\sqrt{T}} \tag{19}$$

where P_{OH} is the OH partial pressure in atmospheres, and the specific growth rate is in c.g.s. units. For oxidation by O_2, the Nagle & Strickland-Constable (1963) expression is used. For an O_2 partial pressure P_{O_2} in atmospheres, the specific oxidation rate is thus

$$R_{O_2} = 12 \times (K_a P_{O_2} \chi' / (1 + K_z P_{O_2}) + K_b P_{O_2} (1 - \chi')) \tag{20}$$

where

$$\begin{aligned} K_a &= 20 \exp(-1.51 \times 10^4 / T) \\ K_b &= 4.46 \times 10^{-3} \exp(-7.64 \times 10^3 / T) \\ K_z &= 21.3 \exp(2.06 \times 10^3 / T) \\ \chi' &= 1/(1 + K_T/(K_b P_{O_2})) \\ K_T &= 1.51 \times 10^5 \exp(-4.88 \times 10^4 / T) \end{aligned} \tag{21}$$

We made the input to our aerosol code compatible with the output of the SANDIA burner code, which provided the profiles of temperature and important chemical species concentrations needed in our flame simulations.

For the conditions of interest in this investigation, the coagulation rates are in the free-molecule regime, occurring at gas kinetic collision frequencies, and thus given by

$$\beta(m, m') = P_c(m, m') \frac{\pi}{4} (D_m + D_{m'})^2 \, \overline{V}_{mm'} \tag{22}$$

$$\overline{V}_{mm'} = \sqrt{\frac{8KT}{\pi} \left(\frac{1}{m} + \frac{1}{m'} \right)}$$

where provision is made for a Van-der Waals enhancement factor P_c. For collision partners of low and similar mass, theory predicts enhancements of the gas kinetic rate by as much as 2.2 (Harris and Kennedy, 1988); we use a nominal value of 1.5 for all interactions.

The dynamic balance equation for the Q_ℓ can be represented as

$$\frac{dQ_\ell}{dt} = \frac{1}{2}\sum_{i=1}^{\ell-1}\sum_{j=1}^{\ell-1} {}^1\overline{\beta}_{i,j,\ell}\, Q_i Q_j - Q_\ell \sum_{i=1}^{\ell-1} {}^2\overline{\beta}_{i,\ell}\, Q_i$$
$$- \frac{1}{2}\,{}^3\overline{\beta}_{\ell,\ell} Q_\ell^2 - Q_\ell \sum_{i=\ell+1}^{M} {}^4\overline{\beta}_{i,\ell}\, Q_i$$
$$+ {}^1G_\ell\, Q_\ell \qquad (23)$$
$$+ {}^2G_{\ell+\ell_N}\, Q_{\ell+\ell_N} - {}^2G_\ell\, Q_\ell + \delta_{\ell 1} S_i(t)$$

$$\ell_N = -1 \qquad G(t) > 0$$
$$= +1 \qquad G(t) < 0$$

where the $\overline{\beta}$ represent sectional coagulation coefficients, ${}^1G_\ell$ are intra-sectional growth coefficients, ${}^2G_\ell$ are inter-sectional growth coefficients, and $S_i(t)$ (see Eqn. 2) is a particle inception rate (mass units) for the initial size class. The value of the index ℓ_n is determined by whether the net growth is positive or negative, and it is understood that the term containing it will not be present for ℓ=1 for net growth, and will not be present for ℓ=M for net oxidation (G(t) greater or less than zero, respectively). Implicit is the assumption of complete particle coalescence after collision, with no aggregate or chain formation.

Because both the surface growth and coagulation rates are factorable into products of functions of mass times functions of time, a considerable simplification of the task of calculating sectional coefficients is made possible because the mass-dependent calculations need be performed only once, with the time dependence imposed during the course of the integration. With the general functional form for the surface growth, Equation 17, the intra-sectional growth coefficients can be calculated analytically as

$${}^1G_\ell = 3\Delta_\ell G(t)\left(\frac{1}{m_{\ell-1}^{1/3}} - \frac{1}{m_\ell^{1/3}}\right) \qquad (24)$$

and the inter-sectional coefficients are related to these by

$${}^2G_\ell = {}^1G_\ell \frac{\overline{m}_{\ell+1}}{\overline{m}_{\ell+1} - \overline{m}_\ell} \qquad G(t) > 0$$
$${}^2G_\ell = {}^1G_\ell \frac{\overline{m}_{\ell-1}}{\overline{m}_{\ell-1} - \overline{m}_\ell} \qquad G(t) > 0 \qquad (25)$$

The inter-sectional coefficients are derived from a number- and mass-conserving algorithm due to Warren and Seinfeld (1985). They govern the rate of mass transfer across size class boundaries due to surface growth or oxidation.

The sectional coagulation coefficients ($\overline{\beta}$) are calculated from the free-molecule collision frequencies, Equation 22, using the general relationships.

$$ {}^{1}\overline{\beta}_{i,j,\ell} = \Delta_i \, \Delta_j \int_{X'_{i-1}}^{X'_i} \int_{X_{j-1}}^{X_j} \frac{\bar{\theta}\, \theta(m_{\ell-1} < m + m' < m_\ell)(m+m')\beta(m,m')}{mm'} \, dXdX' $$

$$ {}^{2}\overline{\beta}_{i,\ell} = \Delta_i \, \Delta_\ell \int_{X'_{i-1}}^{X'_i} \int_{X_{\ell-1}}^{X_\ell} \frac{\bar{\theta}\, (\theta(m+m' > m_\ell)m - \theta(m+m' < m_\ell)m')\beta(m,m')}{mm'} \, dXdX' \tag{26} $$

$$ {}^{3}\overline{\beta}_{\ell,\ell} = \Delta_\ell^2 \int_{X'_{\ell-1}}^{X'_\ell} \int_{X_{\ell-1}}^{X_\ell} \frac{\bar{\theta}\, \theta(m+m' > m_\ell)(m+m')\beta(m,m')}{mm'} \, dXdX' $$

$$ {}^{4}\overline{\beta}_{i,\ell} = \Delta_i \, \Delta_j \int_{X'_{i-1}}^{X'_i} \int_{X_{\ell-1}}^{X_\ell} \frac{\theta(m > m_{min})\beta(m',m)}{m'} \, dXdX' $$

where $\bar{\theta} = \theta(m > m_{min})\theta(m' > m_{min})$. The theta function is unity if the condition expressed in its argument is satisfied, and zero if it is not. m_{min} is a threshold mass for coagulation. Again, the fact that the temperature dependence of β is known makes it possible to do the mass-dependent part of the sectional coefficient calculation once, and then to impose the time-dependent temperature dependence at each point the time derivatives of the Q_ℓ are desired. In the standard MAEROS code, a geometric constraint $m(\ell+1) \geq 2m(\ell)$ is employed to reduce the number of required coefficients. For the nominal diameter range of 0.75 - 300 nanometers of interest to us, this restricts the number of size classes we can use to about M=25. We have created a version of the program in which the geometric constraint is no longer imposed, and the sectional coefficients are calculated using Equations 26. This version is in agreement with the geometric constraint code for values of M such that the geometric constraint is obeyed, and makes it possible to test solution convergence properties by using an essentially unlimited number of size classes. In general, our analytic evaluation of the growth sectional coefficients and the factoring out of the coagulation rate temperature dependence obviate the need to generate a table of coefficients followed by interpolation, and extends the capabilities of the program to the full temperature range of interest in combustion.

With the solution for the Q_ℓ, a number of aerosol properties can be evaluated. The soot volume fraction will be given by

$$ f_v = \frac{1}{\rho_s} \sum_\ell Q_\ell \tag{27} $$

and its rate of change by

$$ \frac{df_v}{dt} = \frac{1}{\rho_s} \sum_\ell {}^{1}G_\ell Q_\ell = \frac{1}{\rho_s} G'(t) A_T \tag{28} $$

where A_T is the total particle surface area (defined below in Eqn. 31). We typically omit the inception size class from the summations. The moments of the diameter distribution are expressible as

$$ < D^n > = \frac{\sum_\ell \int D^n(m) n_\ell(m,t) dm}{\sum_\ell \int n_\ell(m,t) dm} \tag{29} $$

For comparisons with particle diameters obtained from laser light scattering measurements, typically derived by ratioing scattering and extinction, the optical diameter D_{63} is appropriate. This is

$$D_{63} = \left(\frac{< D^6 >}{< D^3 >}\right)^{1/3} = \left(\left(\frac{6}{\pi \rho_s}\right)\frac{\sum_\ell Q_\ell \Delta_\ell (m_\ell - m_{\ell-1})}{\sum_\ell Q_\ell}\right)^{1/3} \tag{30}$$

D_{63} will overweight the larger particles; for a self-preserving size distribution (Lai, Friedlander, Pich, and Hidy, 1972), it will be about 1.43 times the true number density weighted mean diameter. In similar fashion, the total surface area of the particles is given in terms of the Q_ℓ by

$$A_T = \sum_\ell \int_{m_{\ell-1}}^{m_\ell} \pi D^2(m) n_\ell(m,t) dm = 3\pi \left(\frac{6}{\pi \rho_s}\right)^{2/3} \sum_\ell \Delta_\ell Q_\ell \left(\frac{1}{m_\ell^{1/3}} - \frac{1}{m_{\ell-1}^{1/3}}\right) \tag{31}$$

The soot volume fraction is a quantity of great interest because it is usually the most important soot size/density parameter affecting radiative transfer. It corresponds to the first moment of the suspended mass distribution; the MAEROS program gives a good representation of this moment with a modest number of size classes. In most cases, as few as three to five size classes give a good approximation to the volume fraction. The convergence behavior of the various size/ density parameters will be discussed in a following section.

Comparisons to Experimental Data

To compare theory with the soot growth data of Harris and Weiner(1983a) and Bockhorn, et al. (1983), profiles of temperature, benzene and acetylene concentrations, and net surface growth rate are provided to the aerosol code as a function of time or height above the burner surface. The net surface growth rate consists of the mass addition rate for acetylene vapor deposition, minus oxidative terms due to oxygen molecules and OH radicals. The latter typically are dominant low in the flame, and the starting procedure for the aerosol growth analysis is to advance in time or height to the point where the net growth rate first turns positive. As discussed, a provisional inception model is assumed in which benzene acts as an inception species surrogate, and this in turn involves making the assumption that the particle growth mechanisms can be extrapolated into the pre-particle regime. As will be seen, the assumptions about the benzene surrogate role and the starting procedure yield predicted onsets of growth that agree reasonably well with experimental data in most cases. The aerosol code has provision for depletion of the acetylene vapor due to deposition, but this is typically on the order of 10%, and thus does not have a major influence on the results. Certain other assumptions have been made: a size class-independent coalescence sticking probability of 1.5 is assumed, and particles with masses below 150 a.m.u. have been excluded from coalescence. As will be seen, the volume fraction tends to converge in relatively few sections, but the average particle diameter tends to require many more, so that the nominal number of sections assumed in the calculations was 25. The sensitivity of the calculations to assumptions such as these will be discussed later. Unless stated otherwise, all calculations to follow will employ the foregoing assumptions.

For comparison with the Harris flames, CHEMKIN simulations were carried out for C/O ratios of 0.8, 0.92, and 0.96 since temperature profiles were available for these flames. Experimental volume fraction data were available at values of 0.8, 0.84, 0.90, and 0.94. The comparisons of the five surface growth models with the data are shown in Figures 12-16. With the exception of the Frenklach-Wang model, it can be seen that the stoichiometric dependence of the soot volume fraction is approximately satisfied. As discussed, the latter model has little or no dependence on acetylene pressure, and cannot therefore reproduce the stoichiometric dependence with this inception model. It seems unlikely that the observed stoichiometric dependence of the volume fraction could be explained on the basis of inception alone, without a surface growth rate more strongly dependent on the acetylene concentration. The other surface growth models are seen to be reasonably consistent with the data. The FW growth model slightly overpredicts the data which is inconsistent with the presentation by Frenklach and Wang (1990). This difference is due in part to the lower benzene profile (lower by about a factor of two) which was used in the Frenklach and Wang (1990) calculations (see Frenklach and Wang, 1991). All the model calculations tend to suffer from overshoot at early times, particularly in the C/O=0.8 case. Suppression of coagulation involving the smallest particulates tends to raise the particle surface area. Figure 17 shows a simulation using the HW model in which all size classes are allowed to coalesce with unit sticking probability. This combination represents the best overall agreement obtained thus far, although allowing the smallest particles to undergo coalescence might well be dubious. Figure 18 shows the profiles of the total calculated particulate surface areas versus experimental data. The experimental data are reasonably constant with height above the burner. Traditionally, this phenomenon is believed to be due to an approximate balance between area creation by surface growth and destruction of surface area by coalescence. The theoretical surface areas also are sensibly constant, in the regions where there are data. The magnitude of the C/O = 0.8 surface area is in excellent quantitative agreement with the data, but the area predicted for the 0.96 case is low by about 30%.

Comparison of theory and experiment for the two Bockhorn flames is shown in Figures 19 and 20. For the acetylene flame, use of the HW rate with the 31.8 kcal activation energy gives poor agreement, serving as an indication of how uncertain the high temperature surface growth rates are. In fact, there is no reason to expect that surface growth rates can be extrapolated to the temperatures of the acetylene flame since available experimental data for specific soot growth rates is limited typically to below 1700K. Other models give more satisfactory agreement, as seen, with the MODFW model and the FW model (the latter with a 0.1 steric factor) giving the best overall agreement. If one accepts the use of this steric factor at high temperatures, the HW expression, which already gives excellent agreement with the Harris and Weiner soot data (see Figs. 12 and 17), also then describes the acetylene data very well (see Fig. 32). This good agreement is not surprising considering that the HW specific surface growth rates (see Fig. 10) are similar in shape but a factor of 10 above the sterically corrected FW rates for the acetylene flame. It is interesting to note that the simple FW expression (Eqn. 3) as modified with a steric factor provides as good agreement or better as any of the more complex mechanisms - and only acetylene, benzene, and temperature profiles are required.

It should be reiterated that the flame modeled here, with C/O = 1.1, is not the same as that modeled by Frenklach and Wang, for which C/O = 1.3. However, similar results to that reported by Frenklach and Wang have been obtained here with a simpler algorithm. It is also of interest to compare the calculated surface area with the experimental profile reported for the C/O = 1.3 flame, as shown in Figure 21. Calculations are in only approximate agreement with experiment, but this is expected because of the differing stoichiometries. The richer flame has a higher soot yield and might be expected to have a higher total surface area. Oxidation by OH is important in

Figure 12

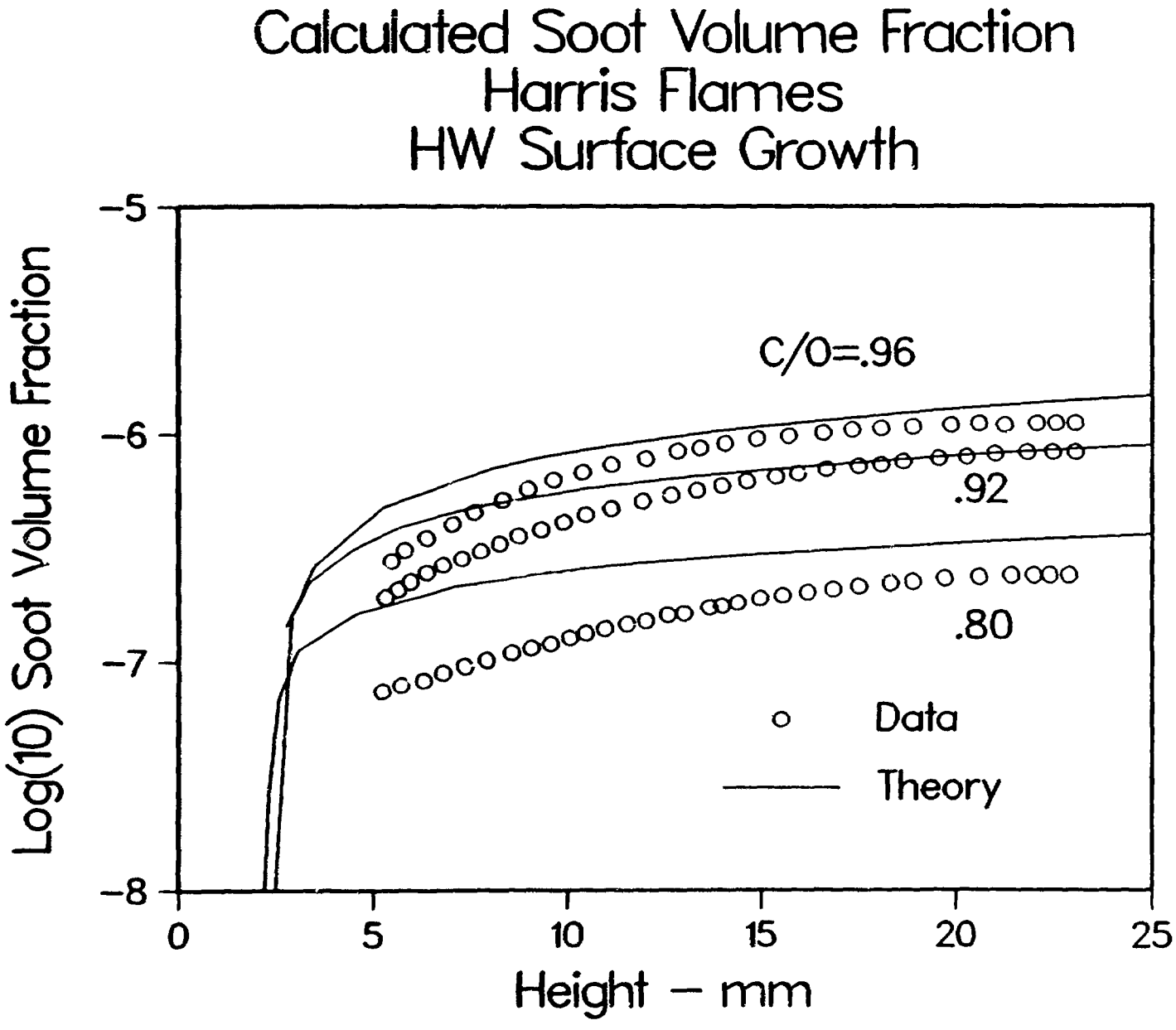
Calculated Soot Volume Fraction
Harris Flames
HW Surface Growth
Log(10) Soot Volume Fraction
-5
-6
-7
-8
C/O=.96
.92
.80
Data
Theory
0
5
10
15
20
25
Height – mm

Figure 13

Calculated Soot Volume Fraction
Harris Flames
5RING Surface Growth

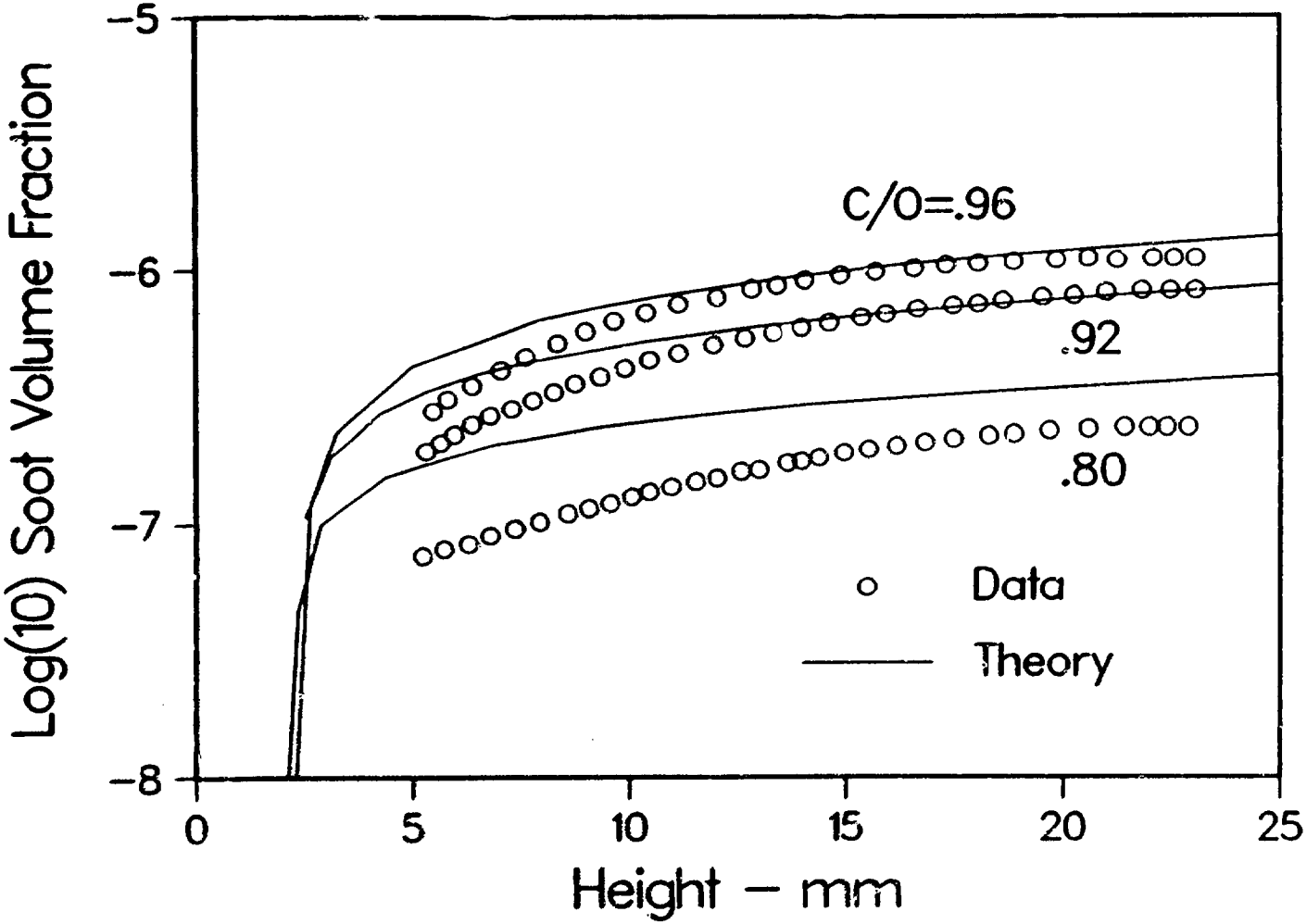

Figure 14

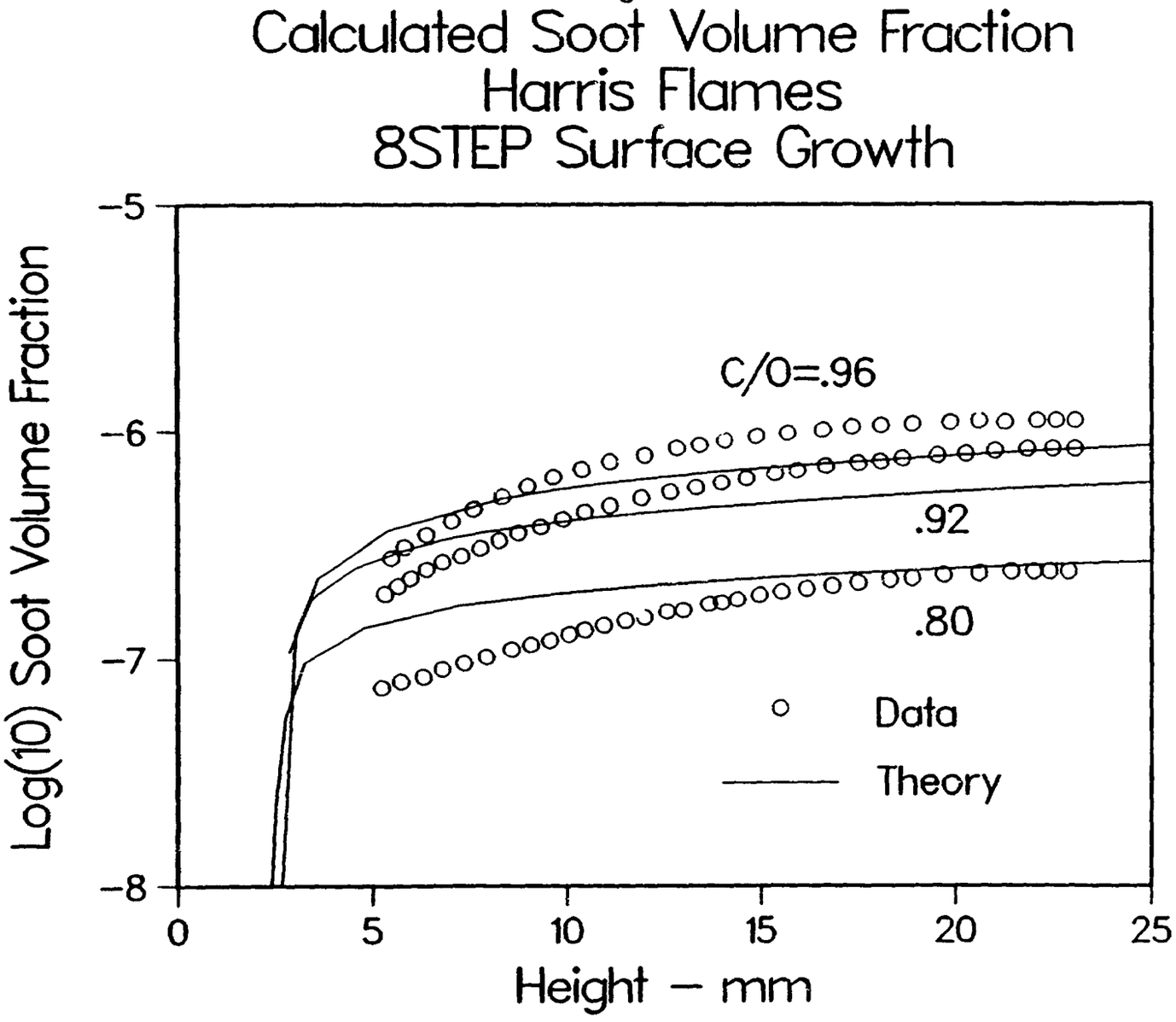
Calculated Soot Volume Fraction
Harris Flames
8STEP Surface Growth
Log(10) Soot Volume Fraction
-5
-6
-7
-8
0
5
10
15
20
25
Height – mm
C/O=.96
.92
.80
Data
Theory

Figure 15

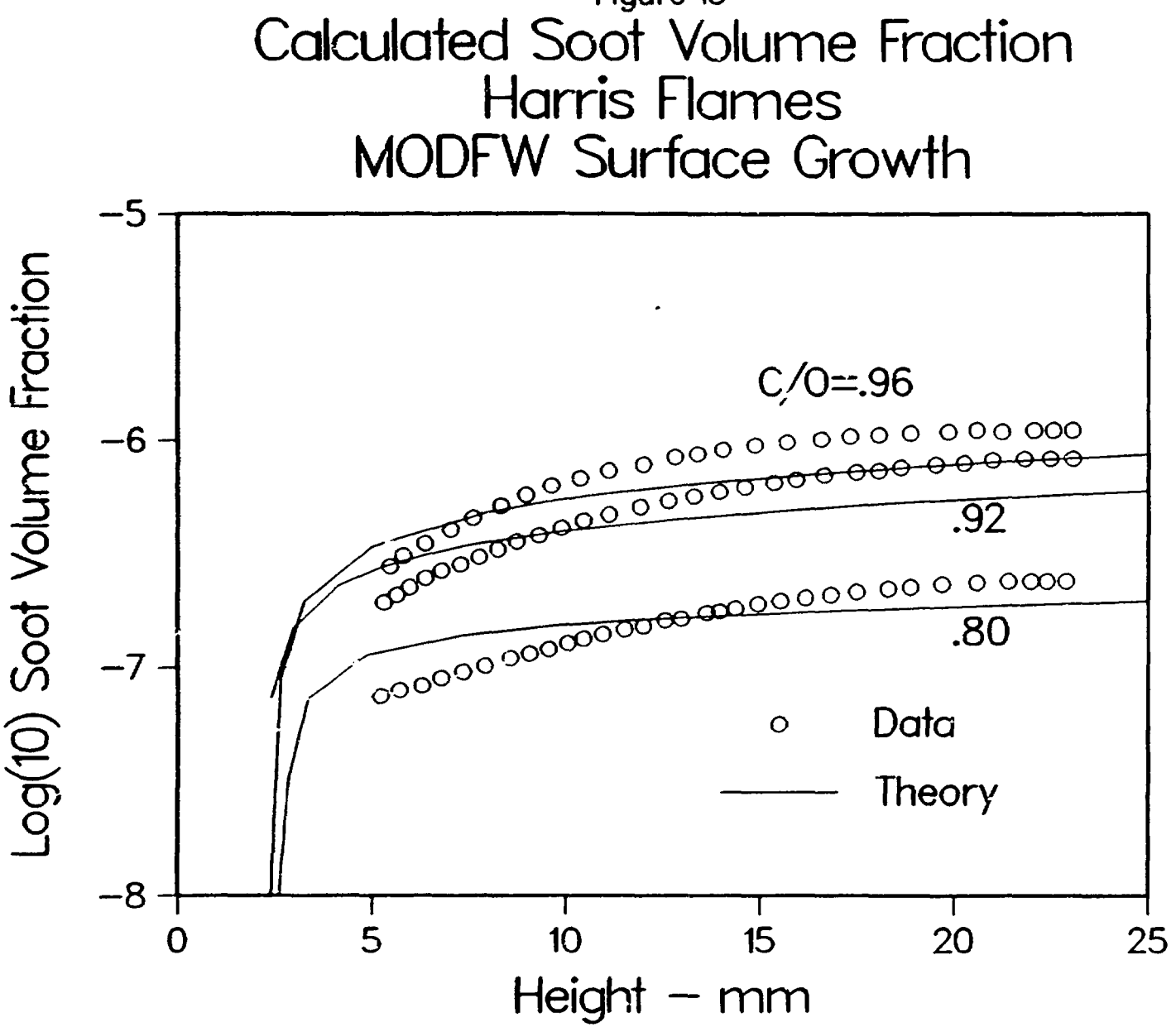
Calculated Soot Volume Fraction
Harris Flames
MODFW Surface Growth
Log(10) Soot Volume Fraction
-5
-6
-7
-8
0
5
10
15
20
25
Height - mm
C/O=.96
.92
.80
Data
Theory

Figure 16

Calculated Soot Volume Fraction
Harris Flames
FW Surface Growth

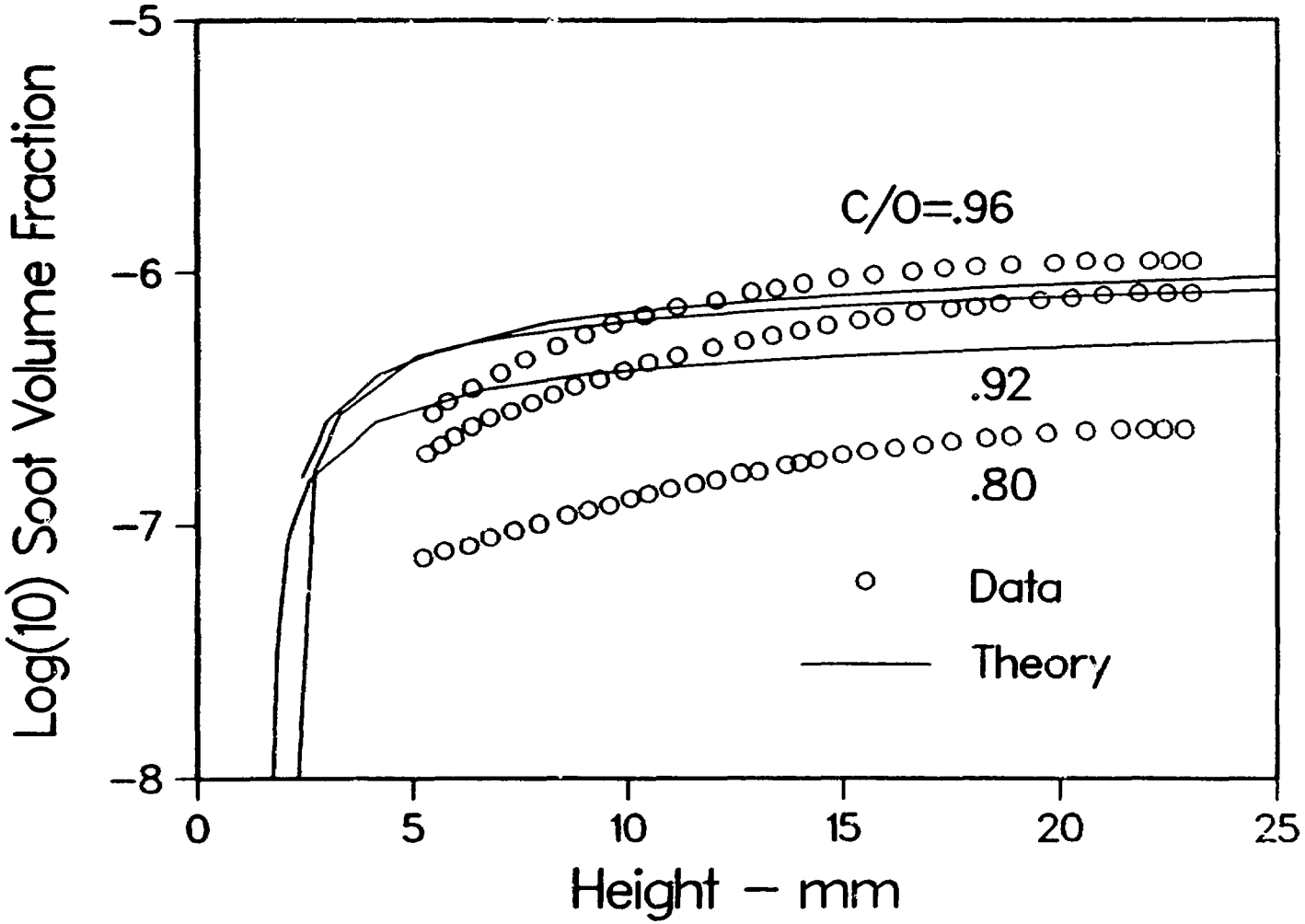

Figure 17

Calculated Soot Volume Fraction
Harris Flames
HW Surface Growth

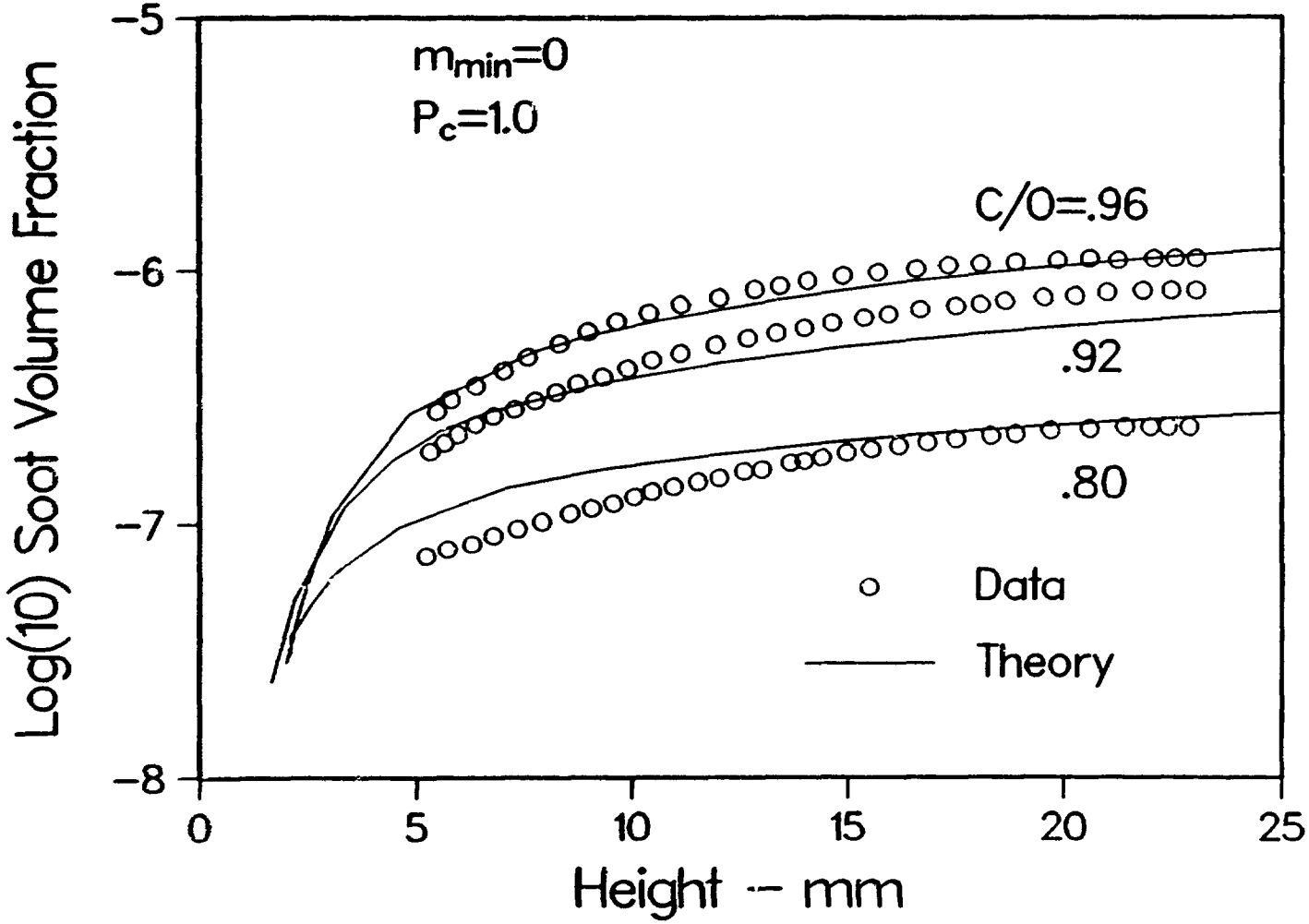

Figure 18

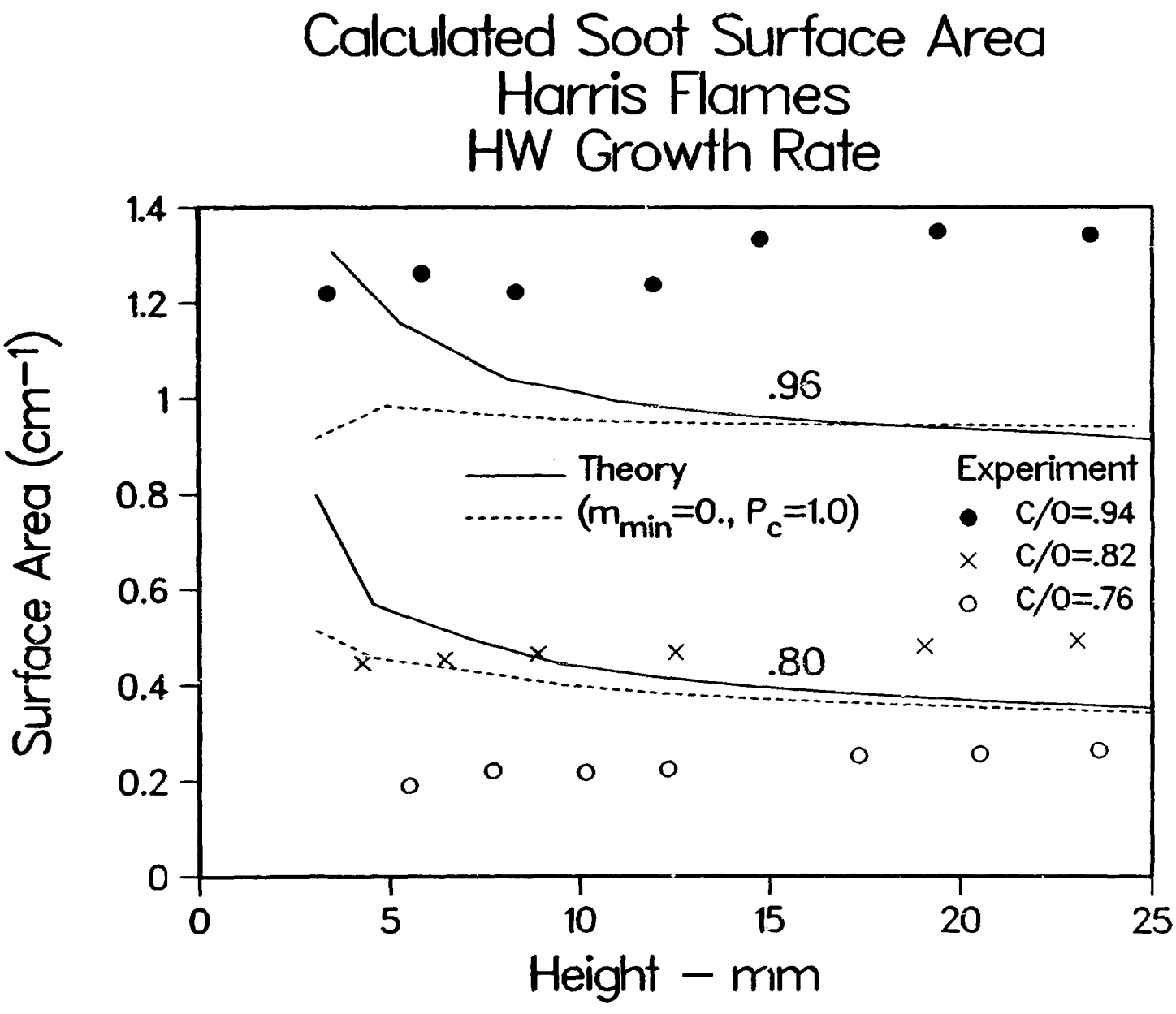
Calculated Soot Surface Area
Harris Flames
HW Growth Rate
Surface Area (cm⁻¹)
Height – mm
1.4
1.2
1
0.8
0.6
0.4
0.2
0
0
5
10
15
20
25
.96
.80
Theory
(m_min=0., P_c=1.0)
Experiment
C/O=.94
C/O=.82
C/O=.76

Figure 19

Calculated Soot Volume Fraction Bockhorn Acetylene Flame Various Growth Models

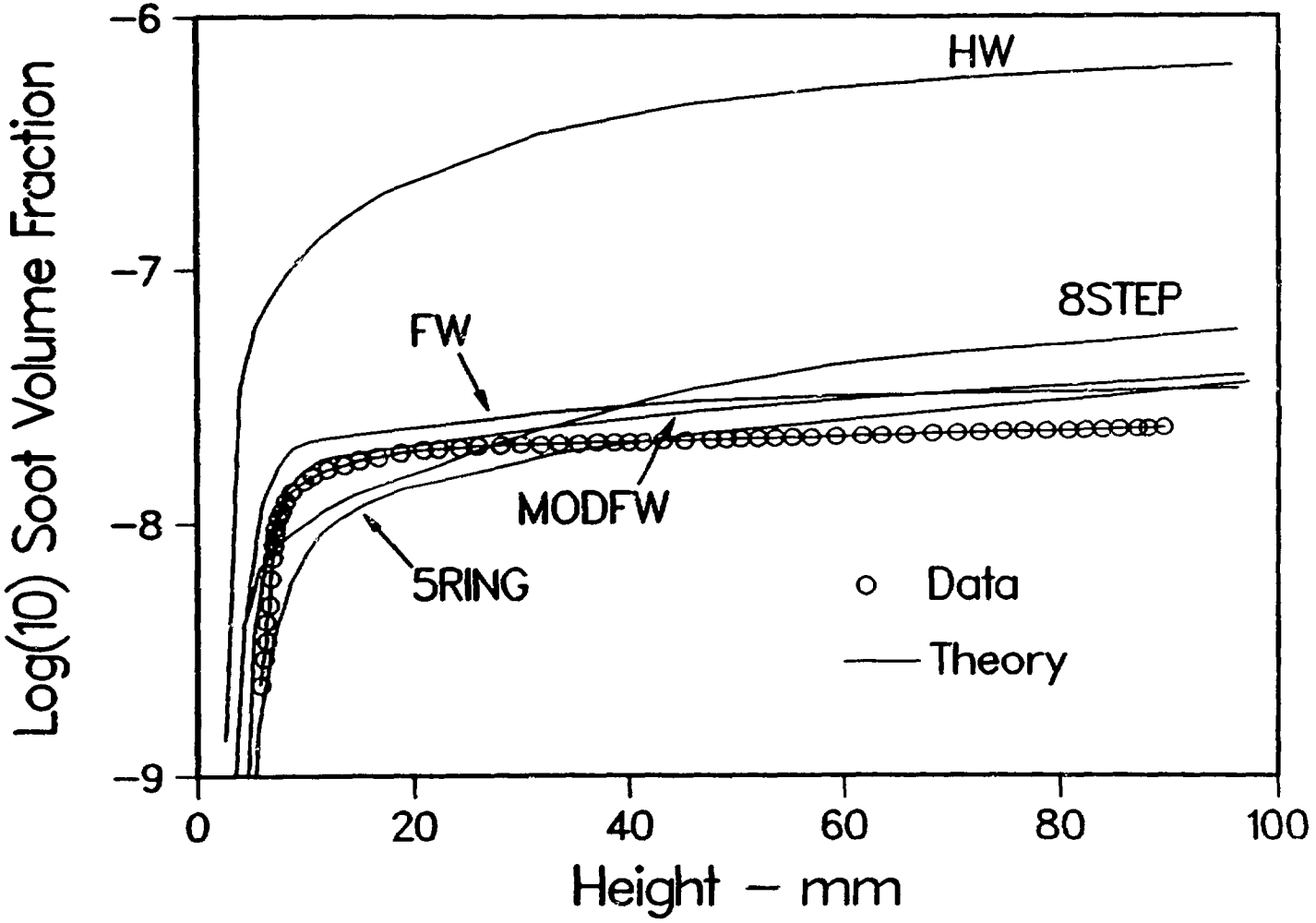

Figure 20

Calculated Soot Volume Fraction Bockhorn Propane Flame Various Growth Models

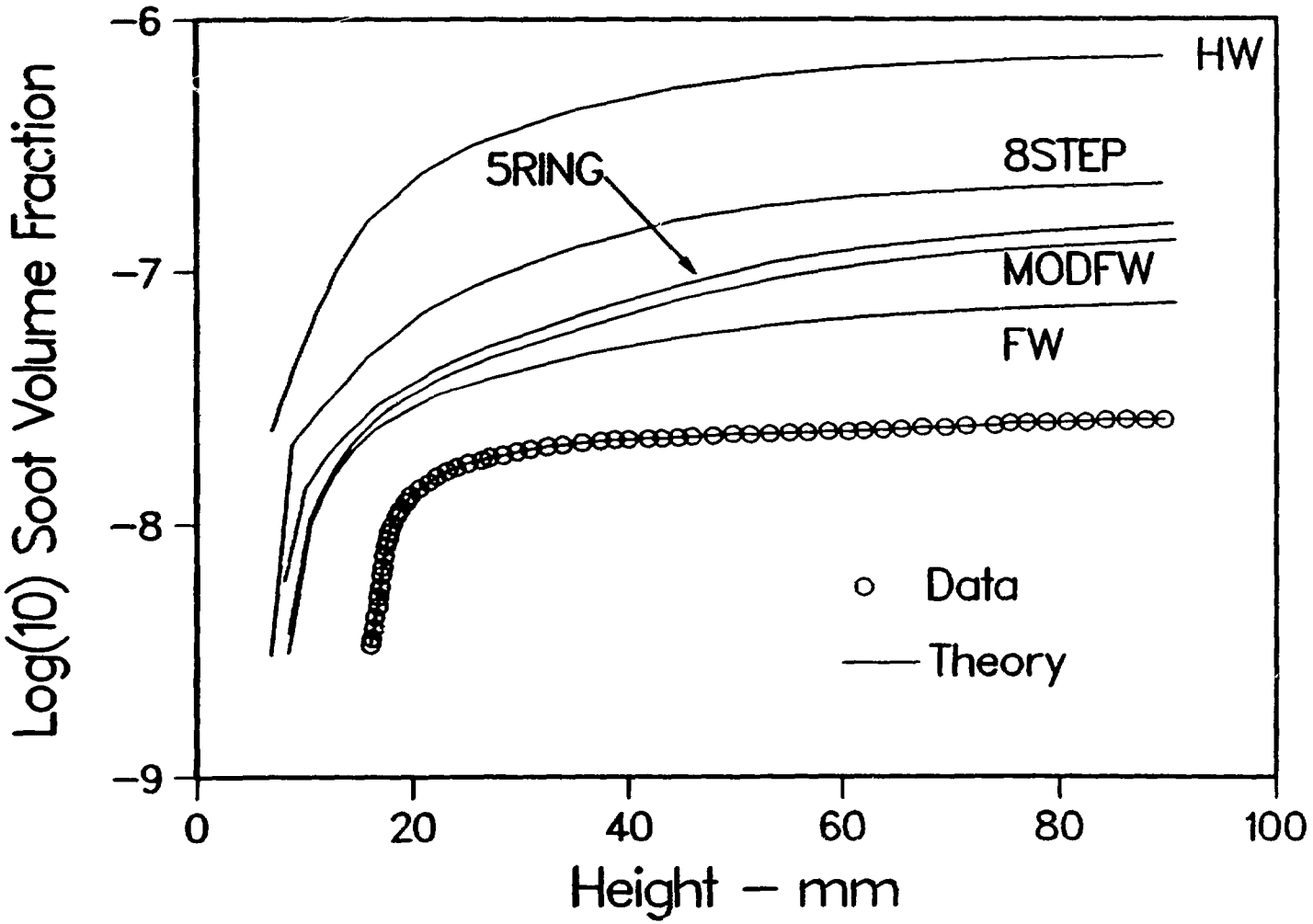

Figure 21

Calculated Soot Surface Area Bockhorn Acetylene Flame

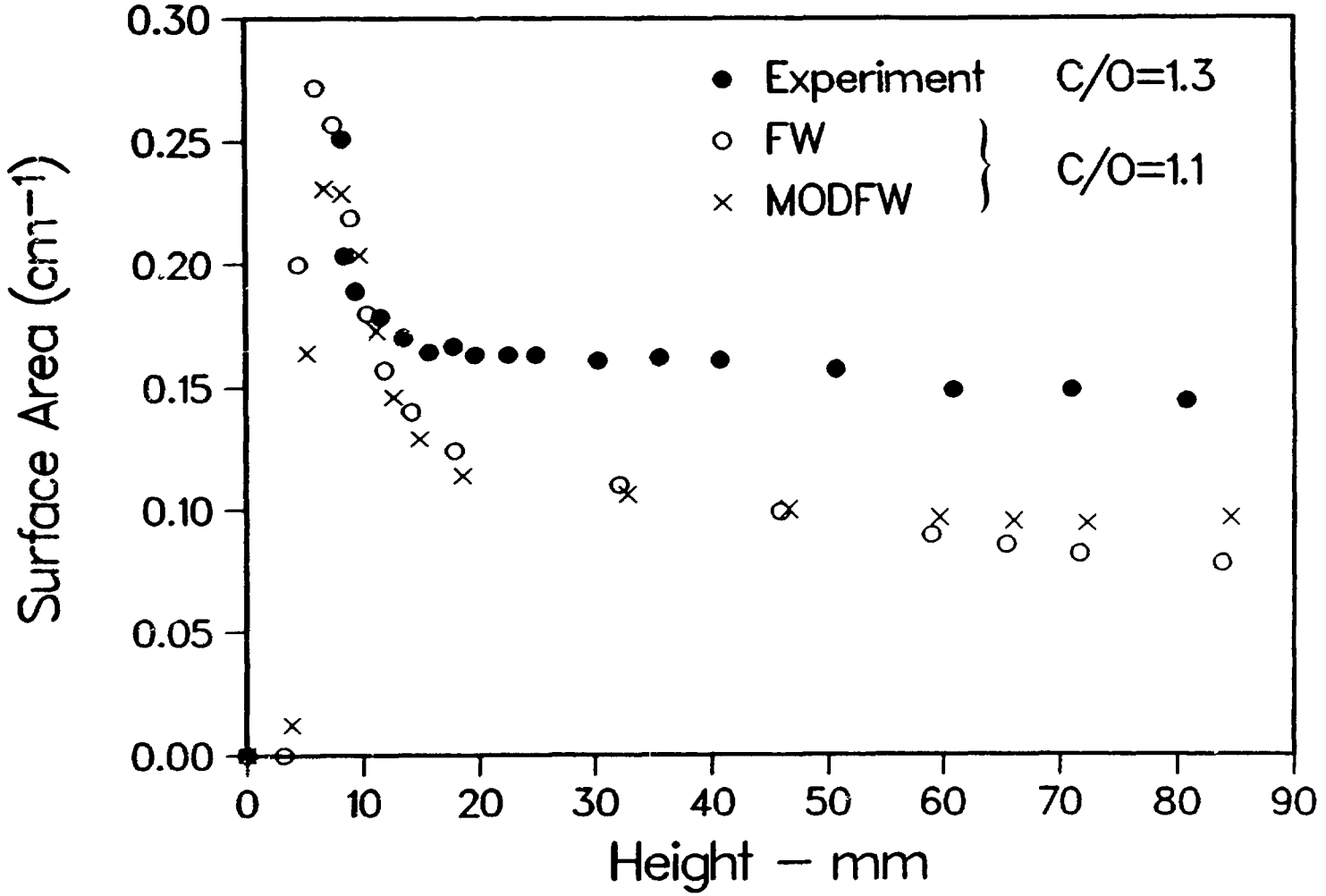

determining the onset of soot in these flames.

For the Bockhorn propane flame, the agreement is generally much less satisfactory for all models, (Figure 20). It is probably the case that introduction of a new steric factor for surface growth in the Frenklach model would result in good agreement. However, it would most likely be on the order of 0.03-0.05, implying a peculiar temperature dependence since the propane flame is typically 100K cooler than the acetylene flame. Given this significant temperature dependence, the fact that the acetylene and propane flames have such similar soot profiles is not understood at this time. As discussed previously, there is an apparent incompatibility between the temperature profile and the other experimental data. It is possible that experimental uncertainties contribute to the lack of agreement for the propane flame. Also of potential interest in modeling this flame is the apparent fact that rapid soot growth occurs in this flame substantially after the peak temperatures and the reaction zone, whereas onset of soot growth for the other flames considered in this study occurs near the flame front and peak temperature zone. This subtle difference may lead to some slightly different controlling processes between these flames.

There is experimental evidence (Haynes and Wagner, 1982; Wieschnowsky, et al., 1988; and Bockhorn, et al., 1984) and theoretical argument involving the surface density of "active sites" (Dasch, 1985; Harris, 1990; and Woods and Haynes, 1991) that the soot growth law is of the form

$$\frac{df_v}{dt} \propto f_v - f_v^* \tag{32}$$

where f_v^* is an equilibrium, asymptotic value. A consequence of this is that a plot of rate of change of volume fraction versus volume fraction should be linear. A surface growth law proportional to total soot surface area can be consistent with Equation 32 if the total surface area is constant and the surface reactivity has a simple exponential decay (Dasch, 1985); therefore, we tested our simulations by making such plots from the best theory-experiment comparisons available from Figures 22-24. For the Harris 0.96 case, there is certainly a region of such linearity at the longer times (Figure 22) where most of the experimental data exist, but in the 0.8 case it is hard to identify any such linear region (Figure 23). Similarly, the acetylene simulation seems somewhat ambiguous (Figure 24), but the region of rapid growth between volume fractions of 10^{-8} and 2×10^{-8} could be said to conform to this law. Our results are not totally inconsistent with the growth law, Equation 32, but do not yet confirm it, either. Even the experimental data (Bockhorn, et al., 1984) seem to have only a limited regime over which Eqn. 32 is valid.

Sensitivity Studies

The sensitivity of the C/O = 0.96 case (ethylene) to the number of size classes is exhibited in Figure 25. The number of classes is being varied, and we specify a mass threshold such that particles of mass less than this value cannot coagulate. As seen, the volume fraction tends to converge quite rapidly, with 3-5 sections giving a good approximation; the surface area has similar convergence properties. The value of volume fraction with 40 size classes differs by no more than one per cent from the value obtained with 5 classes. The optical diameter converges more slowly, requiring 25-30 sections.

Some uncertainty is associated with the proper value of the sticking coefficient, and the sensitivity of the theoretical predictions is given in Figures 26 and 27. Lowering the sticking probability below unity increases the surface area and contributes to much more predicted soot growth for the Harris 0.96 case. For the Bockhorn acetylene flame, however, the sensitivity is less, because the surface growth rate is relatively small except for a limited region low in the flame. The sensitivity of

Figure 22

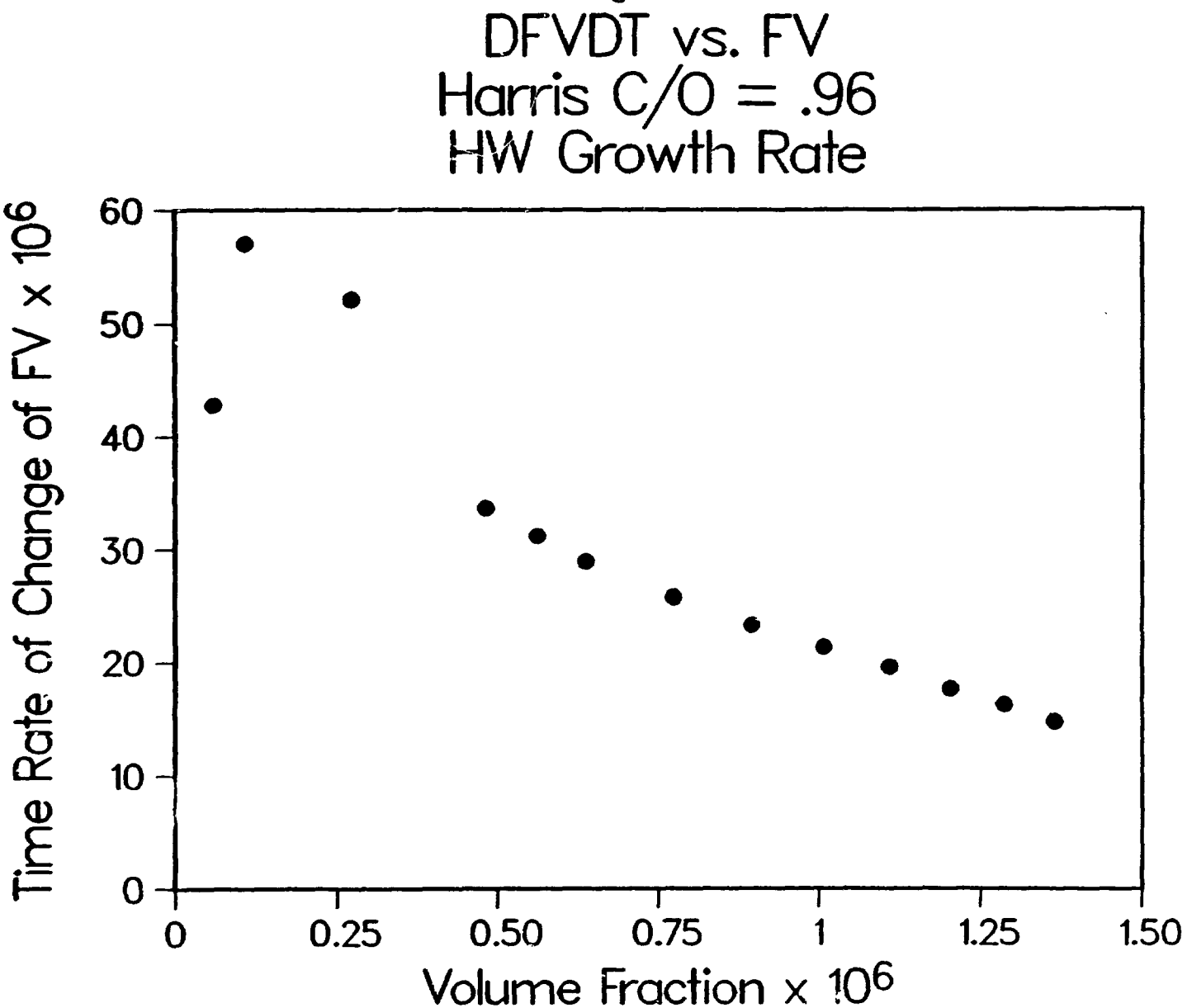
DFVDT vs. FV
Harris C/O = .96
HW Growth Rate
Time Rate of Change of FV x 10^6
60
50
40
30
20
10
0
0
0.25
0.50
0.75
1
1.25
1.50
Volume Fraction x 10^6

Figure 23

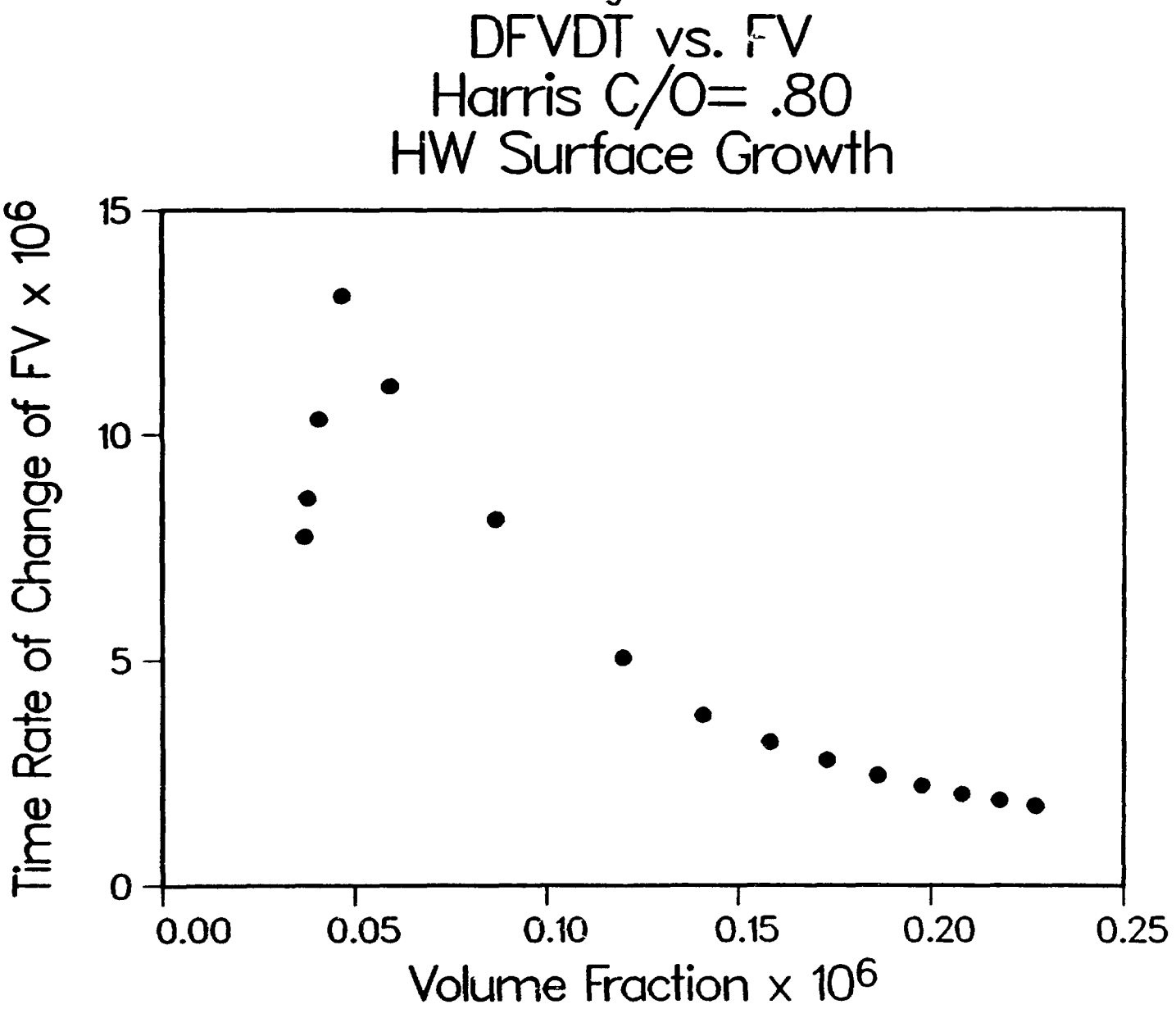
DFVDT vs. FV
Harris C/O= .80
HW Surface Growth
Time Rate of Change of FV x 10⁶
15
10
5
0
0.00
0.05
0.10
0.15
0.20
0.25
Volume Fraction x 10⁶

Figure 24

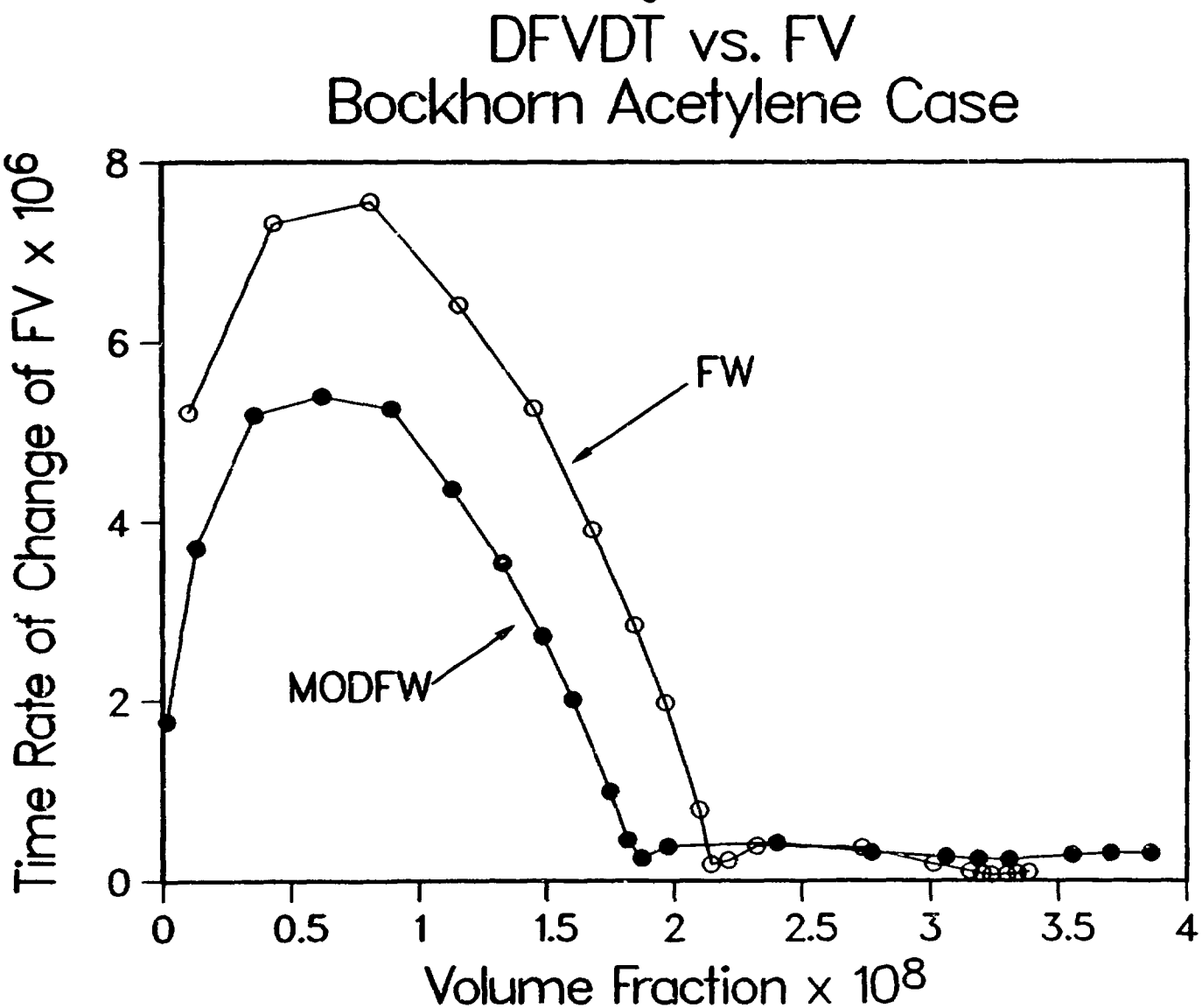
DFVDT vs. FV
Bockhorn Acetylene Case
Time Rate of Change of FV x 10^6
8
6
4
2
0
FW
MODFW
0
0.5
1
1.5
2
2.5
3
3.5
4
Volume Fraction x 10^8

Figure 25

Convergence Properties of Soot Parameters
C/O = .96 Flame
HW Growth Rate

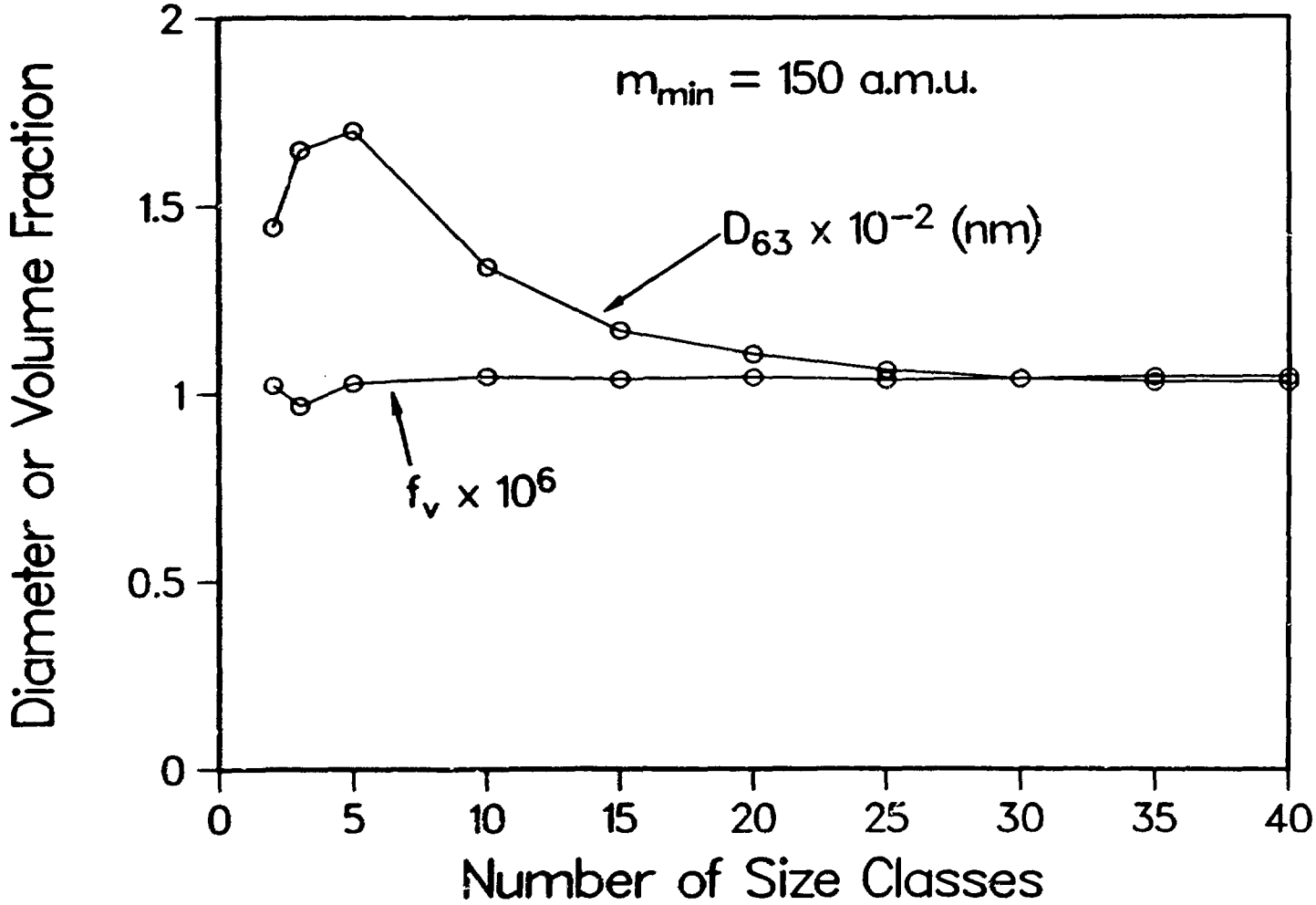

Figure 26

Sensitivity to Sticking Probability
Harris C/O = .96
HW Growth Rate

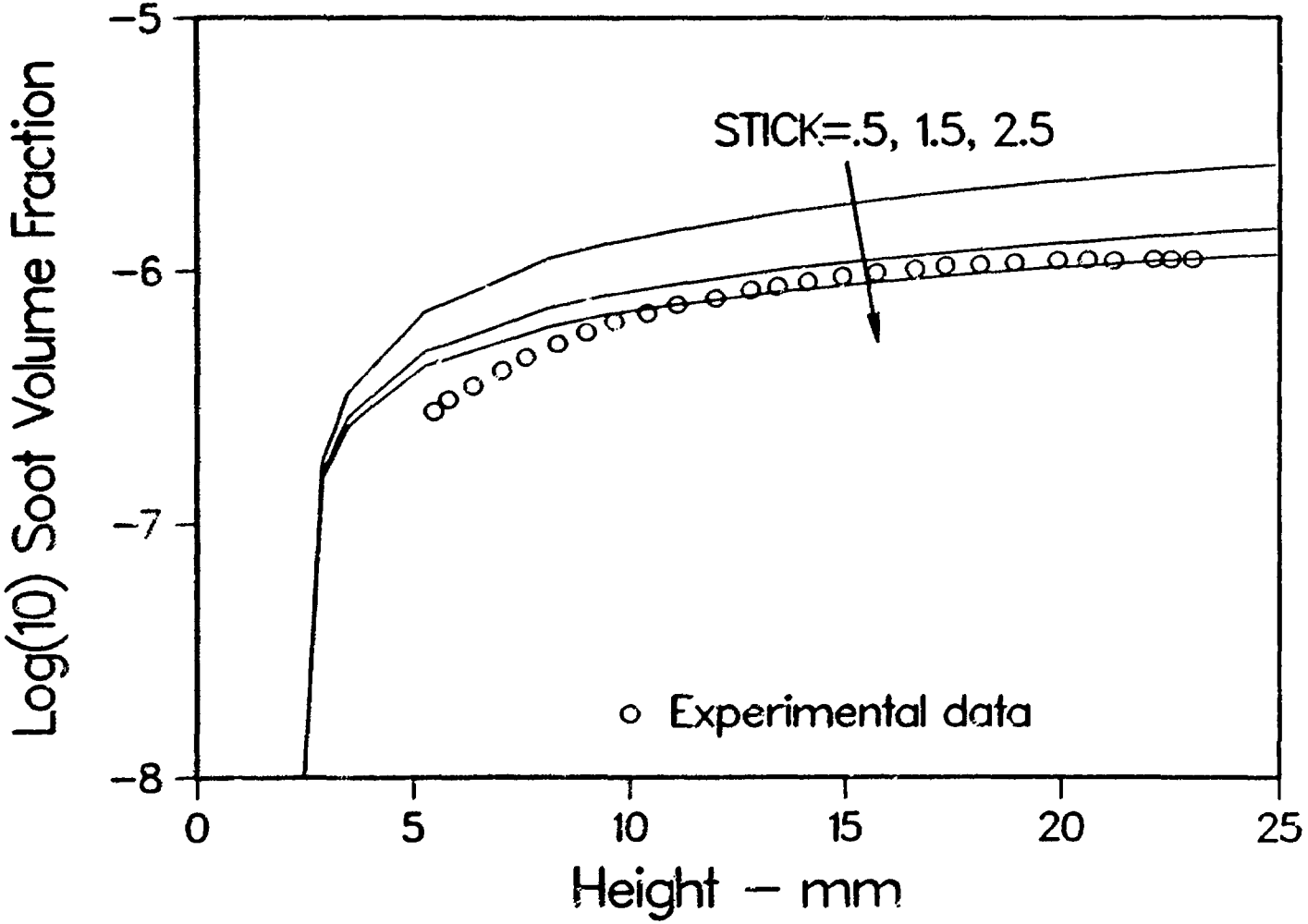

Figure 27

Sensitivity to Sticking Probability
Bockhorn Acetylene Flame
MODFW Growth Rate

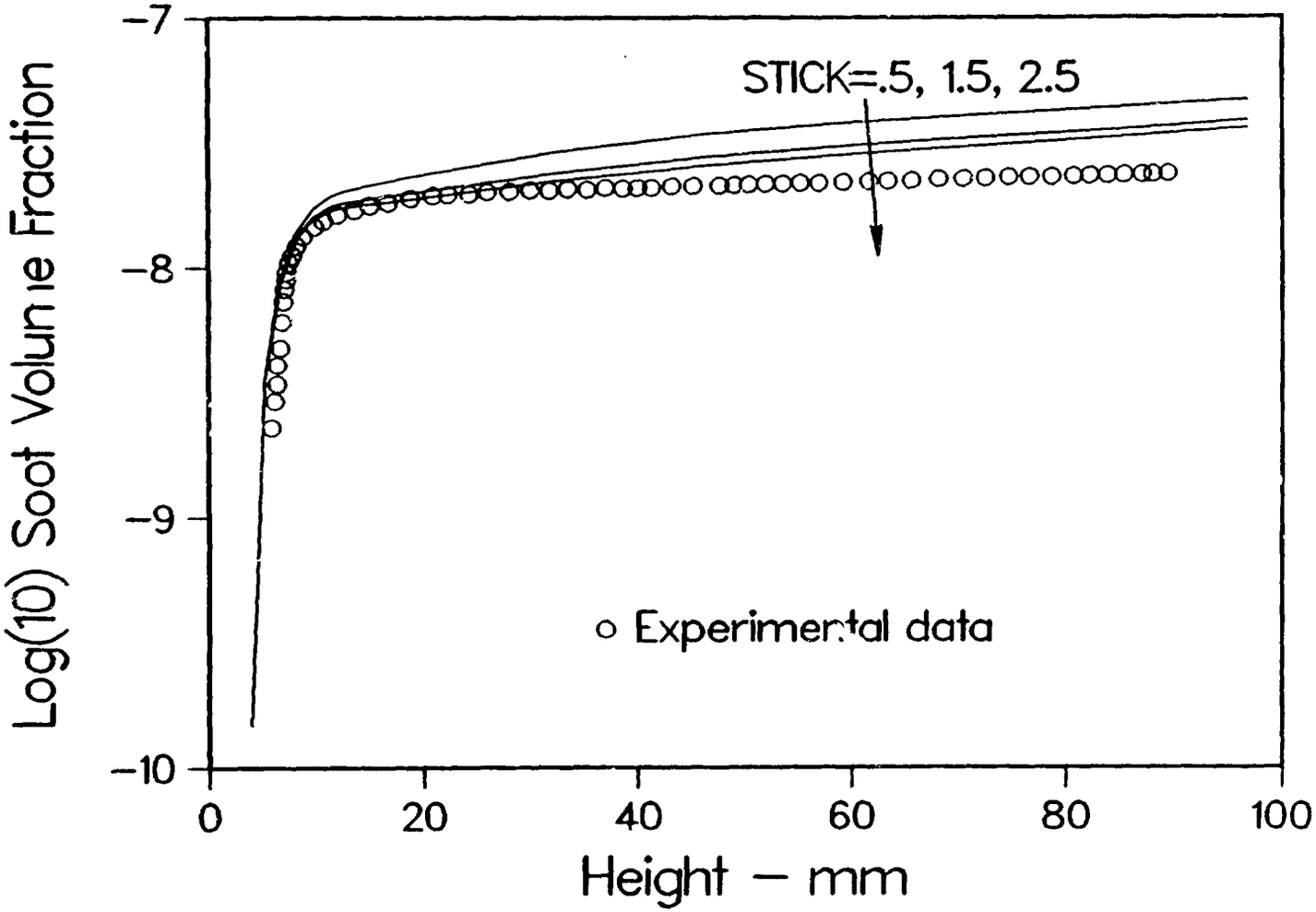

predicted soot volume fraction to coalescence sticking probabilities is tied to the magnitude of the local surface growth rates. Particle number densities and sizes can be expected to be much more sensitive.

If the inception or nucleation source rate is multiplied by constant factors, some impression of the sensitivity of our predictions to source rate can be gained, as shown in Figures 28-30. For the Harris 0.96 and 0.8 cases, multiplication by a factor of ten results in so many inception nuclei that all of the acetylene is scavenged, and growth essentially stops. Similarly, a large increase is predicted for the acetylene flame (Figure 30). The factor of ten increase over a value determined by the benzene production rate is probably unphysical, however. More interesting is the result of dividing the nominal source rate by a factor of ten. Reductions of a factor of two to three are predicted in the soot yields for the Harris flames. For the acetylene flame, the sensitivity to reduced inception rate is somewhat greater, probably because of a relatively slow overall surface growth rate. These simulations probably overstate the sensitivity to inception rates since, when the inception rate is reduced from the value determined by the benzene production rate, the inception size class should be moved to larger particle sizes, giving slightly less sensitivity than has been shown here.

The factor of four to five increase and the factor of two to three decrease in soot formation for the Harris and Weiner flames (see Fig. 28-29) when inception is respectively increased and decreased by a factor of ten was at first surprising, especially in light of recent suggestions. Kennedy, et al., (1990) argued that as soot concentrations in flames increase, the dependence on soot inception decreases and the quantity of soot produced is dominated by growth processes. The recent experiments by Kent and Honnery (1991) support these arguments. The opposing result from our model under selected conditions, we believe, is due to the fact that as inception rates decrease, the losses in surface area due to coalescence are less effective, and relatively high soot growth rates result. These opposing trends highlight the complexity of the soot formation process and the fact that conclusions drawn from one study may not be necessarily applicable to another set of conditions.

Figure 31 displays for the Harris and Weiner 0.96 case the predicted sensitivity to the mass of small particles excluded from coalescence. The curves correspond to excluded masses of approximately 0, 150, 300, and 450 a.m.u. respectively. As seen, the sensitivity is significant. In future efforts, we hope to include the recent results of Miller (1990) regarding size dependent sticking rates for polyaromatic hydrocarbons. In the previous calculations, coalescence was found only to be important for particles whose mass exceeds 800 a.m.u., much larger than those assumed to coalesce in the present study. As stated previously, identification of a more realistic (lower) inception rate will enable the model to address more reasonable descriptions of the coalescence processes.

The importance of temperature to the soot formation process is well established (Glassman, 1988). In the section on gas-phase chemistry, the effect of temperature on benzene profiles (which in turn affects inception rates) was shown to be significant. Changes in inception rates as just discussed lead to nearly linear changes in soot production for most of the flames examined here. Other species, particularly H-atoms which may affect specific surface growth rates, are also a strong function of temperature. In addition, temperature may affect rate constants used in the calculation of specific surface growth rates. To examine a portion of this complex dependence on temperature, we considered the effect of uncertainties in the temperature profile on predictions using just the HW mechanism, since this mechanism only depends on acetylene concentrations, which are weak functions of temperature. For the low pressure acetylene flames, and assuming a steric factor of 0.1 as well as the inception rates used for the base temperature case, soot profiles were calculated with temperature profiles shifted 100K above and 100K below the experimental values. These shifts resulted in about a 40% shift in the specific growth rates as well as a 30 to 50% shift in soot production. The changes in soot production due to shifts in temperature are shown in Fig. 32. Accompanying shifts in benzene profiles can be expected to enhance these differences.

Figure 28

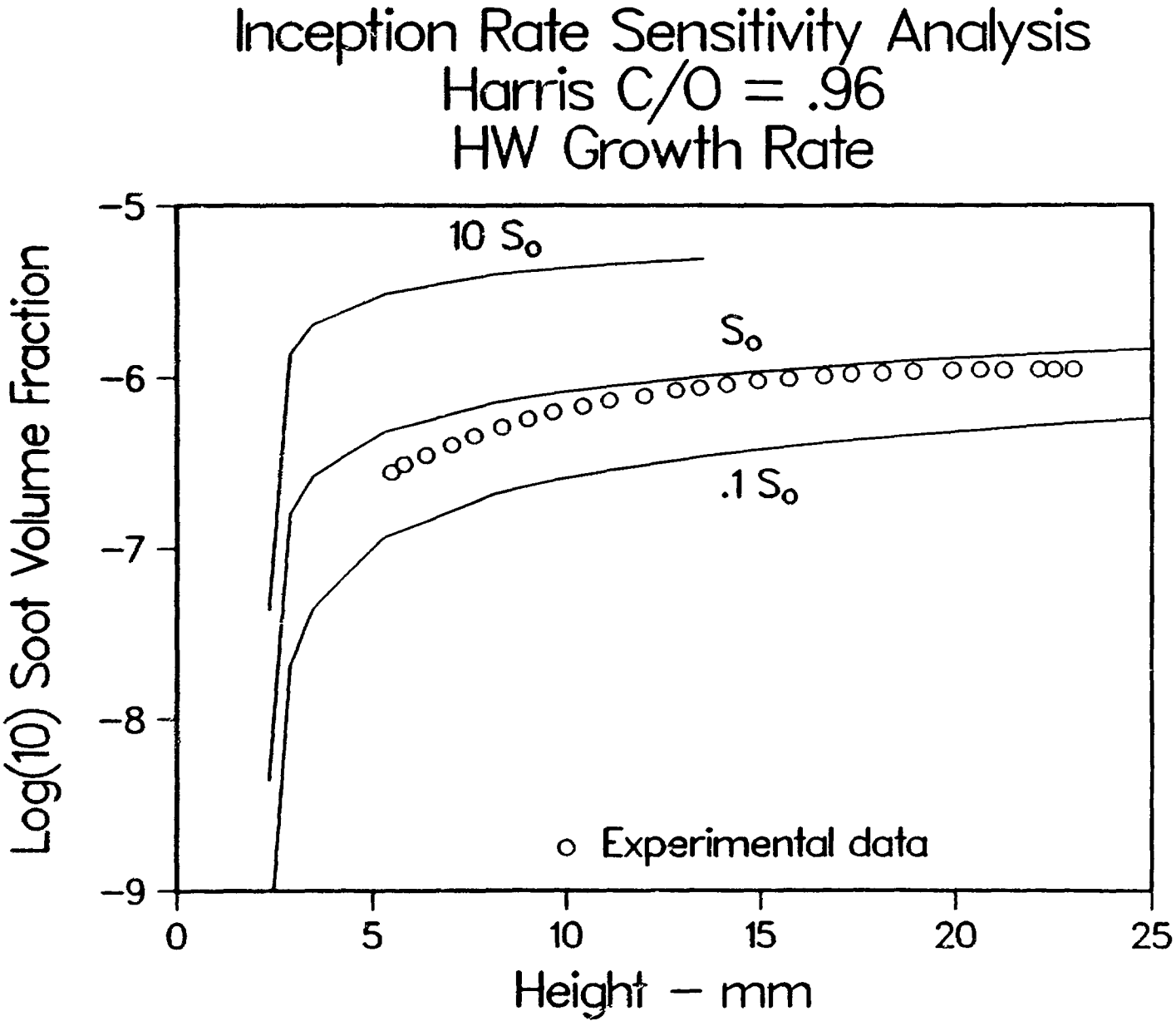
Inception Rate Sensitivity Analysis
Harris C/O = .96
HW Growth Rate
10 S_o
S_o
.1 S_o
o Experimental data
Log(10) Soot Volume Fraction
-5
-6
-7
-8
-9
0
5
10
15
20
25
Height – mm

Figure 29

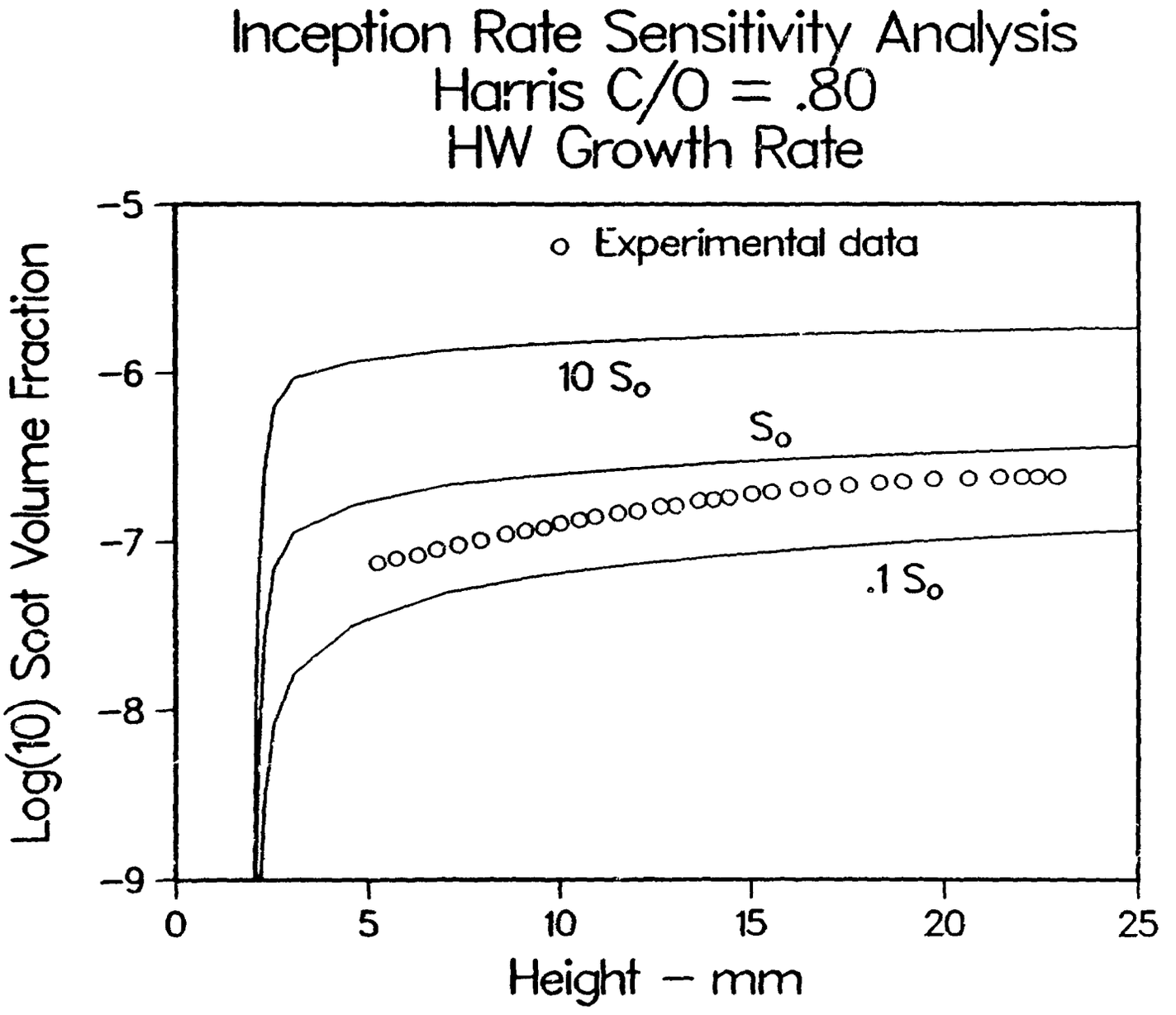
Inception Rate Sensitivity Analysis
Harris C/O = .80
HW Growth Rate
o Experimental data
10 S_o
S_o
.1 S_o
Log(10) Soot Volume Fraction
-5
-6
-7
-8
-9
0
5
10
15
20
25
Height – mm

Figure 30

Predicted Sensitivity to Source Rate Bockhorn Acetylene Flames MODFW Surface Growth

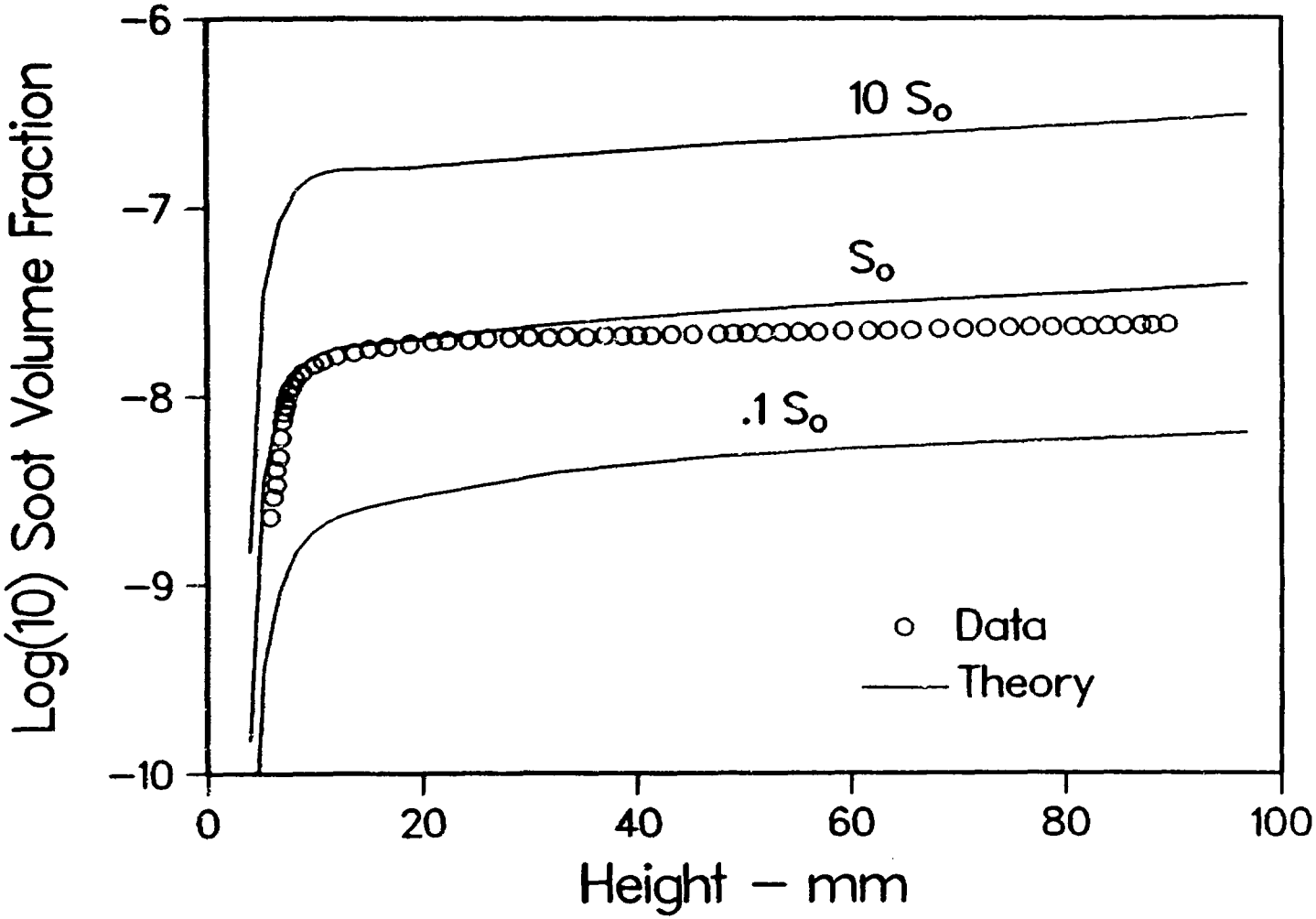

Figure 31

Sensitivity to Coagulation Exclusion
Harris C/O = .96
HW Growth Rate

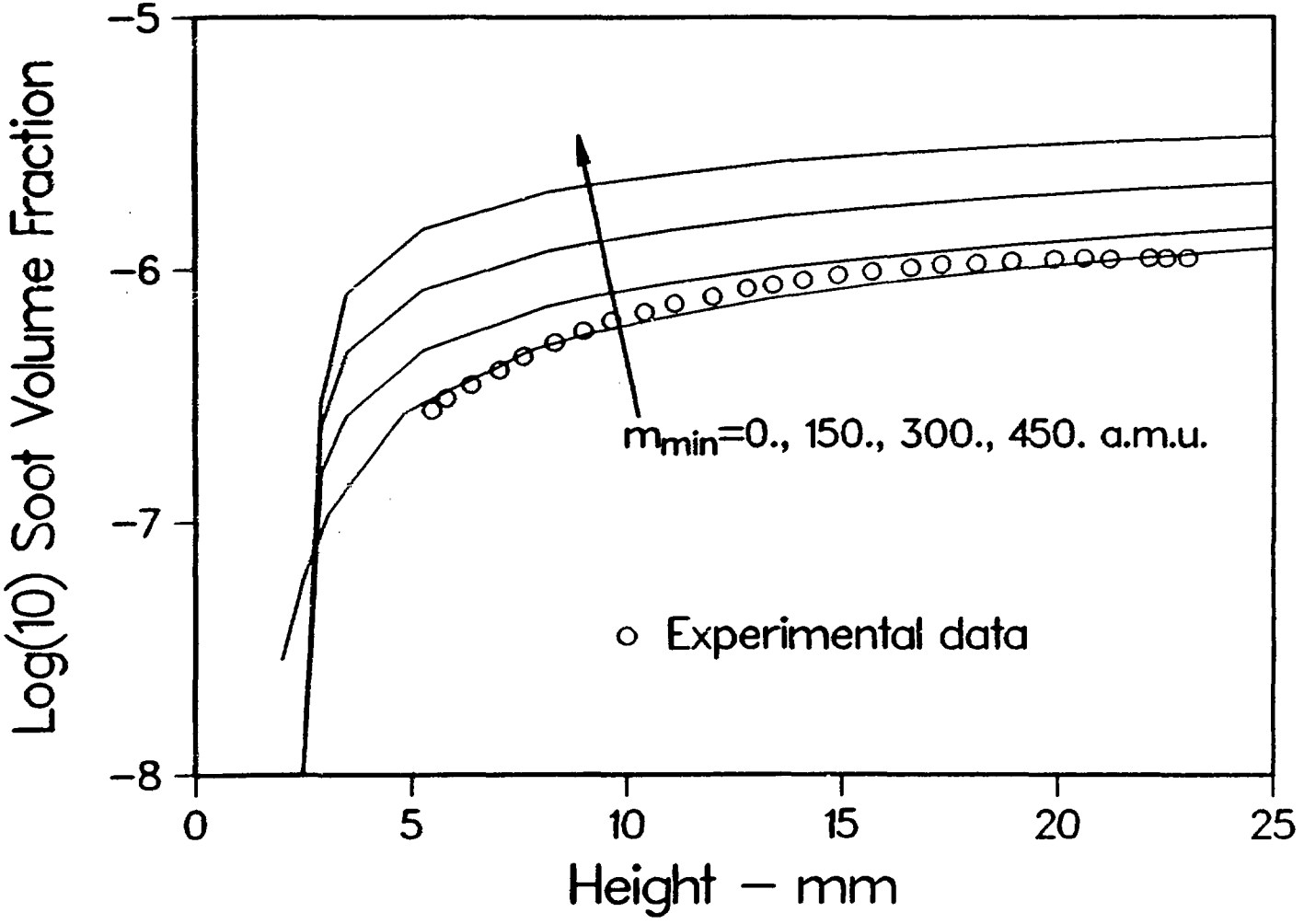

Figure 32

Predicted Temperature Sensitivity of Soot Growth
Acetylene Flame
HW Growth Rate w. Steric Factor=0.1

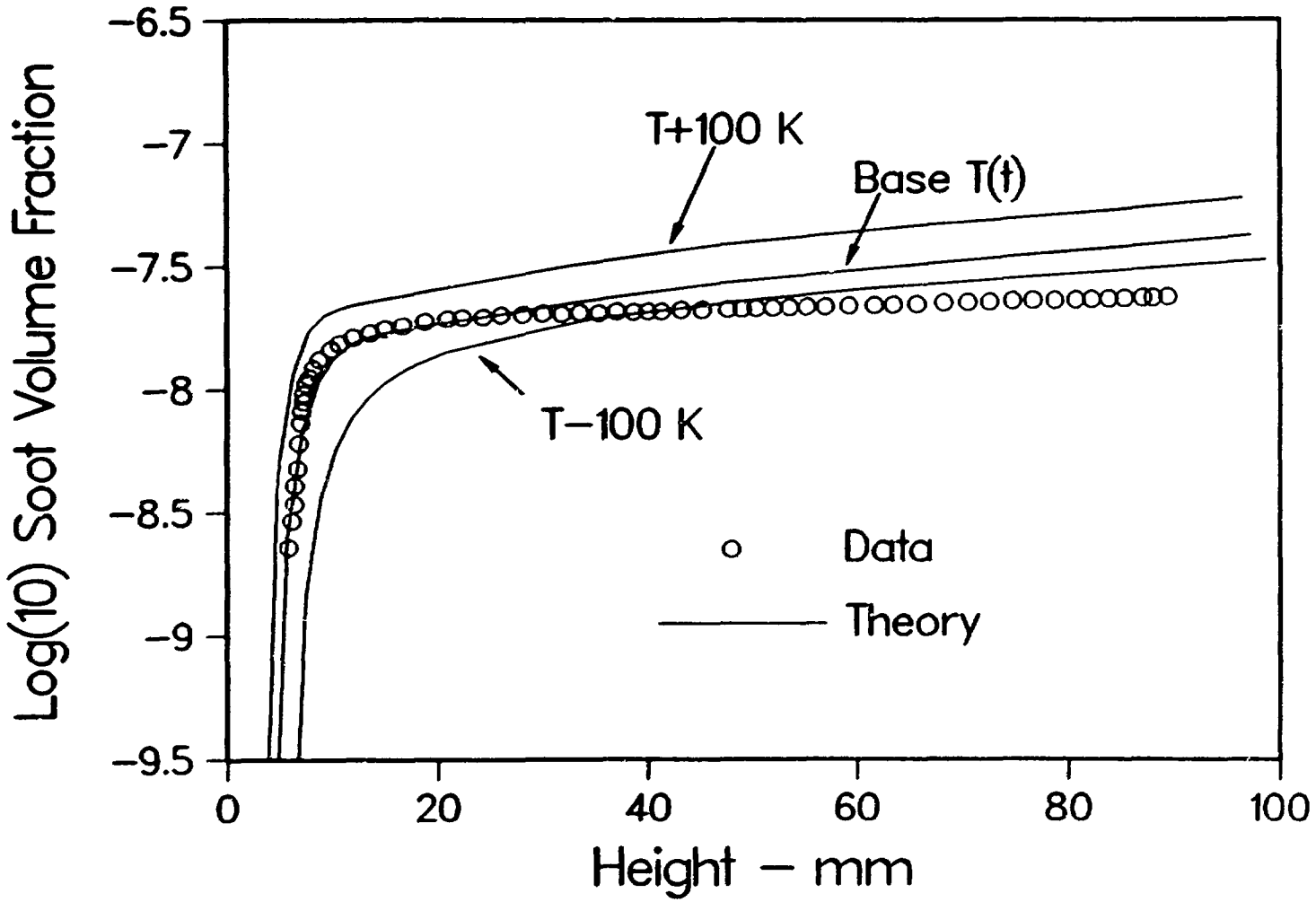

Oxidation plays an important role because of its competition with growth processes. As described previously, soot growth calculations are initiated at the point at which growth first begins to dominate over oxidation. The relative importance of oxygen and hydroxyl radicals changes as flame conditions are altered. For the lower temperature, atmospheric pressure flames of Harris and Weiner, oxygen is the dominant oxidizer. For the higher temperature, low pressure flames of Bockhorn, et al., hydroxyl radical concentrations are much higher and OH becomes the dominant oxidizer as molecular oxygen is depleted in the flames. To examine the sensitivity of soot formation to uncertainties in the calculated OH-radical profile, we doubled the OH concentration. A substantial shift (about 5 mm) was observed in the onset of soot formation, although the total volume fraction rapidly approached the soot profile without the OH modification. These results suggest that uncertainties in OH and oxygen concentrations and/or in rate constants and processes describing the oxidation lead to uncertainties in the point of soot onset and perhaps in the early growth rates, but they do not dramatically alter total soot production. Consideration of O_2 and OH profiles relative to these issues can provide some further insight for the effect of oxidation. Oxygen is depleted dramatically in the flame front as the oxygen is consumed by the fuel. Because its precipitous drop, uncertainties in this profile and in rates of oxidation by O_2 probably have a small effect on the location of soot onset. Therefore, lower temperatures, high pressures will be less sensitive to uncertainties in oxidation processes. Hydroxyl radicals, however, peak within the flame front and slowly decay downstream as the flame cools and the radical concentrations relax to equilibrium conditions. Since this profile is so gradual, uncertainties in absolute concentrations and in rates and mechanisms can lead to substantial errors in predicting the onset of soot formation. The difficulties in accurately predicting the soot profiles for the propane flame could in part be due to uncertainties in predicting the hydroxyl radical concentrations. This analysis indicates that at elevated temperatures and low pressures, when hydroxyl radical concentrations are large, soot predictions may be quite sensitive to uncertainties in oxidation processes.

Summary of Assumptions

These simulations have involved numerous assumptions that have been discussed at various points in the text. These are summarized below.

1. The temperature profile is assumed.
2. Diffusion of higher order hydrocarbons (that is, polyaromatic hydrocarbons) is neglected.
3. Species profiles (except for acetylene) are unperturbed by soot formation. The soot growth and kinetics models are uncoupled.
4. The kinetics model predicts concentrations of gas-phase species with sufficient accuracy.
5. The rate at which benzene is formed is assumed to be the rate of inception; therefore, we assume the actual inception rate is proportional to the rate of benzene formation not only within a given flame but also from flame to flame.
6. Polyaromatic hydrocarbons can be treated as soot (mass, agglomeration processes, growth rates, etc.) with a size-independent density of 1.8 g/cc.
7. Particles coalesce with a sticking coefficient independent of size class.
8. Soot particles grow as individual spheroids with no aggregate formation. Particles are assumed to coalesce upon collision. All surface mass deposition is due to acetylene.
9. Diffusional processes are fast relative to soot growth processes so that concentrations at the surface of a particle can be equated to free stream values. Surface growth occurs at a rate proportional to the particle area.

Conclusions

An analytical model of soot formation in laminar, premixed flames has been presented which is based on coupling the output of flame chemical kinetics simulations with a sectional aerosol dynamics algorithm for spheroid growth. A provisional particle inception model in which benzene acts as a surrogate for the inception species is employed. Justification for the use of this simplified model is provided and its use is motivated by a desire to develop a simple procedure which might be useful for predictions in more practical flames. Surface growth has been based on experimental measurements and ab initio calculations using various possible mechanisms for the surface chemistry. In the latter, the surface growth rate becomes a function of the local values of certain gas phase species concentrations and the gas temperature. Adjustments were made to rate constants for some reactions in order to improve agreement with experiment. Such adjustments, however, were made within the bounds of uncertainty associated with the rates, and the overall mechanisms are presented only as possible explanations for observed growth rates. Detailed comparisons have been made with various flame data by using experimental temperature profiles and calculating profiles of species concentrations needed for the inception rate and surface growth/oxidation calculations. Most of the models appear to overestimate soot production high in the flames. This overestimation is undoubtedly due to the fact that none of the mechanisms include effects due to particle ageing. Recent suggestions that decay of H-atoms is the cause of this 'ageing', although plausible, are inadequate because of differences between the spatial (or temporal) dependence of the decay in the H-atom profiles and the fall-off in specific growth rates observed in laboratory flames. Among the various models for the soot surface growth, best overall agreement is obtained with a modified form of the approach taken by Frenklach and Wang. The result is an analysis that is highly efficient; accurate soot volume fraction calculations can be obtained with only a few growth equations. While various aspects of this simple model can be challenged, it yields agreement with experiment that is comparable to that obtained using more elaborate models.

At least one alternative mechanism was identified (MODFW) which avoided the assumption of a high temperature steric factor, yet which reproduced growth profiles while also providing a linear df_v/dt vs. f_v relationship. The FW mechanism was found to be deficient in that it does not properly describe the stoichiometric dependence observed in the Harris and Weiner flames, while the very simple HW expression could describe these flames as well as the acetylene flames (when the high temperature steric factor is used). Sensitivity analyses have been performed for parameters such as temperature, oxidation, number of size classes, sticking coefficients, inception rates, and coalescence of low molecular weight polyaromatic hydrocarbons. Each of these can have a significant effect on predictions of soot concentration depending on specific flame conditions.

Acknowledgements

This work has been sponsored in part by the Air Force Office of Scientific Research (AFSC), under Contracts No. F49620-88-C-0051 and F49620-85-C-0012. The United States Government is authorized to reproduce and distribute reprints for governmental purposes notwithstanding any copyright notation hereon. The authors are indebted to Dr. Julian Tishkoff, AFOSR contract monitor, for his support. The authors would like to express their appreciation to R. Gelbard for his advice and assistance on matters concerning the aerodynamics analysis. In addition, we would like to thank H. Bockhorn, M. Frenklach, I. Glassman, J. Howard, I. Kennedy, and R. Santoro for many fruitful discussions as well as for their contributions to the literature which helped to guide this research. The able assistance of K. Wicks and H. Hollick in the preparation of the manuscript and figures is gratefully acknowledged.

REFERENCES

E. F. Arefeva, I. S. Rafalkes, and P. A. Tesner, *Khimiya Tverdogo Topliva*, 11:113, (1977).

T. R. Barfknecht, *Prog. Energy Combust. Sci.*, 9:199-237, (1983).

S. W. Benson and H. E. O'Neal, *Kinetic Data on Gas Phase Unimolecular Reactions*, NSRDS-NBS 21, February, (1970).

S. Bhattacharjee and W. L. Grosshandler, "Effect of Radiative Heat Transfer on Combustion Chamber Flows", presented at Western States Sectional Meeting of Combustion Institute, Salt Lake City, March, (1988).

H. Bockhorn, F. Fetting, A. Heddrich, and G. Wannemacher, *Twentieth Symposium (International) on Combustion*, The Combustion Institute, p. 979, (1984).

H. Bockhorn, F. Fetting and H. W. Wenz, *Ber. Bunsenges. Phys. Chem.*, 87:1067, (1983).

L. D. Brouwer, W. Müller-Markgraf, and J. Troe, *J. Phys. Chem.* 92:4905-4914, (1988).

M.B. Colket, "The Pyrolysis of Cyclopentadiene", *Chem. Phys. Proc. Combust.*, paper no. 1, December, (1990).

M. B. Colket and R. J. Hall, "A Soot Growth Mechanism Involving Five-Membered Rings", to be presented at the Eastern Section of the Combustion Institute, Oct. 14-16, (1991).

M. B. Colket, R. J. Hall, J. J. Sangiovanni, and D. J. Seery, "The Determination of Rate-Limiting Steps During Soot Formation", Annual Reports to AFOSR, under Contract No. F49620-88-C-0051, UTRC Report nos. 89-13 and 90-23, April, (1989) and June 8, (1990).

F. Communal, S. D. Thomas, and P. R. Westmoreland, "Kinetics of C3 Routes to Aromatics Formation", Poster paper (P40) presented at the Twenty-Third Symposium on Combustion, Orleans, France, July, (1990).

C. J. Dasch, *Comb. and Flame*, 61:219-225, (1985).

M. Frenklach, *Twenty-Second Symposium (International) on Combustion*, The Combustion Institute, p. 1075, (1988).

M. Frenklach, personal communication, (1991).

M. Frenklach, D. W. Clary, W. C. Gardiner, and S. E. Stein, *Twentieth Symposium (International) on Combustion*, The Combustion Institute, p. 887-901, (1984).

M. Frenklach and H. Wang, *Twenty-third Symposium (International) on Combustion*, The Combustion Institute, p. 1559, July, (1990).

M. Frenklach and H. Wang, "Aromatics Growth Beyond the First Ring and the Nucleation of Soot Particles", presented at the 202nd American Chemical Society, National Meeting, New York, August 25-30, 1991, also *Division of Fuel Chemistry Reprints*, 36(4):1509-1516, (1991).

M. Frenklach and J. Warnatz, *Combust. Sci. Tech.*, 51:265, (1987).

J. J. Gajewski, *Hydrocarbon Thermal Isomerizations*, Academic Press, New York, (1981).

F. Gelbard, *MAEROS User Manual*, NUREG/CR-1391, (SAND80-0822), (1982).

F. Gelbard and J. H. Seinfeld, *J. Coll. Int. Sci.*, 78:485-501, (1980).

F. Gelbard, Y. Tambour, J. H. Seinfeld, *J. Coll. Int. Sci.*, 76:54-556, (1980).

I. Glassman, *Twenty-Second Symposium (International) on Combustion*, The Combustion Institute, p. 295-311, (1988).

R. J. Hall and M. B. Colket, "Simplified Models for the Production of Soot in a Premixed Flame", *Chem. Phys. Proc. Combust.*, paper no. 58, October, (1989).

R. J. Hall, "Discrete Ordinates Solutions to the Equation of Radiative Transfer in Particulate-Laden Media", UTRC86-42, July, (1986).

R. J. Hall and P. A. Bonczyk, "Sooting Flame Thermometry Using Emission/Absorption Tomography", to appear in *Applied Optics*, (1991).

S. J. Harris, *Combust. Sci. Tech.*, 72:67-77, (1990).

S. J. Harris and I. M. Kennedy, *Combust. Sci. Tech.*, 59:443-454, (1988).

S. J. Harris and A. M. Weiner, *Combust. Sci. Tech.*, 31:155-167, (1983a).

S. J. Harris and A. M. Weiner, *Combust. Sci. Tech.*, 32:267-275, (1983b).

S. J. Harris and A. M. Weiner, *Twenty-Second Symposium (International) on Combustion*, The Combustion Institute, p. 333, (1988).

S. J. Harris, A. M. Weiner, R. J. Blint, *Comb. and Flame*, 72:91-109, (1988).

B. S. Haynes and H. Gg. Wagner, *Prog. Energy Combust. Sci.*, 7:229-273, (1981).

B. S. Haynes and H. Gg. Wagner, *Z. Physikalishe Chemie NF*, 133:201, (1982).

J. Howard, personal communication, (1988).

H. S. Hura and I. Glassman, *Twenty-Second Symposium (International) on Combustion*, The Combustion Institute, p. 371, (1988).

R. J. Kee, J. F. Gcar, M. D. Smooke, an J. A. Miller, "A Fortran Program for Modeling Steady Laminar One-Dimensional Premixed Flames", Sandia report, SAND85-8240, (1985).

R. J. Kee, R. M. Rupley, and J. A. Miller, "CHEMKIN II: A Fortran Chemical Kinetics Package for the Analysis of Gas-Phase Chemical Kinetics", Sandia Report, SAND89-8009-UC-401, September, (1989).

I. M. Kennedy, W. Kollmann, and J. Y. Chen, *Comb. and Flame*, 81:73-85, (1990).

J. H. Kent and D. R. Honnery, *Combust. Sci. Tech.*, 75:167-177, (1991).

R. D. Kern, C. H. Wu, J. N. Yong, K. M. Pamidimukkala, and H. J. Singh, "The Correlation of Benzene Production with Soot Yield Determined from Fuel Pyrolysis", presented at the American Chemical Society, National Meeting, Division of Fuel Chemistry, New Orleans, Fall, (1987).

J. H. Kiefer, personal communication, (1991).

F. S. Lai, S. K. Friedlander, J. Pich, and G. M. Hidy, *J. Coll. Int. Sci.*, 39:395-405, (1972).

J. T. McKinnon, PhD. Dissertation, Massachusetts Institute of Technology, (1989).

J. T. Mckinnon and J. B. Howard, *Combust. Sci. Tech.*, 74:175-197, (1990).

C. M. Megaridis and R. A. Dobbins, *Combust. Sci. Tech.*, 63:153-167, (1989).

J. A. Miller and C. T. Bowman, *Progress in Energy and Combustion Science*, 15:287-338 (1989).

J. A. Miller and C. F. Melius, "Kinetic and Thermodynamic Issues in the Formation of Aromatic Compounds in Flames of Aliphatic Fuels", to be published in *Comb. and Flame*, (1991).

J. H. Miller, *Twenty-Third Symposium (International) on Combustion*, The Combustion Institute, p. 91, (1990).

J. Nagle and R.F. Strickland-Constable, *Proceedings of the Fifth Carbon Conference*, Vol. 1, Pergamon Press, p. 154, (1963).

K. S. Narasimhan and P. J. Foster, *Tenth Symposium (International) on Combustion*, The Combustion Institute, p. 253, (1965).

K. G. Neoh, J. B. Howard, and A. F. Sarofim, *Particulate Carbon: Formation During Combustion*, D. C. Seigla and G. W. Smith, eds. Plenum, New York, p. 261, (1981).

E. R. Ritter, J. W. Bozzelli and A. M. Dean, "Kinetic Study on Thermal Decomposition of Chlorobenzene Diluted in H_2", to appear in *J. Phys. Chem.*, (1991).

R. J. Santoro, personal communication, (1990).

O. I. Smith, *Prog. Energy Combust. Sci.*, 7:275-291, (1981).

M.D. Smooke, P. Lin, J. K. Lam, and M. B. Long, *Twenty-Third Symposium (International) on Combustion*, The Combustion Institute, p. 575, (1990).

S.E. Stein and A. Fahr, *J. Phys. Chem.*, 89:3714-3725, (1985).

S.E. Stein, J. A. Walker, M. Suryan and A. Fahr, *Twenty-Third Symposium (International) on Combustion*, The Combustion Institute, p. 85, (1990).

P. A. Tesner, *Comb. Expl. Shockwaves*, 15:111, (1979).

H.G. Wagner, *Seventeenth Symposium (International) on Combustion*, The Combustion Institute, p. 3-19, (1979).

H. Wang and M. Frenklach, "Modeling of PAH Profiles in Premixed Flames", *Chem. Phys. Proc. Comb.*, paper no. 12, October, (1989).

D. R. Warren and J. H. Seinfeld, *Aerosol Sci. Tech.*, 4:31-43, (1985).

C. K. Westbrook and F. D. Dryer, *Prog. Energy Combust. Sci.*, 10:1-57 (1984).

U. Wieschnowsky, H. Bockhorn, and F. Fetting, *Twenty-Second Symposium (International) on Combustion*, The Combustion Institute, p. 343, (1988).

I. T. Woods and B. S. Haynes, *Comb. and Flame*, 85:523, (1991).

M. Zabielski, B. A. Knight, D. J. Seery, " The Influence of Burner Surface Porosity on the Flame Front Structure in Low Pressure Flat Flames", poster paper presented at the Twenty-Third Symposium on Combustion, p. 7, (1990).

APPENDIX B

The Pyrolysis of Cyclopentadiene

THE PYROLYSIS OF CYCLOPENTADIENE

by M. B. Colket
United Technologies Research Center
E. Hartford, CT 06108

Eastern Section: The Combustion Institute
December 3-5, 1990 at Orlando FL

There is increasing experimental evidence that important rate-limiting steps to soot formation are the production and growth of aromatic rings. Detailed modeling and comparison to experimental data has led to a good understanding of mechanisms and rates for the production of benzene (and phenyl radical). A major unknown is the importance of C_5-species on ring growth. Flame studies indicate that cyclopentadiene (CPD) has sooting characteristics similar to that of aromatics, but mechanisms are lacking to explain the rapid conversion to C_6-rings which are believed to dominate in ring growth processes. To develop a better understanding of the decomposition of CPD, a single-pulse shock tube has been used to examine its pyrolysis and rich oxidation as well as the pyrolysis of CPD in the presence of acetylene and biacetyl. These hydrocarbons have been diluted in argon and shock heated over the temperature range of 1100 to 2000K and at total pressures of ten to thirteen atmospheres. Dwell times were about 500-600 microseconds. Collected gas samples were analyzed using gas chromatography for hydrogen, carbon oxides and C_1- to C_{14}-hydrocarbons.

CPD is not sold commercially since it easily dimerizes into dicyclopentadiene (DCP). Initial shock tube experiments using DCP had ambiguous interpretations, so a facility was set up to produce CPD for subsequent tests. DCP was decomposed to CPD at 170°C, the boiling point of DCP. Subsequently, CPD was separated from DCP in a distillation column and then condensed. Purity of the CPD was approximately 96% which could be further refined to 99.6% by bulb-to-bulb distillation when sufficient CPD was produced. Two principal impurities eluted just before CPD and are believed to be C_5-compounds. Based on retention times, the impurities have been tentatively identified as 1-pentene and 1,3-pentadiene.

Interpretation of the data has been complex due to a large number of high molecular weight species, the scarcity of literature mechanisms for the decomposition pathways, and unknowns regarding the role of C_5-species in ring formation or growth. Light hydrocarbon species are plotted as a function of initial post-shock temperatures are provided in Fig. 1 for the pyrolysis. The distribution of products in the case of the oxidative pyrolysis is similar except that the oxidation produces substantially greater relative concentrations of 1,3-butadiene (1,3-C_4H_6) and vinylacetylene (C_4H_4). It is believed that these products arise from an oxidation process of the cyclopentadienyl radical similar to that previously proposed[1]. This decomposition route which includes the formation of C_4-hydrocarbons differs from a proposed pyrolytic process discussed in the next paragraph.

A preliminary mechanism for the pyrolysis is presented in Table I. This proposed mechanism features several decomposition pathways but is limited since it does not include any growth reactions. The principal low temperature decomposition route (Reaction 3) is preceeded by H-atom addition to the 3(or 4)-position on CPD to form cyclopenten-4-yl. Th proposed decomposition of this radical adduct to acetylene and the allyl radical is perhaps the lowest energy decomposition pathway for the C_5-ring (about 10 kilocalories per mole). Further justification for this step is provided by the high concentrations of methane produced in the pyrolysis. Methane is formed during subsequent reactions involving the allyl radical produced in Reaction 3. No other decomposition process easily led to production of methane. At higher temperatures, thermal decomposition of the stabilized radical, cyclopentadienyl, dominates ring fracture. Ethylene is believed to be formed by H-addition to CPD to form cyclopenten-3-yl which decomposes into ethylene and C_3H_3. Propene and allene (or

methylacetylene) are formed by abstraction of H-atoms from CPD by the C_3-radicals. Other possible reactions involve H-atom shifts within the CPD molecule followed by isomerization to a linear aliphatic. Such steps are similar to those proposed for the decomposition of pyrrole[2]. Calculations using this scheme compare qualitatively well with the experimental profiles of acetylene and C_3-hydrocarbons, although ethylene and methane profiles are significantly underpredicted. At 1400K, the model predicts that more than 10% of the CPD is converted to the cyclopentadienyl radical which except for its thermal decomposition is relatively unreactive according to the preliminary model. The fate of the cyclopentadienyl radical will have to be investigated further. GC spectra exhibit large quantities of dimerized products, although some or all of these species may be formed during the quenching process. Cyclopentadienyl radicals probably play a significant role in ring growth reactions. In fact, large quantities of high molecular weight aromatics were observed.

Rapid interchange between C_5 and C_6-rings may in part be responsible for the rapid growth of high molecular weight species. To test this hypothesis, a series of pyrolysis experiments were performed with additives. One of the additives, biacetyl ($(CH_3)_2CO$) was selected since it provides a facile source of methyl radicals and easy modeling techniques are available for estimating the methyl radical concentrations[3]. Methyl radicals in turn may add to the cyclopentadienyl radical to form methylcyclopentadiene. After loss of an H-atom, the resulting radical may isomerize to cyclohexadienyl lose another H-atom and eventually form benzene. This process is similar to the reverse of the mechanism for benzene decomposition recently proposed by Ritter, et al.[4]. A second mechanism for ring interchange was investigated by adding acetylene to the pyrolysis of cyclopentadiene. We speculate that acetylene adds to the cyclopentadienyl radical and the resultant adduct undergoes a ring enlargement reaction to form the benzyl radical, which becomes toluene after H-atom addition. This process is the reverse of a proposed step for the decomposition of the benzyl radical[5], although many different proposals have been made (see for example Ref. 6).

Benzene production from pure cyclopentadiene is compared to benzene production during copyrolysis of cyclopentadiene and biacetyl in Fig. 2. Also included on this plot is data on the two isomers of the intermediate, methylcyclopentadiene. Biacetyl clearly and dramatically increases the concentration of the methylcyclopentadienes as well as significantly increase the concentration of benzene. In Fig. 3, toluene produced from cyclopentadiene pyrolysis and from a mixture of CPD and acetylene are compared. Again large increases in the conversion to aromatics was observed by the presence of an additive. Together these results not only provide evidence supporting recent proposals for ring fracture, but also confirm speculation of rapid interchange mechanisms between C_5 and C_6-rings. If interchange also occurs for multiringed species, then such phenomena should be included in PAH growth models.

An important feature of the data from CPD pyrolysis is the large amount of mass that is converted to high molecular weight material. A plot of the carbon contained in all species with molecular weights of 128 gram/mole and less is shown Fig. 4. This data is compared with that observed during the pyrolysis of other hydrocarbons. This figure demonstrates that cyclopentadiene produces large quantities of high molecular weight material (a qualitative measure of soot production) similar to that of aromatic hydrocarbons and much greater than observed for aliphatic species. This result is not surprising considering the aromatic character of CPD and the resonantly-enhanced stability of the cyclopentadienyl radical. This experimental result further supports concerns about existing models for soot production since none of them include the potential role of C_5-species.

Acknowledgements

This work has been supported in part by the Air Force Office of Scientific Research under Contract No. F49620-88-C-0051.

References

1. A. B. Lovell, K. Brezinsky and I. Glassman, Twenty – Second Symposium (International) on Combustion, The Combustion Institute, pp.1063-1074, 1988.
2. J. C. Mackie, M. B. Colket, P. F. Nelson and M. Esler, "Shock Tube Pyrolysis of Pyrrole and Kinetic Modeling" submitted to the International Journal of Chemical Kinetics, 1990.
3. M. B. Colket, "Formation of C_2-Hydrocarbons and Benzene from Pyrolysis of Biacetyl". 1986 Spring Technical Meeting of the CSS/CI, May 5-6, 1986, Paper no. 1-C2.
4. E. R. Ritter, J. W. Bozzelli and A. M. Dean, "Kinetic Study on Thermal Decomposition of Chlorobenzene Diluted in H_2", to appear in J. Phys. Chem.
5. L. D. Brouwer, W. Müller-Markgraf and J. Troe, *Journal of Physical Chemistry* 92, 4905, 1988. Also see W. Müller-Markgraf and J. Troe, *Journal of Physical Chemistry* 92, 4899, 1988.
6. V. S. Rao and G. B. Skinner, Twenty – First Symposium (International) on Combustion, The Combustion Institute, pp.809-814, 1986.

Table I

Preliminary Mechanism for the Pyrolysis of Cyclopentadiene

	Reactions Considered	Pre Exp	Act Eng
1.	c-C_5H_6↔ H+c-C_5H_5	0.200D+16	81000.
2.	H+c-C_5H_6↔ H_2+c-C_5H_5	0.300D+13	8000.
3.	H+c-C_5H_6↔ C_2H_2+C_3H_5	0.100D+14	12000.
4.	H+c-C_5H_6↔ C_2H_4+C_3H_3	0.500D+13	18000.
5.	H+c-C_5H_6↔ l-C_5H_7	0.100D+13	0.
6.	l-C_5H_7+c-C_5H_6↔ C_5H_8+c-C_5H_5	0.500D+13	6000.
7.	C_5H_8+H↔ C_2H_4+C_3H_5	0.100D+14	8000.
8.	c-C_5H_5↔ C_2H_2+C_3H_3	0.100D+15	74000
9.	C_3H_3+C_3H_3↔ C_6H_5+H	0.100D+14	0.
10.	H+A1↔ H_2+C_6H_5	0.250D+15	16000.
11.	CH_3+C_2H_2↔ CH_3CHCH	0.620D+12	7700.
12.	H+C_3H_4 ↔ CH_3CHCH	0.580D+13	3100.
13.	CH_3CHCH↔ C_3H_5	0.140D+14	36000.
14.	H+ALLENE↔ C_3H_5	0.400D+13	2700.
15.	CH_3+c-C_5H_6↔ CH_4+c-C_5H_5	0.500D+13	5000.
16.	CH_3+H↔ CH_2+H_2	0.724D+15	15100.
17.	C_3H_3+c-C_5H_6↔ C_3H_4+c-C_5H_5	0.100D+13	9000.
18.	C_3H_5+c-C_5H_6↔ C_3H_6+c-C_5H_5	0.100D+13	16000.
19.	C_3H_3+c-C_5H_5↔ A1+C_2H_2	0.400D+13	0.
20.	H + C_2H_2 ↔ C_2H_3	0.550D+13	2500.
21.	H+C_3H_6↔ C_2H_4+CH_3	0.100D+13	5000.
22.	C_3H_6+H↔ C_3H_5+H_2	0.501D+14	3500.
23.	C_3H_5↔ C_3H_4+H	0.398D+14	70000.

Notes: Units in cc, moles, cal

c-C_5H_5 = cyclopentadienyl radical, A1 = benzene

c-C_5H_6 = cyclopentadiene, C_5H_8 = 1,3-pentadiene

Fig. 1 Light Products from CPD Pyrolysis

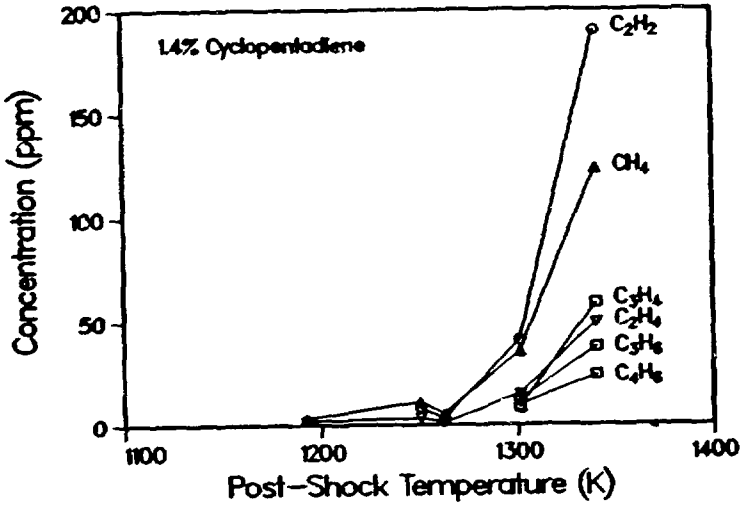

Fig. 2 Formation of Benzene and Methylcyclopentadienes

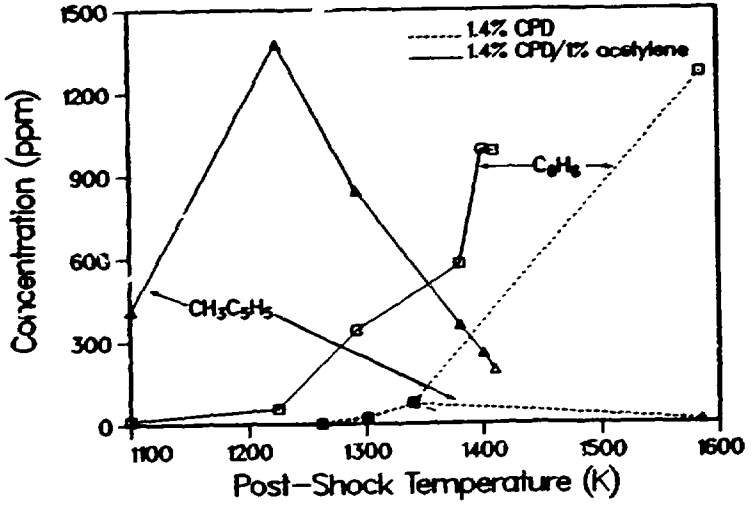

Fig. 3 Formation of Toluene

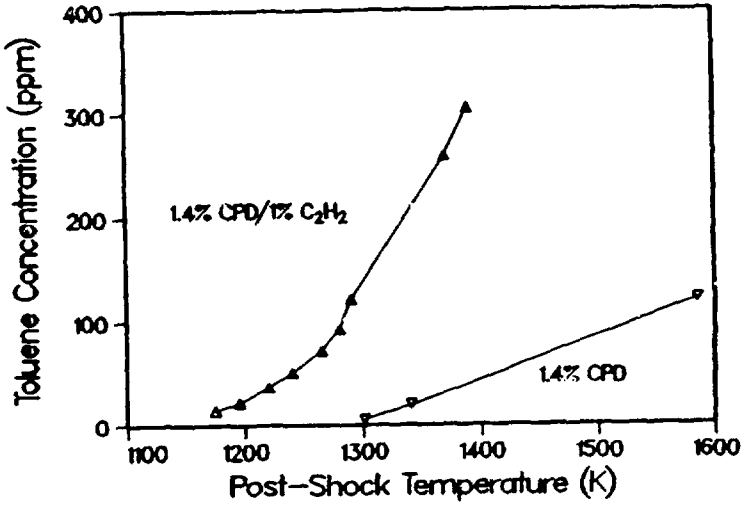

Fig. 4 Mass Recovery Following Pyrolysis in a Single-Pulse Shock Tube

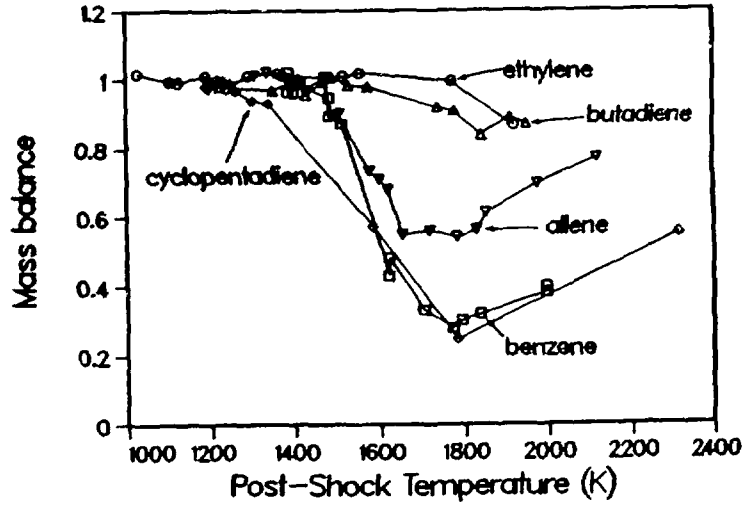

APPENDIX C

A Soot Growth Mechanism

Involving Five-Membered Rings

A SOOT GROWTH MECHANISM INVOLVING FIVE-MEMBERED RINGS

by M. B. Colket and R. J. Hall
United Technologies Research Center
E. Hartford, CT 06108

Eastern Section: The Combustion Institute
October 14-16, 1991 at Ithaca, N.Y.

Conventional proposals regarding growth of polyaromatic hydrocarbons and soot particles focus on formation and growth of six-membered rings. Recently, the rapid conversion of five-membered rings to six-membered rings has been demonstrated in a single-pulse shock tube. Certainly, much of the work detecting polyaromatic hydrocarbons under soot forming conditions in flames demonstrates the presence of large concentrations of species containing five-membered rings. One can thus speculate that five-membered rings play a role in soot growth processes. It is the objective of this paper to examine the evidence and mechanisms for ring interconversions at elevated temperatures, to propose an alternative growth mechanism involving five membered rings and to compare that mechanism to a previous proposal for ring growth via six-membered rings.

Isomerizatiom processes causing ring enlargement and ring contraction are well known (Gajewski, 1981, Benson and O'Neal (1970), Ritter, et al., 1991). Ritter, et al. have recently examined the thermodynamics and kinetics of ring contraction, in particular conversion from a C_6-ring to a C_5-ring. To examine the possibility of ring enlargement, biacetyl (a source of methyl radicals) and acetylene have both been added (Colket, 1990) to the pyrolysis of cyclopentadiene (CPD). In the case of methyl radical addition, a dramatic increase in the formation of (the two isomers of) methyl-cyclopentadiene and benzene were observed. In the case of acetylene addition to CPD, dramatic increases in the formation of toluene were observed. Colket did not discuss specific mechanisms for these processes, although the methyl addition steps are presumably similar to the reverse of the ring contraction processes outlined by Ritter, et al. Kiefer (1991) has suggested that the acetylene addition processes may be related to the reverse diels-alder reaction of acetylene addition to CPD to form norbornadiene. Benson and O'Neal (1970) report rates for unimolecular decomposition of norbornadiene to CPD plus acetylene and for the isomerization of norbornadiene to toluene. Thus one could speculate an overall process for ring enlargement:

$$C_5H_6 + C_2H_2 \leftrightarrow \text{norbornadiene} \leftrightarrow \text{toluene}$$

The overall rate constant for acetylene addition to CPD to form toluene can be estimated from our single-pulse shock tube (SPST) data. ($k = [\text{toluene}]_f/[\text{CPD}]_i/[C_2H_2]_i/t_{dwell}$). This data is plotted in Fig. 1 along with k_a for the reverse diels-alder reaction (obtained from detailed balancing and the rate data from Benson and O'Neal). A l.s.f. of the experimental data gives $k=10^{17}\exp(-58600$ cal/mole/R/T) cm^3/mole/sec. Although the SPST data is slightly higher than a extrapolation of the retro diels-alder rate constant at lower temperatures, the overall activation energy is significantly higher and the pre-exponential is about three orders of magnitude too large for a bimolecular process. We conclude that the dominant process observed in the SPST experiments is a radical process.

Based on the assumption of radical addition processes, we propose the reaction scheme in Fig. 2 as a possible alternative to a growth mechanism involving six-membered rings. The acetylene addition to cyclopentadienyl, formation of norbornadienyl, and isomerization to benzyl radical may be the reverse of a route for benzyl decomposition which has eluded researchers for years. Indene, formed in Reaction 7, has a five membered ring and, after loss of an H-atom (as in Reaction 1 or 2), it may undergo subsequent acetylene addition for further growth of polyaromatic hydrocarbons. Rewriting

this sequence as shown in Table I and assuming steady-state concentrations for all intermediate species, the expression for acetylene addition to 'soot' can be obtained:

$$\frac{d[C(s)]}{dt} = \frac{2(k_1[H] + k_2)k_3k_4k_5[C_2H_2]^2[\text{cyclopentadiene}]}{(k_{-1}[H_2] + k_{-2}[H] + k_{1a})\{k_{-3}(k_{-4} + k_5) + k_4k_5[C_2H_2]\} + k_3k_4k_5[C_2H_2]^2}$$

Reaction 3 and -3 represents the overall reversible process of acetylene addition to cyclopentadienyl to form benzyl radical. Rate constants were initially determined based on literature values for these processes (with CPD) or estimates as necessary. An important difference of this new mechanism is the lower C-H bond strength in the C_5 ring species. The rate constant for acetylene addition to cyclopentadienyl was initially taken to be the reverse of that for the decomposition of benzyl radical. Rate constants were subsequently adjusted to provide better agreement to the soot growth data of Harris and Weiner (1983) and the soot growth rates studied by Bockhorn, et al. (1983) Final adjusted rate constants are shown in Table I where A-factors are in units of cm^3, moles, and seconds. Although these rate constants are relatively close to their initial values, these rates should be considered empirical and not directly related to processes with CPD or its derivatives. The overall soot growth rates as predicted by this equation are shown in Fig. 3 and 4 for the C/O = 0.96 and C/O = 0.80 ethylene flames of Harris and coworkers (1983 and 1988) respectively. Species concentrations were obtained as a function of height by using their kinetic model (Harris, Weiner and Blint, 1988) and the Sandia premixed code. Also shown on these figures are the experimental data and the predictions for soot growth via six-membered rings using the expression and rate constants as provided by Frenklach and Wang (FW) (1991). These predicted curves as well as those obtained using other assumptions (Colket and Hall, 1991) tend to peak early and are all concave upwards, whereas the experimental data is concave downwards. The shape of these 'theoretical' curves is at least partially due to their dependence on H-atom concentrations. For the richer flames, both of the calculated soot growth rates predicts the initial magnitude of the soot growth rate fairly well, although they both fall off too rapidly with increasing height above the burner. For the C/O=0.8 flame, the FW expression does not decrease by a factor of two (relative to the C/O=.94 flame) as the experimental data indicates and leads to substantial overprediction of soot formation in this leaner flame. As Frenklach and Wang explain, their expression, at the conditions in the Harris and Weiner flames, is proportional to H-atoms and independent of the acetylene concentration. Much of the prior work on soot growth including that of Harris and Weiner has been explained by a linear dependence of soot growth on acetylene concentrations. We believe that the inability of the FW expression to descibe the stoichiometric dependence of soot formation in the Harris and Weiner flames is at least partially due to the loss of the dependency on acetylene.

Soot profiles have also been predicted using these models. Both the FW model and this new model describe the soot profile for the C/O = 0.94 flame fairly well. The FW model significantly overpredicts the soot formation for C/O = 0.80 while this five-ringed model, slightly overpredicts soot production early in the flame. The five-ring model describes soot formation in the acetylene flame of Bockhorn without the 0.1 steric factor as suggested by FW. The new model significantly overpredicts (as does the FW model with the 0.1 steric factor) the propane data obtained by Bockhorn, et. al.

Acknowledgements

This work has been supported in part by the Air Force Office of Scientific Research under Contract No. F49620-88-C-0051. Special thanks are owed to Professor John Kiefer of the University of Illinois for valuable discussions on mechanisms of acetylene addition to cyclopentadiene.

References

S. W. Benson and H. E. O'Neal, Kinetic Data on Gas Phase Unimolecular Reactions, NSRDS-NBS 21, February, 1970.

H. Bockhorn, F. Getting, and H. W. Wenz, Ber. Bunsenges. Phys. Chem., 87: 1067(1983).

M. B. Colket, "The Pyrolysis of Cyclopentadiene", ES/CI, Dec., 1990.

M. B. Colket and R. J. Hall, "Successes and Uncertainties in Modeling Soot Formation in Laminar, Premixed Flames", workshop on Mechanisms and Models of Soot Formation, held at Heidelberg, Germany, Sept. 28 - Oct.2, 1991.

M. Frenklach and H. Wang, Twenty – Third Symposium (International) on Combustion, The Combustion Institute, p. 1559, 1990.

J. J. Gajewski, Hydrocarbon Thermal Isomerizations, Academic Press, New York, 1981.

S. J. Harris and A. M. Weiner, Comb. Sci. Tech., 32:267(1983).

S. J. Harris, A. M. Weiner, and R. J. Blint, Comb. Flame, 72:91(1988).

J. H. Kiefer, personal communication, 1991.

E. R. Ritter, J. W. Bozzelli and A. M. Dean, "Kinetic Study on Thermal Decomposition of Chlorobenzene Diluted in H_2", to appear in J. Phys. Chem.

Table I: Preliminary Soot Growth Mechanism Based on Five-Membered Rings

	Reactions Considered	$\log_{10}(A_f)$	E_f	$\log_{10}(A_r)$	E_r
1.	$H+C(s) \leftrightarrow \dot{C}(s)+H_2$	14.40	6	13.70	36
1a.	$\dot{C}(s) \rightarrow$ products	13.70	60	-	-
2.	$C(s) \leftrightarrow \dot{C}(s)+H$	14.78	86	14.48	-
3.	$C_2H_2+\dot{C}(s) \leftrightarrow \dot{C}'(s)$	12.04	12	12.00	70
4.	$C_2H_2+\dot{C}'(s) \leftrightarrow C'(s)\dot{C}_2H_2$	13.00	5	12.30	21
5.	$C'(s)\dot{C}_2H_2 \rightarrow C''(s)+H$	11.4	5	-	-

Figure 1

Effective $k(C_5H_6 + C_2H_2 = \text{Toluene})$

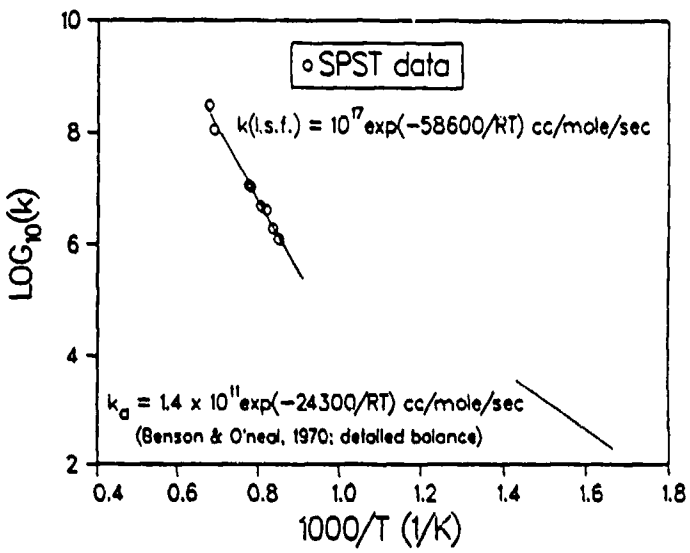

Figure 2: Alternate Ring Growth Mechanism.

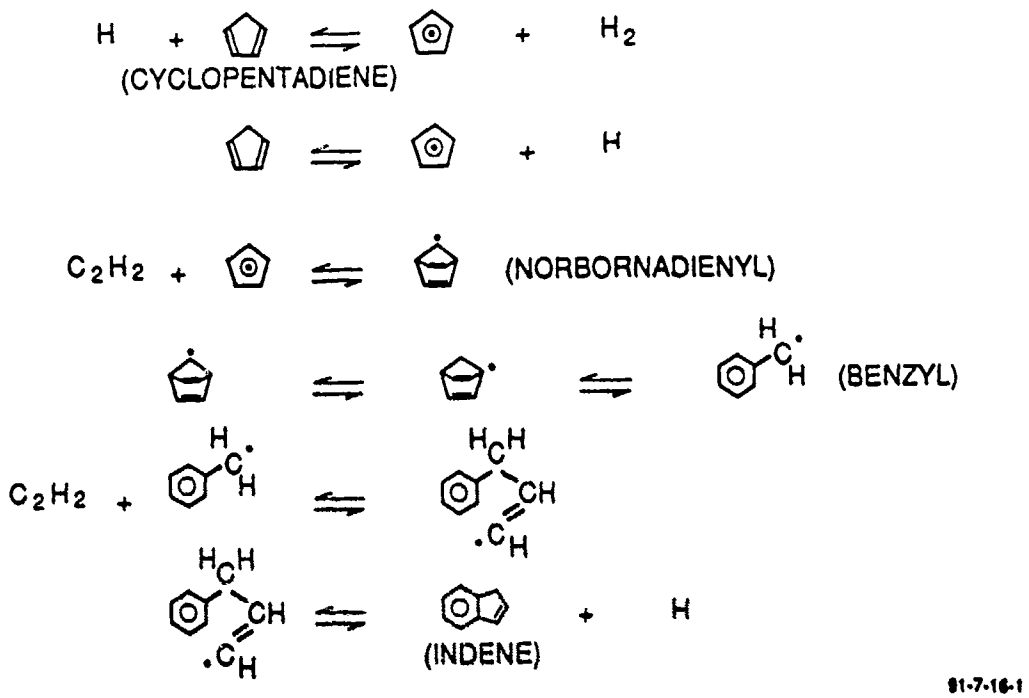

Figure 3
Soot Growth Rate Constant

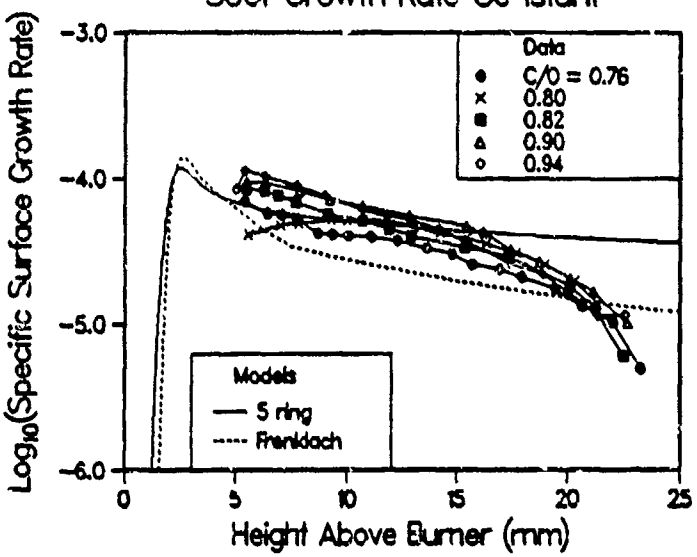

Figure 4
Soot Growth Rate Constant

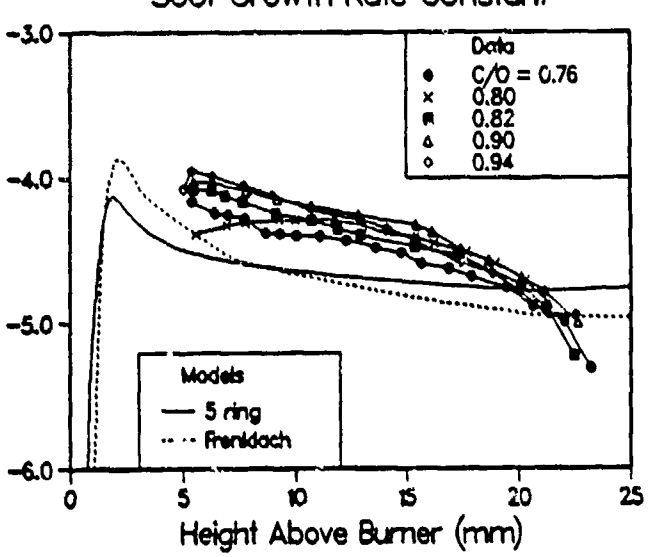

APPENDIX D

On Impurity Effects in Acetylene Pyrolysis

COMMENT

On Impurity Effects in Acetylene Pyrolysis

M. B. COLKET, III, D. J. SEERY

United Technologies Research Center, East Hartford, CT 06108

and

H. B. PALMER

Pennsylvania State University, University Park, PA 16802

In our recent paper [1] (CSP), we concluded that a radical-chain mechanism of acetylene pyrolysis must be appreciable and possibly dominant and argued that impurities, for example acetone, may contribute significantly to chain initiation. To support our conclusions, a model including acetone chemistry was developed but it did not invoke vinylidene reactions or other non-chain processes despite reasonable arguments [2] in support of such steps. Nevertheless, we also recognized, and stated in the paper that the vinylidene mechanism could not be disproven and may in fact play a role.

This analysis apparently prompted Duran, Amorebieta, and Colussi [3] (DAC1) to perform additive experiments. They pyrolyzed acetone/acetylene mixtures at ratios of about 0.2 to 2, selected a decomposition rate expression and determined associated rate constants. Colussi [4] extrapolated this rate expression down to concentration ratios of 0.001 and concluded that the impurity effect can be neglected since it can account for only 2 to 14% of the decomposed acetylene at 910K. In contrast to the suggestion of Colussi, we do not consider these results to be in conflict with our conclusions.

First of all, the uncertainty in extrapolating a rate expression derived from experiments with acetone/acetylene ratios of 0.2 down to ratios of only 0.001 may be significant. Our calculations suggest that at high acetone/acetylene ratios, acetone is rapidly depleted by radical (H-atom, methyl, or vinyl) attack and therefore less is available to initiate the reaction. This possible effect was considered in Appendix I of DAC1 but dismissed since the absolute rate constant for R + acetylene is higher than R + acetone and radicals should be consumed preferentially by acetylene. At low radical concentrations, the effects of the reversibility of the former reaction can be negligible; but as radical concentrations increase (which occurs with high initial acetone concentrations), the rate of R + acetone relative to the *net* rate of R + acetylene increases dramatically. Thus, acetone is rapidly depleted by radical attack, and initiation and overall decomposition rates will be lower than if acetone were not removed by radicals. Rate expressions derived from high concentration experiments may then underestimate decomposition when extrapolated to very low acetone levels. Therefore, we believe that the experiments of DAC1 (which suggest acetone could contribute about 10% to the overall decomposition of acetylene) underestimate the role of low concentrations of acetone.

A second reason for our view of the experi-

0010-2180/91/$3.50

mental results of DAC1 is that the analysis described in our paper suggests that acetone could play a relatively more important role in radical initiation at higher temperatures. As stated in the conclusions of our paper, 900K is approximately the lower limit for which acetone was predicted to play a significant role. Our lower limit is very close to the temperature of the DAC1 study, 910K.

The comment by Colussi implies that trace acetone concentration levels cannot appreciably accelerate overall rates of acetylene pyrolysis. This statement is not apparent from the pre-publication manuscript (DAC1), since acetone and acetylene were copyrolyzed at comparable concentrations. Typical concentrations were 51.4 torr acetylene and 100 torr acetone. Low-level impurity experiments apparently were not performed.

We have performed some calculations based on the conditions cited by Duran, Amorebieta, and Colussi [5] (DAC2) for pyrolysis of neat acetylene. We have slightly modified our published mechanism to account for the pressure dependence. The modifications include selection of $k/k_\infty = 0.5$ for the following reactions.

$$H + C_2H_2 \rightarrow C_2H_3 \qquad (2)$$

$$CH_3COCH_3 \rightarrow CH_3 + CH_3CO. \qquad (5)$$

In addition, the high pressure rate constant recommended by Benson and O'Neal [6] is used fr Reaction 5. At 910K and 100 torr acetylene, we calculate a steady-state decomposition rate (after a transient less than two seconds) to be 2.2×10^{-8} moles/cm^2/sec (2.2×10^{-5} M s^{-1}) and a rate constant of 7.1×10^3 cm^3/moles/sec (7.1 M^{-1} s^{-1}). These values are very close to the values cited by DAC1 and DAC2. The excellent agreement is probably fortitous, but these calculations were performed using a chain mechanism, an impurity of 0.1 torr of acetone, and did not include contributions of vinylidene. Detailed product information is not available from these publications for comparison.

It should be emphasized that the thermochemistry for several radical intermediates potentially important to acetylene decomposition cannot be considered to be well known. Consequently it is difficult to draw definitive conclusions based on such arguments. The uncertainty in the heat of formation of C_4H_3 isomers was cited as an example in CSP, but uncertainties in the entropy also exist. Values vary depending on the estimation (calculation) technique as well as the individual performing the evaluation. Most evaluations are unpublished, but examples of some reported values of $\Delta H^0_{f,298}$, S^0_{298}, and $C_p(T)$ for the i—C_4H_3 radical are reproduced in Table I. Also included are calculations of the rate constant for the suggested reaction

$$C_2H_2 + C_2H_2 \rightarrow i\text{—}C_4H_3 + H \qquad (1a)$$

After DAC1, k_{1a}'s were calculated assuming the reverse, recombination rate constant is 5×10^{13} cm^3/mole/sec. DAC1 estimated that Reaction 1a

TABLE I

Reported Thermodynamics for 1-Buten-3-yn-2-yl (i—C_4H_3)

$\Delta H^\circ_{f,298}$ kcal/mole	S°_{298} cal/mole/K	C_p° cal/mole/K 300	500	800	1000	1500	k_{1a}* cm^3/mole/sec	Ref
110.8	63.7	16.3	21.9	27.8	29.8	33.1	0.37	8
115.2	66.1	16.9	22.1	27.0	29.3	33.0	0.11	9
114.5	68.3	17.5	22.5	27.4	29.6	33.2	0.56	10
116.1	68.1	16.8	22.2	27.1	29.3	32.8	0.19	11
102.0	65.4	17.4	22.4	27.1	29.2	32.5	126	12
110.0	71.6	17.4	22.4	27.1	29.2	32.5	33.8	13

*assuming a $k_{-1a} = 5 \times 10^{13}$ cm^3/mole sec

Note: The low heat of formation calculated by Ref. 12 is probably in error, but is the value included in many thermodynamic compilations. The relatively high value of entropy determined by Melius [13] has recently been supported by additional calculations [14].

had to have rate of at least 85 cm^3/mole/sec at 910K in order for it to contribute to acetylene pyrolysis. As can be seen from the different values listed in Table I, various conclusions can be drawn, although most recent estimates using group addivity techniques support the conclusion of DAC1 regarding the importance of Reaction 1a.

Lacking sufficiently accurate thermochemical data, one must consider experimental evidence. It is our own interpretation [1] that available data supports contribution from a chain mechainsm. Radical initiation, if not from Rection 1a or similar step, could arise from impurities or walls. Although we have argued that acetone plays an important role, acetone is not always present. Acetylene made from water and calcium carbide, for example, will not contain acetone, although other impurities (possibly inorganic) could be present. If the impurity has a relatively weak bond, large concentrations are not required.

The difficulty of accurately making measurements of acetylene pyrolysis near 1000K should not be underestimated. In addition to being susceptible to radical sources from impurities (see CSP), the pyrolysis is extremely exothermic. Formation of vinylacetylene, benzene, or solid carbon plus hydrogen is 19, 48, and 54 kilocalories exothermic per mole of acetylene decomposed, respectively. Thus, nearly ninety percent of the potential energy release arises just by forming benzene and helps to explain the explosive behavior of neat acetylene. Assuming that only 2% of the acetylene forms benzene (an important low temperature product) and taking $c_p(C_2H_2) \approx 16$ cal/mole/K, the temperature rise is 60K for undiluted samples of acetylene. For a reaction with E = 40 kcal/mole, the rate constant would rise by a factor of 2.5. For larger extents of reaction, this problem will be more severe. Formation of vinylacetylene, benzene and other higher molecular weight species will lead to a reduction in the number of moles and to a pressure reduction (for constant volume reactors) as the reaction progresses. The pressure cannot be directly related to the rate of reaction unless detailed information on product distribution is also known. An additional complication in interpreting pressure traces arises from the temperature rise due to the heat of reaction. The temperature rise would lead to a pressure increase (ideal gas law) which partially offsets the pressure decay due to reaction. For flow reactors in which constant pressure can be maintained, the above effects lead to changes in velocity which complicate determination of reaction time. On-line diagnostics such as mass spectrometers may be pressure sensitive and so calibrations and experiments must be carefully interpreted. In some reactor designs, energy release from the reaction may be absorbed by the walls, but in such situations, the rate of wall collisions must be high and there may be surface contributions to the chemistry. Pretreatment of vessels at elevated temperatures may simply 'stabilize' the source of radical production/termination at the walls. The difficulty in accurately measuring the rate of pyrolysis of neat acetylene is dramatically illustrated by the scatter (factor of two to three) obtained in the work of DAC2 (Fig. 1) but is significantly less (≈ 20%) when a stable source of radicals (acetone or neopentane) is added (see Figs. 1-3 in DAC1). The scatter in the 'neat' acetylene experiments may be due to run-to-run variations in impurities or wall effects.

As we consider the varying evidence and conclusions from previous work, the need for careful documentation in future experiments becomes evident. Levels of impurities must be measured and specified. Equipment sensitive to concentrations lower than 1000 ppm acetylene must be used. Based on the confused situation identified in Table 3 of CSP, the reaction order should be redetermined *and* demonstrated to readers. (Towell and Martin [7], for example claimed second order dependence, but their data indicated an order much closer to 1.5.) Based on the literature cited in CSP, the last time experimental data was presented showing second order behavior was 1964; since then there have been may dissimilar results. Considering the relative sophistication of present-day experimental techniques, it should be straightforward to establish the kinetic order of acetylene pyrolysis.

In conclusion, we are convinced that there are uncertainties still to be resolved in the acetylene

system. The trace impurity experiment has not yet been performed. An extapolation of a rate expression to low acetone concentrations suggests a contribution of 10% to the overall rate at about 900K. We feel that the results of DAC1 do not disprove our suggestion that even small concentrations of impurities can have a significant impact on acetylene pyrolysis.

REFERENCES

1. Colket, M. B., Seery, D. J., and Palmer, H. B., *Combust. Flame* 75:343-366 (1989). (CSP).
2. Kiefer, J. H. and Von Drasek, W. A., *Int. J. Chem. Kin.* 22:747-786 (1990).
3. Duran, R. P., Amorebieta, V. T. and Colussi, A. J., *Int. J. Chem. Kin.* 21:947-958 (1989) (DAC1).
4. Colussi, A. J., *Combust. Flame*, 84: (1991).
5. Duran, R. P., Amorebieta, V. T. and Colussi, A. J., *J. Am. Chem. Soc.* 109:3154 (1987). (DAC2).
6. Benson, S. W. and O'Neal, "Kinetic Data on Gas-Phase Unimolecular Reactions," NSRDS-NBS 21, U.S. Govt. Printing Office, Washington, D.C. (1970).
7. Towell, G. D. and Martin, J. J., *A.I.Ch.E. Journal* 7:693 (1961).
8. Bittner, J., "A Molecular Beam Mass Spectrometer Study of Fuel-Rich and Sooting Benzene-Oxygen Flames," Ph.D. Dissertation, Appendix P, Massachusetts Institute of Technology, 1981.
9. Ghibaudi, E. and Colussi, A. J., *J. Phys. Chem.* 92:5839 (1988).
10. Westmoreland, P. R., "Prediction of Kinetics for C_4 Species which form Benzene," *American Chemical Society, Fuel Chemistry Preprints* 32:480 (1987). NOTE: The original reference incorrectly lists the heat of formation of i-C_4H_3 (personal communication from P. R. Westmoreland).
11. Stein, S. E., National Bureau of Standards, Gaithersburg, MD, Personal Communication, 1987.
12. Cowperthwaite, M. and Bauer, S. H., *J. Chem. Phys.* 36:1743 (1962).
13. Melius, C., Sandia National Laboratories, Personal Communication, 1988.
14. Montgomery, J. A., and Michels, H. H. United Technologies Research Center, Personal Communication, 1989.

APPENDIX E

Aerosol Dynamics of Soot Particle Growth in Flames

AEROSOL DYNAMICS SIMULATIONS OF SOOT PARTICLE GROWTH IN FLAMES*.

Robert J. Hall and Meredith B. Colket, United Technologies Research Center, East Hartford, CT 06108.

Soot particle growth in flames has been modeled as a classical aerosol dynamics problem using a modified version of the MAEROS program. The carbon particle size range of interest is divided into discrete size classes, or sections, and a master equation for the population in each size class is solved with terms representing nucleation, surface growth by deposition of condensible vapor, and coagulation. Provision is also made in the surface growth terms for oxidative removal of mass. Appropriate temperature dependences have been given to the surface growth and oxidation rates, and the temperature range of the MAEROS code has been extended.

We first tested the simplifying idea of extrapolating these particle dynamics concepts into the pre-particle regime. In comparisons with available pre-mixed flame data, acetylene was assumed to be the condensible vapor, and the nucleation rate was chosen to be that of the lowest order closed ring species, benzene or napthalene. The model in its simplest form thus requires only the gas temperature, the acetylene and oxygen concentrations, and an estimate of the benzene or napthalene source rate, data that are available, together with soot density measurements, in certain well-characterized flames. Generally encouraging agreement has been obtained using this simplifying assumption, and we will discuss the sensitivity of the predicted soot density and size parameters to the rates for the various processes. A discussion of important rate-limiting steps in pre-particle chemistry will also be given, and we will show how particle thermal radiation can be calculated from the growth solution.

* Sponsored by Air Force Office of Research Under Contract F49620-88-C-0051